THE ANTENNA LABORATORY

UNPUBLISHED PRELIMINARY DATA

RESEARCH ACTIVITIES in --

Automatic Controls — *Antennas* — *Echo Area Studies*
Microwave Circuits — *Astronautics* — *E M Field Theory*
Terrain Investigations — *Radomes* — *Systems Analysis*
Wave Propagation — *Submillimeter Applications*

Measurements of the Optical Constants of Magnesium Oxide and Calcium Tungstate in the Spectral Region Between 10 cm^{-1} and 100 cm^{-1} at 300°K and 90°K

by

R.F. Rowntree

Grant No. NSG-74-60

1093-13 28 February 1963

Department of ELECTRICAL ENGINEERING

THE OHIO STATE UNIVERSITY
RESEARCH FOUNDATION
Columbus, Ohio

NOTICES

When Government drawings, specifications, or other data are used for any purpose other than in connection with a definitely related Government procurement operation, the United States Government thereby incurs no responsibility nor any obligation whatsoever, and the fact that the Government may have formulated, furnished, or in any way supplied the said drawings, specifications, or other data, is not to be regarded by implication or otherwise as in any manner licensing the holder or any other person or corporation, or conveying any rights or permission to manufacture, use, or sell any patented invention that may in any way be related thereto.

The Government has the right to reproduce, use, and distribute this report for governmental purposes in accordance with the contract under which the report was produced. To protect the proprietary interests of the contractor and to avoid jeopardy of its obligations to the Government, the report may not be released for non-governmental use such as might constitute general publication without the express prior consent of The Ohio State University Research Foundation.

Qualified requesters may obtain copies of this report from the ASTIA Document Service Center, Arlington Hall Station, Arlington 12, Virginia. Department of Defense contractors must be established for ASTIA services, or have their "need-to-know" certified by the cognizant military agency of their project or contract.

REPORT

by

THE OHIO STATE UNIVERSITY RESEARCH FOUNDATION
COLUMBUS 12, OHIO

Cooperator	National Aeronautics and Space Administration 1520 H Street Northwest Washington 25, D.C.
Grant No.	NSG-74-60
Investigation of	Receiver Techniques and Detectors for Use at Millimeter and Submillimeter Wavelengths
Subject of Report	Measurements of the Optical Constants of Magnesium Oxide and Calcium Tungstate in the Spectral Region Between 10 cm^{-1} and 100 cm^{-1} at 300°K and 90°K (1.0 to .1 mm)
Submitted by	R.F. Rowntree Antenna Laboratory Department of Electrical Engineering
Date	28 February 1963

The material contained in this report is also used as a dissertation submitted to the Graduate School of The Ohio State University as partial fulfillment for the degree Doctor of Philosophy.

ABSTRACT

33694

Using the new Ohio State University far infrared spectrometer, incorporating an interferometric modulator, the optical constants n and κ of MgO and $CaWO_4$ were directly measured at 300°K and 90°K in the spectral region between 10 and 100 cm^{-1} (1.0 to 0.1 mm). The refractive indices n were computed from the maxima and minima of channeled spectra, while the extinction coefficients κ were computed from point-by-point transmission measurements. Through the use of wire grating polarizers, both the ordinary ray and extraordinary ray optical constants of $CaWO_4$ were obtained. The measured refractive indices at both 300°K and 90°K are believed to be correct to 1.0 percent in the region between 30 and 80 cm^{-1}, with the possible error increasing to 2.4 percent outside of that region. The 300°K extinction coefficient values are believed to be correct to 14 percent, while the 90°K values may be in error by as much as 50 percent. Selected representative values of the refractive indices were squared and plotted versus the square of frequency and a linear relation obtained. The resulting lines were extrapolated to zero frequency and the following values were found for the static dielectric constants: MgO; 300°K, $\epsilon_o = 9.79$; 90°K, $\epsilon_o = 9.56$; $CaWO_4$: $E \perp c$-axis (ordinary ray). 300°K, $\epsilon_o = 10.88$; 90°K, $\epsilon_o = 10.61$; $E \parallel c$-axis (extraordinary ray) 300°K, $\epsilon_o = 9.16$; 90°K, $\epsilon_o = 8.92$. The values of the dielectric constant (real part) ϵ' followed the predictions of classical dispersion theory, while the values for the dielectric constant (imaginary part) ϵ'' did not; this finding is in agreement with those of other workers. The measured values of the $CaWO_4$ optical constants were compared with those predicted from the dispersion parameters, calculated by A.S. Barker, Jr. from reflection measurements in the mid infrared; small corrections were made to the dispersion parameters and an excellent fit was obtained. The data for MgO was shown to confirm the findings of Smart, et al., and Saksena and Viswanathan that the eigenfrequency is in the region of 400 cm^{-1}, rather than 570 cm^{-1} as had been previously reported. The eigenfrequency data of Smart, together with the present dielectric constant results for MgO, were applied to the first and second Szigeti relations. The effective charge parameter s was found to be 0.60 at 300°K and 0, 61 at 90°K; the ratio of the calculated compressibility to the measured compressibility was found to be 0.91 at 300°K and 0.88 at 90°K. The formulas suggested by other authors to improve the Szigeti relations were evaluated for MgO. The infrared absorption in this region was discussed in terms of the two-phonon process.

FOREWARD

The body of this technical report is the dissertation of Dr. Robert F. Rowntree, which was submitted in partial fulfillment of the requirements for his Ph.D. degree (1963) from The Ohio State University. The research reported in this dissertation was supported, in part, at different times, by two sponsors:

> The Air Force Cambridge Research Laboratories through Contract AF 19(604)-4119 with The Ohio State University Research Foundation, Professor Ely E. Bell, supervisor;
>
> The National Aeronautics and Space Administration, Grant Number NsG-74-60 to The Ohio State University Research Foundation, Dr. William S.C.Chang, supervisor.

Copies of this report are being supplied to both sponsors.

Preliminary reports of the measurements described in this dissertation have been given at the following scientific meetings:

> "A New Far Infrared Submillimeter Spectrometer Utilizing Interferometric Modulation," by R.F.Rowntree, E.E.Bell, M.E.Vance and R.A.Oetjen, Symposium on Molecular Structure and Spectroscopy, Columbus, Ohio, June 1962;
>
> "Measurement of the Properties of Laser Crystals at Submillimeter Wavelengths," by R.F.Rowntree and W.S.C., The Ohio State University Antenna Laboratory Lasers and Applications Symposium, Columbus, November 1962;
>
> "Properties of Materials for Submillimeter Masers," by W.S.C.Chang and R.F.Rowntree, Third International Symposium on Quantum Electronics, Paris, February 1963.

The far infrared spectrometer used to make the measurements described in this report was constructed with the partial support of the aforementioned Air Force Cambridge contract and a grant from the National Science Foundation. The present report is part of a program of studies of the spectra of gases, of the optical properties of materials, and of quantum electronic devices in the submillimeter wavelength region being performed at The Ohio State University with the aid of this instrument.

CONTENTS

CONTENTS - Continued

ILLUSTRATIONS

ILLUSTRATIONS - Continued

TABLES

CHAPTER I

INTRODUCTION

A. The decline and revival of the study of the infrared properties of dielectric crystals

The study of the interaction of infrared radiation with dielectric crystals was an area of major interest in solid state physics in the 1930's.[1] However, in the following decades, which have seen great improvements in the state of infrared instrumentation, this interest has lagged in favor of investigation of other phases of the solid state, particularly the properties of semi-conductors.

The direction of the improvements in infrared instrumentation have doubtless contributed to this decrease in interest. The development, following World War II, of detectors and crystal-growing techniques resulted in advances in spectroscopy first in the near infrared and then subsequently at longer wavelengths. Some of the properties of greatest interest in the elemental semi-conductors silicon and germanium (e.g., the width of the forbidden band and the location of

---

[1] References to much of this work may be found in the bibliography of E. Palik, J. Opt. Soc. Am. 50, 1329 (1960).

impurity centers within it) were accessible to study in the near infrared where the instrumentation advances were first felt.

Most dielectric crystals (without impurities), on the other hand, exhibit few properties of interest, other than dispersion, in the near infrared ($\lambda < 4\mu$). Indeed, the majority of the studies of such materials, in the decade following 1945, were measurements of their dispersion, with the aim of establishing their usefulness for prisms and windows in infrared instruments.

The phenomena of major interest in polyatomic dielectrics, the strong absorptions associated with the optically active vibrations of the crystal lattice, occurs primarily at relatively long wavelengths (seldom less than 15μ), and often lie in the far infrared spectral region (defined, for purposes of this report, as $50\mu > \lambda > 1.0$ mm or 200 $cm^{-1} < \nu < 10$ cm^{-1}). Aside from the development of the Golay radiation detector[2] (an innovation whose significance we do not mean to deny) instrumentation for spectroscopy in the far infrared showed a relatively slow advance in the post-war decade. The few far infrared measurements of dielectrics in this period were primarily efforts to find window end transmission filter materials for further instrumentation.[3]

---

[2] M. Golay, Rev. Sci. Inst. 18, 357 (1947).

[3] T.K. McCubbin, Far Infrared Spectroscopy from 100 to 700 Microns, Ph.D. Dissertation, The Johns Hopkins University, 1951; R.L. Hansler, Ph.D. Dissertation, The Ohio State University, 1952, unpublished.

In the last five years, however, the "instrumentation explosion" has reached the far infrared region.[4] In this period there have been reported[5] a number of low temperature ($T < 4^{\circ}K$) detectors which offer a considerable improvement over the Golay Cell. Of probably greater importance (certainly for the present work) has been the application of interferometric techniques to the far infrared region,[6] permitting the construction of spectrometers which can be operated to beyond 1000μ.

Almost simultaneously with this improvement in far infrared instrumentation, there has occurred a revival of interest in the infrared properties of dielectrics. Several laboratories have reported measurements in the regions of the lattice absorptions, at low temperatures

---

[4] An excellent survey of the field has been given by L. Genzel, Preprint C-106, International Symposium on Molecular Structure and Spectroscopy, Tokyo, 1962.

[5] W. Boyle, W. Rodgers, J. Opt. Soc. Am. 49, 66 (1959); D. Martin, et al., Cryogenics 1, 159 (1960); Optica Acta 7, 185 (1960); F. Low, J. Opt. Soc. Am. 51, 1300 (1961); E. Putley, J. Phys. Chem. Solids 22, 241 (1961).

[6] L. Genzel, R. Weber, Z. angew. Physik 10, 127 (195), 195 (1958). J. Strong, G. Vanesse, J. Opt. Soc. Am. 49, 844 (1959); H. Gebbie in J. Singer (ed.), Advances in Quantum Electronics (Columbia University Press, New York, 1961), p. 155; M.E. Vance, Ph.D. Dissertation, The Ohio State University, 1962.

as well as ambient.[7] In addition, at least two groups[8] have reported measurements on the optical constants of dielectric crystals at wavelengths considerably longer than those of the lattice absorption.

Together with this renewed interest in far infrared measurements, the last five years have also seen the publication of a number of papers on the theory of dielectrics.[9] These works cover two areas: 1) relations between the static and optical dielectric constants, and the frequency of the lattice absorption; and 2) explanations of the spectral structure of the absorptions associated with the lattice vibrations.

The interest in the far infrared properties of dielectric crystals has also been stimulated from another direction. The advance of the limit of microwave research up into the far infrared (called "submillimeter" by microwave workers) region[10] with the advent of laser technology has led communications engineers to raise the question of

---

[7] R.L. Brown, Ph.D. Dissertation, The Ohio State University, 1959; G. Jones, D. Martin, P. Mawer, C. Perry, Proc. Roy. Soc. (London) A261, 10 (1961); see also footnote 1.

[8] At Freiburg and Frankfurt (W. Germany), under L. Genzel; and at King's College, University of London (England), under W.C. Price and G.R. Wilkinson.

[9] References to this work will be given in Chapter II, below.

[10] The Millimeter and Submillimeter Conference, Orlando, Florida, January 1963.

the possibility of developing similar submillimeter stimulated emission devices. In order to develop such devices the properties of dielectrics for laser host crystals, for antenna windows, etc., must be known.

Thus we see that in twenty five years the wheel has turned a full circle and that the study of the infrared properties of dielectric crystals is again a topic of interest to physicists, and to engineers and technologists as well.

B. The present work

The construction at The Ohio State University of a new far infrared spectrometer,[11] capable of making measurements, with a high degree of spectral purity, throughout the region from 100 to 1000μ and able to accept cryostats for low temperature measurements, now permits this Laboratory to make a contribution to the study of the infrared properties of dielectrics at room temperature and low temperatures.

Because physicists usually prefer to study first the simpler types of problems, the cubic diatomic alkali halide crystals have been the most frequent subjects of investigation. A second group of cubic diatomic crystals, the alkaline earth oxides, were often included in the studies during the 1930's. The most readily available member

---

[11] R.F. Rowntree, M.E. Vance, E.E.Bell, R.A. Oetjen, Symposium on Molecular Structure and Spectroscopy, Columbus, Ohio, 1962.

of this group is magnesium oxide (MgO), and we have chosen it for one of the subjects of this investigation.

Of the more complicated polyatomic crystals, quartz (SiO_2)[1] and calcite ($CaCO_3$)[1] received considerable attention during the earlier period and, more recently, corundum or sapphire (Al_2O_3) has also been studied.[12]

Calcium tungstate ($CaWO_4$) is another such polyatomic crystal which has just recently become of interest to spectroscopists through its use as a host crystal for the study of the fluorescence and energy transfer processes of rare earth ions, and as host for a number of near infrared laser devices with such rare earth ions as the active material. We have selected $CaWO_4$ as the second crystal for study in this investigation.

1. Magnesium oxide

Magnesium oxide is an extremely hard, high melting-point material[13] (it is used as an abrasive and as a refractory material) and is transparent to visible light. Its crystal structure is that of sodium chloride[14] (face-centered cubic) and its only apparent major difference

[12]S. Roberts, D. Coon, J. Opt. Soc. Am. 52, 1023 (1962).

[13]S. Ballard, K. McCarthy, W. Wolfe, Optical Materials for Infrared Instrumentation, Infrared Information and Analysis Center, The University of Michigan, Ann Arbor, 1959.

[14]R. Wyckoff, Crystal Structures (Interscience Publishers, Inc., New York, 1948).

from NaCl is the double valency of the chemical bond. Being cubic, MgO exhibits the same optical constants for all radiation polarizations relative to the crystal.

As was mentioned above, MgO was the subject of a number of infrared spectral investigations in the 1930's, and, indeed, the literature contains a wealth of physical data of all sorts for MgO.

The earliest reported infrared spectral investigation of MgO was by Tolksdorf,[15] in 1928, who studied the transmission of the powder between 2 and 15μ. Strong,[16] using reststrahlen techniques, measured the transmission of thin layers of MgO, collected by fuming magnesium ribbon in air, at seven wavelengths between 7 and 33μ. He similarly measured the reflectance of a sample of the pressed powder (magnesia) at eleven wavelengths from 20 to 150μ. Fock,[17] in 1934,studied the transmission of fumed layers out to 40μ. Barnes, Brattain and Seitz,[18] in 1935, made a detailed study of the transmission of thin plates of single crystal MgO out to 15μ. Strong and Brice,[19] in 1935, measured

---

[15] S. Tolksdorf, Z. physik Chem. 132, 161 (1928).

[16] J. Strong, Phys. Rev. 37, 1565 (1931), 38, 1818 (1931).

[17] J. Fock, Z. Physik 90, 44 (1934).

[18] R. Barnes, R. Brattain, F. Seitz, Phys. Rev. 48, 582 (1935).

[19] J. Strong, B. Brice, J. Opt. Soc. Am. 25, 207 (1935).

the refractive index in the visible. Burstein, Oberley, and Plyler,[20] in 1948, measured the transmission of single crystal plates between 6 and 13μ, and the reflection from a single crystal out to 35μ. Willmott,[21] in 1950, measured the transmission of fumed layers and the transmission and reflection of single crystal samples, and calculated optical constants of MgO out to 25μ. Stephens and Malitson,[22] in 1952, measured the refractive index, and its temperature dependence, from the visible to beyond 5μ. Momin[23] in 1953, studied the transmission of fumed layers between 1 and 21μ. Saksena and Viswanathan,[24] in 1956, made an analysis of the results of Stephens and Malitson and Willmott reinterpreting the latter's results. Within the past year Plyler, Yates and Gebbie[25] have published curves of the transmission of thin MgO plates in the 70-200μ region. All the above measurements were made at room temperature.

---

[20] E. Burstein, J. Oberley, E. Plyler, Proc. Indian Acad. Sci. A28, 398 (1948).

[21] J. Willmott, Proc. Phys. Soc. (London) A63, 389 (1950).

[22] R. Stephens, I. Malitson, J. Research Natl. Bur. Standards 49, 249(1952).

[23] A. Momin, Proc. Indian Acad. Sci. A37, 254 (1953).

[24] B. Saksena, S. Viswanathan, Proc. Phys. Soc. (London)B69, 129 (1956).

[25] E. Plyler, D. Yates, H. Gebbie, J. Opt. Soc. Am. 52, 860 (1962).

Recently, at King's College, University of London, W.C. Price and G.R. Wilkinson[26] have begun a program of measurement of infrared properties of a large number of crystals at room temperature and at liquid nitrogen temperature. Working in their laboratory Smart,[27] in 1960, measured the transmission and reflection of single-crystal plates and of evaporated (not fumed) layers of MgO at 300°K and 90°K from 10 to 50μ, and Inglis[26] measured the transmission of a thin plate at 90°K from 50μ to beyond 200μ. Using this data, Smart programmed a computation through the Kramers-Kronig relation and so obtained values for the optical constants of MgO at 300°K and 90°K from 10μ (1000 cm^{-1}) to DC (0 cm^{-1}).

In the work below we report[28] direct measurements of the optical constants of MgO from 90 to 800μ at 300°K and 90°K, and their interpretation in the light of current theory and the above-mentioned earlier work.

---

[26] W. Price, G. Wilkinson, et al., Molecular Spectroscopy Report, U.S. Army Contract DA-91-591-EUC 1958-1959 (ASTIA AD 231584, TAB 60-2-3, p. 61), 1959-1960 (ASTIA AD 262665, TAB 61-4-4, p. 190).

[27] C. Smart, Ph.D. Thesis, University of London (England), 1962, unpublished.

[28] A preliminary report of the present experimental results has been presented elsewhere: R.F. Rowntree, W.S.C. Chang, Symposium on Lasers and Applications, Columbus, Ohio, November, 1962; note 11.

2. Calcium tungstate

Calcium tungstate is a hard, visibly transparent crystal which occurs naturally as the mineral scheelite. Unlike the case of MgO, the literature contains very little physical data of any sort about $CaWO_4$ or scheelite.

The crystal structure of $CaWO_4$ is tetragonal[14] and thus it is uniaxial,[29] exhibiting different optical constants for radiation polarized perpendicular ("ordinary ray") and parallel ("extraordinary ray") to the crystalline c-axis.

W.W. Coblentz,[30] in 1908, measured the infrared reflection of an unoriented sample of scheelite out to 14μ. Nisi,[31] in 1935, studied the Raman spectrum of unoriented scheelite. Bentley and Jones,[32] in 1960, reported the spectra of a number of solid powders, including $CaWO_4$, dispersed in Nujoll.

Recently, Barker[33] has measured the room temperature reflection of $CaWO_4$, for both radiation polarizations, from the near

---

[29]R.W. Ditchburn, Light (Interscience Publishers, Inc., New York, 1953) p. 523.

[30]W.W. Coblentz, Supplementary Investigations of Infrared Spectra, Publication No. 97, The Carnegie Institution of Washington, Washington, 1908, p. 16.

[31]H. Nisi in Pieter Zeeman: 1865-25 mei-1935 (Martinus Nyhoff, The Hague, 1935), p. 261.

[32]F. Bentley, W. Jones, Spectrochim. Acta 16, 135 (1960).

[33]A.S. Barker, Jr., private communication.

infrared to beyond 50μ; he has analyzed his data in terms of classical theory and obtained a set of dispersion parameters from which one may compute the optical constants.

In this work we report[28] direct measurements of the optical constants of $CaWO_4$, for both polarizations, at 300°K and 90°K, from 90 to 800μ; we also show the extent of the agreement between our room temperature results and those obtained from the dispersion parameters of Barker.

CHAPTER II
THEORY

In this chapter we will display expressions, from classical electrodynamics, which describe the power transmitted through a medium by an electromagnetic wave in terms of optical constants, macroscopic parameters whose form is independent of the structure of the medium and whose value is determined by the medium. The optical constants are, in general, functions of the frequency of the electromagnetic wave; we shall show how the optical constants may be simply computed from measurements of the power transmitted by the medium in a given spectral region.

We shall then show how, in classical dispersion theory, the macroscopic optical constants are related to the microscopic structure of the medium, on the assumption that it is composed of a set of damped harmonic oscillators. Because this classical theory is contained in numerous texts[1] on physical optics and monographs[2] on the

---

[1] See e.g. R. Ditchburn, Light (Interscience Publishers, Inc., New York, 1953); M. Born, E. Wolf, Principles of Optics (Pergamon Press, New York, 1959).

[2] T. Moss, Optical Properties of Semi-Conductors (Butterworths Scientific Publications, London, 1959); H. Fan, in K. Lark-Horovitz, V. Johnson (eds), Methods of Experimental Physics (Academic Press, New York, 1959) Vol. 6, Part B, pp. 249-278, "Optical Properties".

measurement of optical properties, we will give detailed derivations only where the argument extends beyond that contained in these common sources.

Finally, we shall discuss some extensions of the classical theory and some modifications of it in the light of more recent ideas. These developments are the work of many authors and the arguments are still in a state of flux, so that the areas of agreement and disagreement are unclear. For this reason we shall not attempt a unified explanation of the recent ideas, but will only present the various authors' conclusions, and their implications in the light of the data obtained in the present work.

A. Measurement of the optical constants

The propagation of an electromagnetic wave, in a specified direction in a medium, may be written in terms of the electric vector,[3]

$$\vec{E}(x, t) = \vec{E}_o \exp\left[i\omega\left(t - \hat{n}\,\frac{x}{c}\right)\right], \qquad \text{(II-1)}$$

where x is the direction of propagation, ω the circular frequency of the wave, c the velocity of light in vacuum, and $\hat{n}$ the complex

---

[3] Moss, op. cit., p. 1; Ditchburn, op. cit., p. 441; Born and Wolf, op. cit., p. 611; Fan, loc. cit., p. 249.

refractive index, consisting of a real part, n, the refractive index, and an imaginary part, κ, the extinction coefficient.

(II-2) $$\hat{n} \equiv n - i\kappa \ .$$

In general $\hat{n}$ is a function of frequency. For $\hat{n}$ to be independent of position, the medium must be homogeneous (i.e., $\hat{n}$ changes only at boundaries between media). Unless the medium is isotropic, $\hat{n}$ will exhibit different values for different specified directions of polarization ($\vec{E}_o$) relative to the medium. Since the present work is restricted to media that are either isotropic or uniaxial (having one defined direction called the crystalline c-axis), the electric vector may be completely specified by components parallel and perpendicular to the c-axis. Thus it is sufficient to note that the remainder of the argument applies to a given one of these directions.

For an electromagnetic wave incident normally on the interface between vacuum ($n = 1$, $\kappa = 0$) and an infinitely thick medium, application of the boundary conditions yields,[4] for the ratio of power reflected to the power incident, the reflection coefficient

(II-3) $$R = \frac{(n-1)^2 + \kappa^2}{(n+1)^2 + \kappa^2} \ .$$

---

[4]Moss, op. cit., p. 6; Ditchburn, op. cit., p. 443; Born and Wolf, op. cit., p. 617; Fan, loc. cit., p. 250.

For the case $n >> \kappa$, (II-3) reduces to

$$R = \frac{(n-1)^2}{(n+1)^2} \quad . \tag{II-4}$$

In the visible spectral region, for common window materials $n = 1.5$, yielding $R = 0.04$. For $n \cong 3.0$, a typical value for the present work, $R = 0.25$.

Similarly, for a wave incident normally on a slab of material with parallel sides separated by a distance ℓ, application of the boundary conditions, or consideration of the multiple internal reflections, yields[5], for the power transmission coefficient

$$\mathcal{T} = \frac{(1-R)^2 D}{(1-RD)^2 + 4RD \sin^2 \phi} \quad , \tag{II-5}$$

$$D = \exp\left(-4\pi \kappa \frac{\ell}{\lambda}\right) \quad ,$$

$$\phi = 2\pi n \frac{\ell}{\lambda} \quad ,$$

where λ is the vacuum wavelength of the incident radiation.

In the remainder of the present work we shall use the spectroscopists' notation

$$\nu = \frac{1}{\lambda} = \frac{\omega}{2\pi c} \quad ,$$

---

[5] Moss, op. cit., p. 13; Fan, loc. cit., p. 263; the complete expression also includes a reflection phase angle ψ, $\tan \psi = \frac{2\kappa}{n^2 + \kappa^2 - 1}$, but $\psi \cong 0$ for the present work, and so we shall neglect it.

and refer to ν as "the frequency in [units of] cm^{-1}." Thus, in (II-5)

$$(II\text{-}5') \qquad D = \exp(-4\pi\kappa\,\nu\ell)$$

$$\phi = 2\pi n\nu\ell \ .$$

In engineering work the quantity D is often expressed in terms of the absorption coefficient α,

$$(II\text{-}5'') \qquad D = \exp(-\alpha\ell),$$

$$\alpha = 4\pi\kappa\nu \ .$$

If the power transmitted by the slab is measured as a function of frequency, in a spectral region where D is close to unity, $\mathcal{T}$ exhibits maxima and minima, called a "channeled spectrum",[6] due to the second term in the denominator of (II-5):

$$(II\text{-}6) \qquad \mathcal{T}_{max} = \frac{(1-R)^2\,D}{(1-RD)^2}, \quad \phi = b\pi;$$

$$\mathcal{T}_{min} = \frac{(1-R)^2\,D}{(1+RD)^2}, \quad \phi = (b+1/2)\pi \ .$$

$$b = 0, 1, 2, 3, \cdots \ .$$

Thus, if the frequencies of the extrema of the transmitted power are measured the refractive indices at those frequencies

---

[6] J. Strong, Concepts of Classical Optics (W.H. Freeman and Co., San Francisco, 1958), p. 225.

are given by

$$(II\text{-}7) \qquad n_b = \frac{b}{2\ell \nu_b} \qquad \text{maxima,}$$

$$n_{b'} = \frac{b' + 1/2}{2\ell \nu_{b'}} \qquad \text{minima.}$$

If the slab is sufficiently thick, so that the spectral pass-band of the measuring instrument exceeds the separation of adjacent maxima $\left(\Delta\nu_1 > \frac{1}{2n\ell}\right)$, then the channeled spectrum is no longer resolved and the measured power transmission coefficient becomes (upon averaging (II-5) over $0 \leq \phi \leq 2\pi$)[7]

$$(II\text{-}8) \qquad \mathcal{T} = \frac{(1-R)^2 D}{1-R^2 D^2} \quad .$$

If D is sufficiently small so that $R^2 D^2 << 1$, then (II-8) reduces to

$$(II\text{-}9) \qquad \mathcal{T} = (1 - R)^2 D.$$

The program of measurement consisted of first recording the spectrum of the power transmitted by a thin plate of the material and determining the frequencies in the resulting channeled spectrum. The refractive index n was then computed using (II-7) and the single-surface reflection coefficient R was computed from (II-4). The

---

[7] Moss, op. cit., p. 14; this expression is obtained directly if one disregards the phase difference between the reflections at the two surfaces, see H. Yoshinaga, R. Oetjen, Phys. Rev. 101, 526 (1956).

results of the present measurements show that the condition for using (II-4), $n >> \kappa$, is satisfied throughout.

Quantitative measurements of the power transmission coefficient $\mathcal{T}$ of thicker samples were then made at selected frequencies. Using the value of R computed from (II-4), the quantity D was then obtained from (II-8) or (II-9), as appropriate. Finally, the extinction coefficient was computed from the definition of D in (II-5'):

(II-10) $$\kappa = (4\pi \nu \ell)^{-1} \ln D^{-1} .$$

It should be noted that this method of measurement of the optical constants follows directly from the electromagnetic wave equation solution (II-1), and involves no a priori assumptions about the microscopic nature of the medium, other than that of homogeneity.

B. Classical dispersion theory

In (II-1) above, the propagation of an electromagnetic wave in a medium was described in terms of the complex refractive index $\hat{n}$. It is also possible to describe the propagation in terms of a complex dielectric constant $\hat{\epsilon}$, where the relationship between $\hat{\epsilon}$ and $\hat{n}$, and between their respective real and imaginary parts, is given by[8]

---

[8] Moss, op. cit., pp. 2,15; Ditchburn, op. cit., p. 453; Born and Wolf, op. cit., pp. 83, 610.

$$\hat{n}^2 = \hat{\epsilon} \equiv \epsilon' - i\epsilon'' ,$$

(II-11)

$$\epsilon' = n^2 - \kappa^2 , \quad \epsilon'' = 2n\kappa .$$

In electrical engineering usage, ϵ' is called the dielectric constant and the ratio of ϵ'' to ϵ' the loss tangent:

(II-11') $$\frac{\epsilon''}{\epsilon'} \equiv \tan \delta .$$

In classical electromagnetic theory the macroscopic parameters $\hat{\epsilon}$ (or $\hat{n}$) were related to the microscopic structure of the medium on the assumption that the medium consisted of a set of damped harmonic oscillators. These oscillators were characterized by a mass m and charge e, damping constant $m\omega_o\gamma$, and force constant $m\omega_o^2$. The damping was assumed to be small, so that the oscillator's resonant frequency ν_o was $2\pi\nu_o = \omega_o$. The polarization $\vec{P}$ of the medium was then described in terms of the familiar expression for the motion of the oscillator under the influence of the impressed electric field $\vec{E}(\nu)$.[9] Under the restrictions imposed in Section A, above, $\vec{E} \,||\, \vec{P}$. The complex dielectric constant was then obtained from[8]

$$\vec{P} = \hat{\chi}\,\vec{E}, \quad \hat{\epsilon} = 1 + 4\pi\,\hat{\chi}$$

---

[9]Moss, op. cit., pp. 15-18; Ditchburn, op. cit., pp. 452-457; Born and Wolf, op. cit., pp. 89ff, 621-624.

yielding the desired relation between the macroscopic parameters of the electromagnetic field and the microscopic parameters of the medium

$$\hat{\epsilon}(\omega) = 1 + (4\pi\ Ne^2\ m^{-1})(\omega_o^2 - \omega^2 + i\gamma\omega_o\omega)^{-1}\ , \tag{II-12}$$

where N is the number of oscillators per unit volume.

With the advent of quantum mechanics, the classical model was taken over,[9] with the resonance at ν_o representing an allowed transition of the system having an oscillator strength f. Also, the system was generalized to one with a number of different allowed transitions, each with frequency ν_g (the equivalent of the assumption that the medium contains more than one kind of oscillator). With these additions, (II-12) becomes

$$\begin{aligned}\hat{\epsilon} &= 1 + \sum_g (4\pi\ N_g e_g^2 f_g m_g^{-1})(\omega_g^2 - \omega^2 + i\gamma_g\omega_g\omega)^{-1} \\ &= 1 + \sum_g \frac{A_g}{(1 - \Omega_g^2) + i\gamma_g\Omega_g}\ ,\end{aligned} \tag{II-13}$$

with

$$A_g = 4\pi N_g e_g^2 f_g \omega_g^{-2} m_g^{-1},$$

and

$$\Omega_g = \frac{\nu}{\nu_g}\ ,$$

where the sum extends over all the allowed transitions.

In the case of dielectric solids, the transitions ν_g are split into two groups well-separated from one another. Those with the lowest frequencies, ν_j, lie in the infrared, while the remainder, ν_k, lie in the ultraviolet, or beyond. The region of separation between these groups corresponds to the visible and near infrared, where these materials are non-absorbing. Thus we rewrite (II-13)

$$\hat{\epsilon} = 1 + \sum_k \frac{A_k}{(1-\Omega_k^2) + i\gamma_k\Omega_k} + \sum_j \frac{A_j}{(1-\Omega_j^2) + i\gamma_j\Omega_j}$$

and finally, if we restrict the frequency ν at which we are to determine $\hat{\epsilon}(\nu)$ to the infrared, we have

$$\text{(II-13')} \qquad \hat{\epsilon}(\nu) = \epsilon_\infty + \sum_j \frac{A_j}{(1-\Omega_j^2) + i\gamma_j\Omega_j}, \quad (\nu \ll \nu_k)$$

$$\epsilon_\infty = 1 + \sum_k \frac{A_k}{(1-\Omega_k)^2 + i\gamma_k\Omega_k} .$$

The sum on j now extends only over those resonances ν_j which lie in the infrared; the effects of the remainder of the resonances are contained in ϵ_∞. Finally, upon combining (II-11) with (II-13'), we obtain the classical dispersion relations

$$\text{(II-14)} \qquad \epsilon'(\nu) = n^2 - \kappa^2 = \epsilon_\infty + \sum_j A_j \frac{(1-\Omega_j^2)}{(1-\Omega_j^2)^2 + \gamma_j^2\Omega_j^2}$$

$$\epsilon''(\nu) = 2n\kappa = \sum_j A_j \frac{\gamma_j \Omega_j}{(1-\Omega_j^2)^2 + \gamma_j^2 \Omega_j^2} ,$$

(II-15)

$$\Omega_j = \frac{\nu}{\nu_j} .$$

These expressions relate the macroscopic optical constants to the microscopic parameters of the medium. In the conventional nomenclature, the quantities appearing in (II-14) and (II-15) are called the classical dispersion parameters: ν_j is the eigenfrequency, A_j the oscillator strength, γ_j the damping constant, and ϵ_∞ the optical dielectric constant "extrapolated to zero frequency". Operationally ϵ_∞ is taken as the constant term in the Sellmeier-type equation[10] to which refractive index measurements in the visible and near infrared are usually fitted.

A special case of (II-14) and (II-15) is that for zero frequency,

$$\epsilon_o \equiv \epsilon'(o) = \epsilon_\infty + \sum_j A_j ,$$

(II-16)

$$\kappa(o) = 0, \qquad n_o^2 = \epsilon_o ,$$

where ϵ_o is called the static dielectric constant.

For a cubic diatomic crystal there is but one resonance, so that

---

[10]Ditchburn, op. cit., p.457; Born and Wolf, op. cit., pp. 95-96.

(II-16a) $$\epsilon_o = \epsilon_\infty + A,$$

(II-14a) $$n^2 - \kappa^2 = \epsilon_\infty + \frac{(\epsilon_o - \epsilon_\infty)}{(1-\Omega^2)^2 + \gamma^2 \Omega^2} ,$$

(II-15a) $$2n\kappa = \frac{(\epsilon_o - \epsilon_\infty)\gamma\Omega}{(1-\Omega^2)^2 + \gamma^2 \Omega^2} .$$

In the present work the highest frequencies of measurement are considerably lower than the eigenfrequency, consequently we expand the denominators of (II-14) and (II-15), keeping only the lowest powers in Ω, and obtain

(II-14') $$n^2 - \kappa^2 = \epsilon_o + \nu^2 \sum_j \frac{A}{\nu_j^2}, \quad 1 >> \frac{\nu^2}{\nu_j^2} >> \frac{\nu^4}{\nu_j^4}, \quad \gamma_j^2 << 1;$$

(II-15') $$2n\kappa = \nu \sum_j \frac{\gamma_j A_j}{\nu_j}, \quad \frac{\nu}{\nu_j} >> \frac{\nu^3}{\nu_j^3} .$$

Since we find that in our spectral region $n^2 >> \kappa^2$, (II-14') shows that a graph of the square of the measured values of n versus the square of frequency should yield a straight line, and that the extrapolation of this line to zero frequency gives the value ϵ_o. Similarly, (II-14') indicates that a plot of the product of the measured values of n and κ should be linear in frequency.

An alternative form of (II-14a) is useful in the wider frequency range if the frequency of the single resonance is known and the damping constant is small:

$$(\text{II-14a}') \qquad n^2 = \epsilon_o + (\epsilon_o - \epsilon_\infty)\left[\frac{1}{1-\Omega^2} - 1\right] ,$$

$$\Omega = \frac{\nu}{\nu_o} \qquad \gamma^2 \Omega^2 << (1-\Omega^2)^2 .$$

A plot of n^2 versus the quantity in square brackets should be linear, with a zero intercept of ϵ_o and a slope equal to $(\epsilon_o - \epsilon_\infty)$.

In summary, then, classical dispersion theory provides some simple expressions, (II-14'), (II-15'), (II-14a'), through which its validity may be readily tested by the present work. While classical theory makes no explicit statements about the temperature dependence of the optical constants, the implication is that the oscillator strengths A_j (and, consequently, ϵ_o) should be independent of temperature, because they involve only transition probabilities and other relatively temperature-independent quantities, and that the major temperature dependence should occur in the damping constant (the "line width") and, consequently, in κ. The present work will also provide a test of these implications.

C. Some remarks on more recent theories

1. The Kramers-Kronig relations

Inspection of the classical dispersion relations (II-14), (II-15) discloses that both $\epsilon'(\nu)$ and $\epsilon''(\nu)$ are determined by the same parameters and that, consequently, there may exist some more general relationship between ϵ' and ϵ'' beyond that of (II-14), (II-15). Indeed, such a relationship does exist, one which relates the real and imaginary parts of a quantity which describes the behavior of a linear system in terms of some variable (often the frequency). The basic consequence of the relationship is that if one of the parts of the complex quantity is known for all possible values of the variable, then the other part is also determined for all values of the variable. The first application of this relationship to the analysis of the dielectric constant was by Kronig[11] and Kramers.[12] Macdonald and Brachman have discussed these relations as part of the broader subject of "Linear System Integral Transform Relations" in a review article.[13]

---

[11] R. Kronig, J. Opt. Soc. Am. 12, 547 (1926).

[12] H. Kramers, Atti Congr. dei Fisici, Como, 545 (1927).

[13] J. Macdonald, M. Brachman, Rev. Mod. Phys. 28, 393 (1956).

The form of the relation for the real and imaginary parts of the dielectric constant is[14]

$$(II\text{-}17) \qquad \epsilon'(\nu') = 1 + \frac{2}{\pi} \int_0^\infty \frac{\epsilon''(\nu)\nu\, d\nu}{\nu^2 - \nu'^2}$$

$$= 1 + \frac{2}{\pi} \int_0^\infty \frac{\epsilon''(\Omega)\Omega d\Omega}{\Omega^2 - 1}, \quad \Omega = \frac{\nu}{\nu'} \quad .$$

The second line of (II-17) illustrates the real reason for the interest in this relation: ϵ' is determined primarily by those values of $\epsilon''(\nu)$ lying close to ν'. More particularly, for $\nu' = 0$,

$$(II\text{-}18) \qquad \epsilon_o = 1 + \frac{2}{\pi} \int_0^\infty \epsilon'' \frac{d\nu}{\nu} \quad ,$$

and finally, following the notation of (II-13),

$$(II\text{-}19) \qquad \epsilon_o - \epsilon_\infty = \frac{2}{\pi} \int_0^\infty \epsilon''_{IR} \frac{d\nu}{\nu} \quad ,$$

where ϵ''_{IR} includes only those contributions that lie in the infrared. A similar relation, between the refractive index and the extinction coefficient, is[15,11]

---

[14] Moss, op. cit., p. 24.

[15] Ibid., p. 27.

$$(II\text{-}20) \qquad n(\nu') = 1 + \frac{2}{\pi} \int_0^\infty \frac{\kappa\, \nu\, d\nu}{\nu^2 - \nu'^2} \quad ,$$

$$n_o = 1 + \frac{2}{\pi} \int_0^\infty \frac{\kappa\, d\lambda}{\lambda} \quad , \qquad (\nu' = \frac{1}{\lambda'} = 0);$$

$$n_o = 1 + \frac{1}{2\pi^2_o} \int_0^\infty \alpha\, d\lambda \quad , \quad \left(\alpha \equiv \frac{4\pi\kappa}{\lambda}\right) \quad .$$

The last line of (II-20) is especially useful because the absorption coefficient α (defined previously in (II-5'') is often directly measurable when n is not. A special form of (II-20) which utilizes only the infrared absorption is

$$(II\text{-}21) \qquad n_o - n_\infty = \frac{1}{2\pi^2} \int_0^\infty \alpha_{IR}\, d\lambda \quad .$$

The reports[16] of the group under Price and Wilkinson at King's College, London, include some data testing the validity of (II-21).

The most used form of the Kramers-Kronig relation is that between the modulus and phase of the amplitude reflection coefficient,[4]

$$(II\text{-}22) \qquad \hat{r} = re^{-i\psi} = r\cos\psi - ir\sin\psi$$

$$= \frac{n - i\kappa - 1}{n - i\kappa + 1} \quad .$$

---

[16] Chapter I, footnotes 26, 27.

Note that $\hat{r}$ is the amplitude reflection coefficient while R, (II-3), is the power reflection coefficient $R \equiv \hat{r}\hat{r}^* = \hat{r}^2$.

For the reflectivity parameters the form of the Kramers-Kronig relation is[17]

$$\text{(II-23)} \qquad \psi(\nu') = -\frac{2\nu'}{\pi}\int_0^\infty \frac{\ln r(\nu)}{\nu^2 - \nu'^2}\, d\nu$$

$$= \frac{\nu'}{\pi}\int_0^\infty \frac{\ln R(\nu)}{\nu^2 - \nu'^2}\, d\nu \ .$$

Thus, from measurements of the power reflection coefficient R one can compute ψ from (II-23) and then the optical constants from (II-22), both with the use of a high speed computing machine, of course. Integrating (II-23) by parts yields

$$\text{(II-24)} \qquad \psi(\nu') = \frac{1}{2\pi}\int_0^\infty \left(\ln\frac{\nu - \nu'}{\nu + \nu'}\right)\frac{d}{d\nu}(\ln R)\, d\nu \ .$$

This shows that $\psi(\nu')$ is insensitive to changes in R far from ν', so that in order to use (II-24), R need only be measured over the reststrahlen peaks in the infrared in order to obtain the infrared constants. Use of this method has been reported by a number of

---

[17] Moss, op. cit., p. 25; T. Robinson, Proc. Phys. Soc. (London) B65, 910 (1952); B66, 969 (1953).

authors,[18] however it has been shown[19] to produce incorrect results for κ in regions of small absorption (e.g., that of the present work). This is hardly surprising, in view of the definition of R (II-3), or footnote 5, above: in the region of small absorption the reflection from a medium is very insensitive to changes in the absorption and, consequently, κ.

2. The theory of the dielectric constant

Attempts to obtain general relations, for cubic diatomic crystals, between the eigenfrequency, ν_o, and the static and high frequency dielectric constants, ϵ_o and ϵ_∞, have been one aspect of the present problem which has received continuing attention during the past fifteen years. The Kramers-Kronig relations, discussed above, provide one such link. The theories discussed in this section, however, utilize not the entire absorption associated with the eigenfrequency, but only its frequency.

The major stimulant of this interest has been the work of B. Szigeti. In two early papers he obtained expressions which have been the point of departure for much of the later work of other authors.

---

[18] Footnotes 17-27, Spitzer and Kleinman, note 19 below.

[19] W. Spitzer, D. Kleinman, Phys. Rev. 121, 1324 (1961); R. Geick, Z. Physik 166, 122 (1961).

In the first paper[20] (henceforth Szigeti I) he obtained an expression for the static dielectric constant of a cubic diatomic crystal from the contributions due to a) the electronic structure (the high frequency dielectric constant ϵ_∞), and b) the polarization of the ions as determined by the mechanical forces in the crystals and the electrical forces resulting from the polarizations:

$$\text{(II-25)} \qquad \epsilon_o - \epsilon_\infty = \left(\frac{\epsilon_\infty + 2}{3}\right)^2 \frac{4\pi N(Zse)}{M\omega_o^2} \quad ,$$

$$M = \left(\frac{1}{m_1} + \frac{1}{m_2}\right)^{-1} \quad , \quad \omega_o = 2\pi\nu_o ,$$

$$N = (2r_o^3)^{-1} \quad .$$

In this expression (and henceforth) M is the reduced mass of a pair of unlike ions, ν_o is the eigenfrequency, N is the number of ion pairs per unit volume or the reciprocal of the volume of a unit cell (r_o is the distance between the nearest neighbors), and Zse the charge on each ion (Z = 1 for the alkali halides, Z = 2 for MgO) with e the electronic charge.

The parameter s is introduced because (II-25) does not provide an exact fit with experiment; Szigeti justifies this parameter with the argument that the overlap of the ions distorts the electron

---

[20] B. Szigeti, Trans. Faraday Soc. 45, 155 (1949).

cloud associated with each ion, thus the polarization is described by an effective charge $Ze^* = Zse$ which is less than that of the free ion. All the quantities in (II-25) are experimentally measurable except s. Szigeti computed s for some nineteen cubic diatomic crystals (including MgO) and obtained values ranging between 0.7 and 1.1; the only crystals exhibiting $s > 0.95$ were those for which some of the experimental data were in doubt. We shall see, below, that the value obtained for MgO ($s = 0.88$) was also due to incorrect experimental data. Most of the subsequent work, discussed below, has been directed toward this problem of the effective charge and of alternative means for calculating it.

In the second paper[21] (henceforth Szigeti II) an expression was obtained[22] for the compressibility K^*:

$$\text{(II-26)} \qquad \frac{1}{K^*} = \frac{M\omega_o^2}{6r_o}\left(\frac{\epsilon_o + 2}{\epsilon_\infty + 2}\right) \quad .$$

In his derivation Szigeti assumed that only central forces were acting on an ion and that the mechanical forces were only due to nearest neighbors, while the electrical forces arose from the

---

[21] B. Szigeti, Proc. Roy. Soc. (London) A204, 51 (1950).

[22] A Similar expression was independently obtained by V. Odelevski, Izv. AN USSR, Ser. Fiz. 14, 232 (1950).

polarization of the entire crystal sample. Again, the conventional form for the evaluation of (II-26) has been the ratio K^*/K, where K is the measured compressibility. Szigeti stated that (II-26) should provide values of K^*/K closest to unity for those crystals showing the least mechanical anisotropy (i.e., the alkali halides) and that results further from unity should be expected for MgO, whose elastic constants show a definite anisotropy. He computed K^*/K for some seventeen substances and obtained $1.13 > K^*/K > 0.85$ for the alkali halides (with a few exceptions where the experimental data were in doubt) and $K^*/K = 0.45$ for MgO. Again, we shall see, below, that this result was based on incorrect data. Szigeti noted that room temperature data were used for these computations while the derivation was, strictly speaking, good only at the absolute zero.

It should be noted that both Szigeti I and II rely heavily on relations between various modes of vibration of the crystal lattice deduced, in a well-known paper, by Lyddane, Sachs, and Teller.[23] Born and Huang,[24] in their work on lattice dynamics, also obtained the Szigeti relations (II-25) and (II-26), although by a somewhat different argument.

---

[23] R. Lyddane, R. Sachs, E. Teller, Phys. Rev. 59, 673 (1941).

[24] M. Born, K. Huang, Dynamical Theory of Crystal Lattices (The Clarendon Press, Oxford, 1954), pp. 111, 112.

In order to incorporate the elastic anisotropy of crystals into the results of Szigeti, Lundqvist[25] applied Löwdin's[26] theory of lattice dynamics, in which three-body forces appear, and obtained,

$$\text{(II-27)} \qquad \frac{K^*}{K} = \frac{1}{(1 + K(c_{44} - c_{12})} \ .$$

Here c_{44} and c_{12} are elastic constants of the material. If the Cauchy relation for elastic isotropy ($c_{44} = c_{12}$) holds, then (II-27) says that $K^*/K = 1$. Lundqvist also obtained an expression for the effective charge:

$$\text{(II-28)} \qquad Ze^* = r_o^2 (1.159\, c_{44} + 1.717 c_{12})^{\frac{1}{2}}.$$

In the Lundqvist model $c_{44} = 0.348\, Z^2 e^2 / r_o^4$; consequently, if the Cauchy relation holds, then $e^* = e$. Because in the Löwdin lattice dynamics the crystal is assumed to be at 0^oK, the results of Lundqvist are expected to hold better at low temperatures than at room temperature.

A direct quantum mechanical calculation of the dielectric constant in terms of the total energy of the polarized crystal has been attempted by Yamashita.[27] He was not particularly successful

---

[25] S. Lundqvist, Arkiv Fysik 9, 435(1955); 12, 263(1957).

[26] P. Löwdin, Arkiv Mat. Astr. Fys. 35, No. 30 (1948).

[27] J. Yamashita, Progr. Theoret. Phys. (Kyoto) 8, 280(1952); 12, 454 (1954).

in obtaining agreement with experimental results for MgO and LiF, and his approach has been criticized in a number of respect by Lundqvist[25] and by Levin and Offenbacher.[28] The latter authors presented a recalculation, for LiF, following the approach of Yamashita, and obtained good agreement with (II-25) for s; however, their results for ϵ_o and ϵ_∞ differed significantly from the observed values. Yamashita and Kurosawa[29] reversed the procedure of the former and obtained a quantum mechanical expression for the energy of a polarized crystal in terms of the dielectric constant, eigenfrequency, and other measurable quantities. They obtained reasonable results for the alkali halides but not for MgO. Use of the correct experimental data for MgO produces results consistent with those of the alkali halides; however, we shall not discuss their results further because it is not pertinent to the present work.

Szigeti's derivations were criticized in a conference paper by Tolpygo,[30] who suggested that the effect of the polarization on the electrons should also be considered. He presented an alternative

---

[28] E. Levin, E. Offenbacher, Phys. Rev. 118, 1142 (1960).

[29] Y. Yamashita, T. Kurosawa, J. Phys. Soc. Japan 10, 610 (1955).

[30] K. Tolpygo, Second All Union Conference on the Physics of Dielectrics, Transactions, Izv. AN USSR, Ser. Fiz., 24, No. 2 (1960) (Trans. Bulletin 24, 167 (1960)); Uspekhi Fiz. Nauk. 74, 269 (1961), Soviet Phys.-Uspekhi 4, 485 (1961).

theory and a tabulation of data for a number of crystals. We cannot attempt to evaluate Tolpygo's theory in the light of the present work because in the one paper available it is not clear which are the input data and which are the results; his original papers were published in journals[31] not available to the present author.

In the above theories the ions were treated as charged lattice points. In two papers Dick and Overhouser,[32] and Hanlon and Lawson[33] independently proposed what is now called the shell model. In this model the ion is assumed to consist of a shell of outer electrons bound isotropically to a core, consisting of the nucleus and the remaining electrons. The dominant repulsive force between ions is taken to be that between shells. This approach is justified by Dick and Overhouser as a result of a calculation of the force between noble gas atoms. The major problem of the shell model is that of determining the number of electrons in the shell. Dick and Overhouser assumed that an ion had the same number of electrons as that of the iso electronic noble gas atom; the latter could be calculated from measured optical data. Dick and Overhouser also introduced the concept of "exchange charge polarization", produced by

---

[31] e.g. Ukr. fiz. Zhur. (Ukranian Journal of Physics) 2, 242 (1957); 4, 72 (1959).

[32] B. Dick, A. Overhouser, Phys. Rev. 112, 90 (1958).

[33] J. Hanlon, A. Lawson, Phy. Rev. 113, 472 (1959).

the change in the distribution of the exchange charge during relative motion of the ions; the computation of this effect required a number of assumptions.

Havinga[34] has considered the works of Dick and Overhouser, and Hanlon and Lawson and deduced a somewhat smaller number of electrons in the shell. Rather good agreement with the values of s from (II-25) are obtained from Havinga's formulas, without recourse to the exchange charge polarization effect. Havinga also pointed out some inadequacies in the work of Hanlon and Lawson.

One formula obtained by Havinga is

$$(II\text{-}29) \qquad (1-s)^2 = \left(\frac{\epsilon_o + 2}{\epsilon_\infty + 2}\right) \frac{M\omega_o^2}{(Ze)^2} (\alpha_+ + \alpha_- - \alpha_\infty),$$

where α_+ and α_- are the free ion polarizabilities of the cation and anion, and α_∞ the crystal polarizability (computed from ϵ_∞). Perry, et al.,[35] have reported rather good agreement of (II-29) with (II-25) for various halides with both 300°K and 4°K experimental data in (II-25), although they had to use estimates of the 4°K values of ϵ_o. On the assumption that the repulsive force between ions will contain most of the dependence on temperature and pressure, Havinga

[34] E. Havinga, Phys. Rev. 119, 1193 (1960).

[35] G. Jones, D. Martin, P. Mawer, C. Perry, Proc. Roy. Soc. (London) A261, 10 (1961).

obtained two additional expressions for the effective charge parameter:

$$(\text{II-30}) \qquad (1-s)^2 = \frac{\frac{\epsilon_\infty - 1}{\epsilon_\infty + 2}\Gamma + \frac{3}{(\epsilon_\infty + 2)^2}\frac{\partial \epsilon_\infty}{\partial T}}{\frac{\epsilon_o - 1}{\epsilon_o + 2}\Gamma + \frac{3}{(\epsilon_o + 2)^2}\frac{\partial \epsilon_o}{\partial T}} ,$$

$$(\text{II-31}) \qquad (1-s)^2 = \frac{\frac{\epsilon_\infty - 1}{\epsilon_\infty + 2}K + \frac{3}{(\epsilon_\infty + 2)^2}\frac{\partial \epsilon_\infty}{\partial P}}{\frac{\epsilon_o - 1}{\epsilon_o + 2}K + \frac{3}{(\epsilon_o + 2)^2}\frac{\partial \epsilon_o}{\partial P}}$$

where Γ is the volume coefficient of thermal expansion and the partial derivatives are the changes of the static and high frequency dielectric constants with temperature and pressure. Havinga found experimental data to test (II-30) and (II-31) for NaCl and (II-30) for KCl, and obtained reasonable agreement with (II-29) and (II-25).

Tests of a number of the above formulas for NaCl and KCl at 82°K were reported by Hass;[36] unfortunately his paper appeared almost simultaneously with Havinga's and so the latter's work was not included. Hass obtained the best agreement from a combination of the shell model with the work of Lundqvist, as suggested by Hanlon and Lawson. However, this relation appears to contradict the generally accepted results of Lyddane, Sachs, and Teller,[23] and,

---

[36] M. Hass, Phys. Rev. 119, 633 (1960).

as mentioned above, Havinga has found other discrepancies in the work of Hanlon and Lawson.

The concept of the shell model has been used by Cochran[37] to modify the Szigeti relations and to calculate the lattice vibrations of various cubic crystals; we shall consider the latter application in the next section. Cochran obtains, for the effective charge parameter s, the relation

$$s = 1 + d_+ - d_- , \tag{II-32}$$

where d_+ and d_- are measures of the distortion polarizabilities (following Szigeti's explanation of s) of the positive and negative ions, respectively. He also proposes a modification of Szigeti II (II-26):

$$\frac{1}{K^*} = \frac{M\omega_o^2}{6r_o}\left(\frac{\epsilon_o + 2}{\epsilon_\infty + 2}\right) + \frac{e^2}{6r_o}\left(\frac{d_+^2}{\alpha_+} + \frac{d_-^2}{\alpha_-}\right). \tag{II-33}$$

By comparing the data for various alkali halides he obtained values for d_+ and d_- from (II-32) which were then substituted in (II-33). The values of K^* so obtained were stated to be a few percent larger than the measured values of the compressibility.

In a later paper (III) Szigeti[38] performed a quantum mechanical calculation of $\epsilon_o - \epsilon_\infty$ for a potential including third and fourth order

---

[37] W. Cochran, Phil. Mag. 4, 1082 (1959).

[38] B. Szigeti, Proc. Roy. Soc. (London) A252, 217 (1959).

terms as well as the harmonic one, and for a dipole moment expression containing second and third order terms as well as the linear one. In his result he identified the leading term, resulting from the harmonic potential and the linear dipole moment, with his earlier result (Szigeti I, (II-25)), while the remaining, higher order terms were called "anharmonic effects". In his next paper (Szigeti IV)[39] he calculated the infrared absorption, for the same potential and dipole moment expressions, and then applied the Kramers-Kronig relation (II-19) to demonstrate agreement with the result obtained in the previous paper (Szigeti III). We shall return to this calculation of the infrared absorption in the next section. Finally, in a fifth paper, Szigeti[40] computed, from the temperature dependence, the size of the anharmonic contribution to $(\epsilon_o - \epsilon_\infty)$ for KCl and NaCl (whose Debye temperatures are 230°K and 275°K, respectively) and for LiF (whose Debye temperature is 650°K). He concluded that the anharmonic effect represented only 3 to 7 percent of $(\epsilon_o - \epsilon_\infty)$ and that, consequently, the failure of (II-25) to yield $s = 1$ could not be charged to anharmonicity.

---

[39]B. Szigeti, Proc. Roy. Soc. (London) A258, 377 (1960).

[40]B. Szigeti, Proc. Roy. Soc. (London) A261, 274 (1961).

A recent study of the temperature dependence of the static dielectric constant of cubic diatomic crystals was reported by Fuchs.[41] By differentiation of Szigeti I, (II-25), he separated the temperature dependence into two parts. One part, which he called the "volume dependence", was determined by the thermal expansion, while the other part, the "pure temperature effect", included the changes due to temperature with volume held constant. Fuchs evaluated his differentiation in terms of the published room temperature data for LiF, NaCl, KCl, and MgO. He concluded that some temperature dependence of the effective charge parameter s was necessary to produce agreement with experiment. This work of Fuchs may be criticized for his failure to utilize the measured temperature variations of the eigenfrequency, ω_o; instead he chose to calculate the temperature dependence of ω_o from the repulsive potential of Born.[42]

In summary, then, the recent increase in interest in the theory of the static dielectric constant of cubic diatomic crystals has resulted in a number of formulas which we shall test in Chapter VI, below.

---

[41] R. Fuchs, Temperature Dependence of the Dielectric Constant of Ionic Crystals, Technical Report 167, Lab. for Insulation Research; MIT, Cambridge (1961);(ASTIA AD 267 278, TAB 62-1-4).

[42] Born and Huang, op. cit., p. 25.

D. The infrared absorption and lattice dynamics

From the time of the earliest measurements of Czerny and Barnes on NaCl,[43] it was known that the infrared absorption of cubic diatomic crystals exhibited secondary maxima, at frequencies other than the eigenfrequency, which are not predicted by classical theory (II-15a). The problem of modifying classical theory, or of obtaining a quantum mechanical theory, to predict correctly these subsidiary maxima was attacked by a number of authors in the period before World War II.[44] Born and Huang,[45] in their treatise mentioned above, offered an exhaustive quantum mechanical treatment, starting with the inclusion of higher order (anharmonic) terms in the potential function, and non-linear terms in the dipole moment.

These calculations predicted secondary structure at frequencies corresponding to sums and differences of the eigenfrequency with other vibration frequencies of the crystal lattice. Unfortunately, these predictions did not agree with the experimental results. Born and Huang[46] concluded that the broadening of the central

---

[43] R. Barnes, M. Czerny, Z. Physik 72, 447 (1931).

[44] A. Bilz, L. Genzel, H. Happ, Z. Physik 160, 535 (1960), notes 5-10.

[45] Born and Huang, op. cit., Chap. 7.

[46] Ibid., p. 364.

(eigenfrequency) absorption was primarily due to the anharmonic potential while the secondary structure was primarily due to the non-linear dipole moment. They chose to incorporate their results into the classical dispersion relations (II-14), (II-15) by making the damping constant frequency dependent. They also stated explicitly[47] the temperature dependence mentioned at the end of Section B above: that the real part of the dielectric constant was independent of temperature while the damping constant was not.

At this point it would seem appropriate to digress and review a few pertinent details,[48] as well as mention some recent experimental results,[49] about the dynamics of crystal lattices. The description of the vibrations of a three-dimensional crystal with a simple structure, such as that of the alkali halides, is extremely complex. For

---

[47] Ibid.,p. 360.

[48] For a more complete discussion see, e.g., C. Kittel, Introduction to Solid State Physics (John Wiley and Sons, Inc., New York, 1956); F. Seitz, Modern Theory of Solids (McGraw-Hill Book Co., Inc., New York, 1940); L. Brillouin, Wave Propagation in Periodic Structures (Dover Publications, Inc., New York, 1953); J. Ziman, Electrons and Phonons (Clarendon Press, Oxford, 1960); R. Smith, Wave Mechanics of Crystalline Solids (John Wiley and Sons, Inc., New York, 1961).

[49] A recent review of the subject of lattice vibrations is J. Krumhansl, J. Appl. Phys. 33, 307 (1962).

simplicity, let us first consider the linear chain (Figure 1),[50] consisting of masses (or atoms) m_1 and m_2, separated by a distance a, and connected together with springs of force constant β. The solution of the problem of finding the modes of vibration of this chain is straightforward, and some pertinent results are shown in Figure 1. Conventionally, the vibrations are given by a dispersion curve, where the phonon frequencies u are given in terms of the wave vector $\vec{q}$, $|\vec{q}| = \frac{2\pi}{\lambda}$ ($\vec{q}$ is a vector quantity because it describes the direction of propagation of the vibration; in the case of the linear chain this can be one of two directions). One of the features of the vibration of such a periodic structure[51] is that, for the description of the vibration to be single-valued, the wavelength of the vibration cannot be smaller than twice the smallest measure of the periodicity of the structure (alternately, vibrations with wavelengths smaller than this can always be described in terms of combinations of these with longer wavelengths). Thus the wave vector $\vec{q}$ is restricted in magnitude to $0 < |\vec{q}| \leq \frac{2\pi}{\lambda_{max}}$, and the vibrations of the crystal (phonon spectrum) can be completely described in terms of the wave vectors within this one Brillouin zone, whose boundary is described by $\bar{q} = \bar{q}_{max}$. In the graph in Figure 1, $|\vec{q}| = \frac{\pi}{2a}$ is the

---

[50] Following Kittel, op. cit., p. 111.

[51] Brillouin, op. cit.

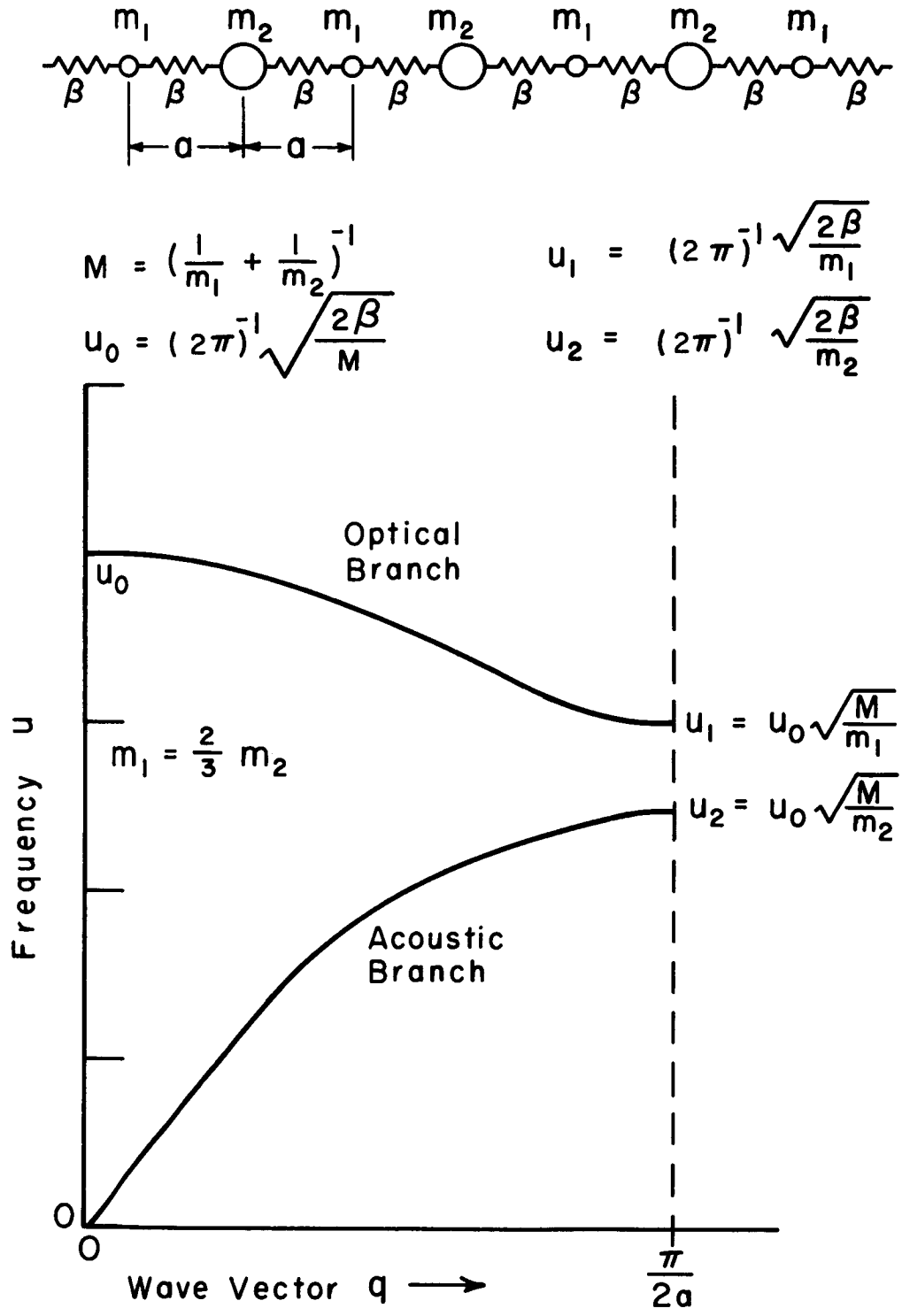

Fig. 1. Dispersion curve for the vibrations of a linear diatomic chain.

zone boundary (the zone is symmetric about $\vec{q} = 0$). The solution of equations of motion for the one-dimensional diatomic chain yield an acoustic branch and an optical branch. In the acoustic branch the vibration with zero wave vector ($\vec{q} = 0$) corresponds to a translation of the entire crystal, and thus has zero frequency. The optical vibration of zero wave vector, however, is one where consecutive atoms move oppositely, and so it has a non-zero frequency (u_o in Figure 1). If the atoms are oppositely charged (ions), then such a vibration will produce a dipole, which can interact with an electromagnetic wave. Now, the lattice constant a is no larger than a few Angstroms, while the wavelength of an electromagnetic wave, whose frequency is that of the optical branch, lies in the infrared and is of the order of 10^5 a; consequently, for the crystal vibration to remain in phase with the electromagnetic wave, $\lambda \sim 10^5$ a, or $|\vec{q}| \sim 0$: the electromagnetic wave (with $\nu = u_o$) interacts strongly with the transverse optical mode of (approximately) zero wave vector. In the present work this is called the eigenfrequency.[52] To the zeroth

[52] There is an unfortunate tendency in a number of the theoretical papers, consulted for the present work, to confuse the word eigenfrequency (the frequency of maximum absorption) with the words reststrahl frequency (the frequency of the reflectance maximum). There is, however, a significant difference in these frequencies; the reststrahl frequency always lies higher than the eigenfrequency. This point has been discussed in detail by Born and Huang (p. 117ff). Since the measured values of both frequencies are often tabulated separately, a continuation of this confusion could lead to a faulty comparison of theory with experiment.

order, then, the infrared spectroscopist is only interested in the eigenfrequency (u_o in Figure 1). We shall see below, however, that this interest must be expanded. Particularly, the frequencies at the zone boundary (u_1 and u_2 in Figure 1) will be of interest; in the case of the linear chain these are readily calculable from a knowledge of only the masses of the ions and the eigenfrequency (Figure 1).

In the three dimensional case the picture becomes much more complicated. In general, each one-dimensional branch breaks up into three: two transverse modes and one longitudinal mode each for both the optical and the acoustic branches. In addition, the dispersion curves are now different for different directions. For more complex crystals (e.g., $CaWO_4$) there will be several triplets of optical branches as well as the triplet of acoustic branches. Until recently there has been no means for measuring the dispersion curves of real lattices, and the primary use of theoretical calculations has been for the determination of specific heats, in which the dispersion curves are averaged. The literature contains relatively few theoretical calculations of real crystal dispersion curves[53] because such work is extremely difficult. All these calculations

---

[53] NaCl: E. Kellermann, Phil. Trans. Roy. Soc. London 238, 513 (1940). KCl: M. Iona, Phys. Rev. 60, 822 (1941). Diamond: H. Smith, Phil. Trans. Roy. Soc. London 241, 105 (1948).

were based on the point ion model, however, different interionic force systems have been tried.

In recent years, the above-described picture has changed. The advent of high resolution slow neutron spectroscopy now permits the phonon spectrum (the dispersion curve) to be directly measured.[54] The quantity of such work as yet is small, but one rather complete set of measurements on a cubic diatomic crystal is available: that of Woods, Cochran and Brockhouse[55] (henceforth WCB) on sodium iodide (NaI) at 110°K. They obtained values for a number of points in each branch for three symmetry directions (where the transverse modes are degenerate). They also made a theoretical calculation of the phonon spectra, on the point ion model, and found that it failed to match the experimental results in a number of respects, both qualitative and quantitative. Cochran[55] also made a calculation of the dispersion curves, using the shell model discussed in the previous section, and obtained good agreement with experiment. Subsequently, Cochran[56] also used the shell model to calculate

---

[54] B.N. Brockhouse, A.T. Stewart, Revs. Mod. Phys. 30, 236 (1958).

[55] A. Woods, W. Cochran, B. Brockhouse, Phys. Rev. 119, 980 (1960).

[56] W. Cochran, Proc. Roy. Soc. (London) A253, 260 (1959).

the phonon spectra of germanium; again he achieved good agreement with the results of neutron scattering experiments.

A modification of the point ion model which seems to be similar to that of the shell model has been proposed by Tolpygo.[57] He and his co-workers have used this model to calculate the dispersion curves for NaCl, KCl, and KBr.[58] They obtained curves similar to those of Cochran,[55] with the same variations from the point ion model predictions which WCB found were necessary to match the experimental results for NaI.

The results of the work on NaI are shown in Figure 2, for the three symmetry directions indicated by brackets [ ]. The solid curves are a composite of the experimental points and the shell model calculations; the dashed curves are branches which were calculated only. It should be noted that the curves in the [110] direction extend beyond the zone boundary; the boundary lies at a distance (3/4 3/4 0) and is shown by the vertical line at that point. The values of the NaI linear chain frequencies at the zone boundary (u_1 and u_2), computed from the measured u_o, have been added to

---

[57] K. Tolpygo, Izvestiya AN USSR, Ser. Fiz. 21, No. 1 (1957); (Trans. Bulletin 21, 44 (1957)).

[58] The original papers are in journals not available to the present author (e.g., note 31, above).

Figure 2. They are seen to lie somewhat too low to be considered representative of the transverse optical mode and the acoustic modes, respectively. One phenomenon of considerable interest for the present work is exhibited in the [110] direction dispersion curve. This is the crossing of the longitudinal (LA) and the transverse (TA) acoustic branches, at approximately the zone boundary. WCB state that there is a degeneracy between the transverse and longitudinal modes at the (100) and (110) positions, as shown by the dotted lines in Figure 2. The present author can see no reason why this should be a phenomenon unique to NaI; it would appear to be a result of the geometry of the Brillouin zone,[59] and consequently a property of (at least) all crystals with the sodium chloride structure. We shall return to this point presently. We shall have occasion to refer to Figure 2 in the discussion below.

We can now return to the question of the infrared absorption in cubic diatomic crystals in regions separated from the eigenfrequency. The processes described in recent papers[60] on the theory of the infrared absorption are no longer restricted to combinations of lattice vibrations including the eigenfrequency, but now accept any

---

[59]See R. Smith, op. cit., Fig. 6.8, p. 223.

[60]Notes 39, 44, above, and 61, 62, 63, below.

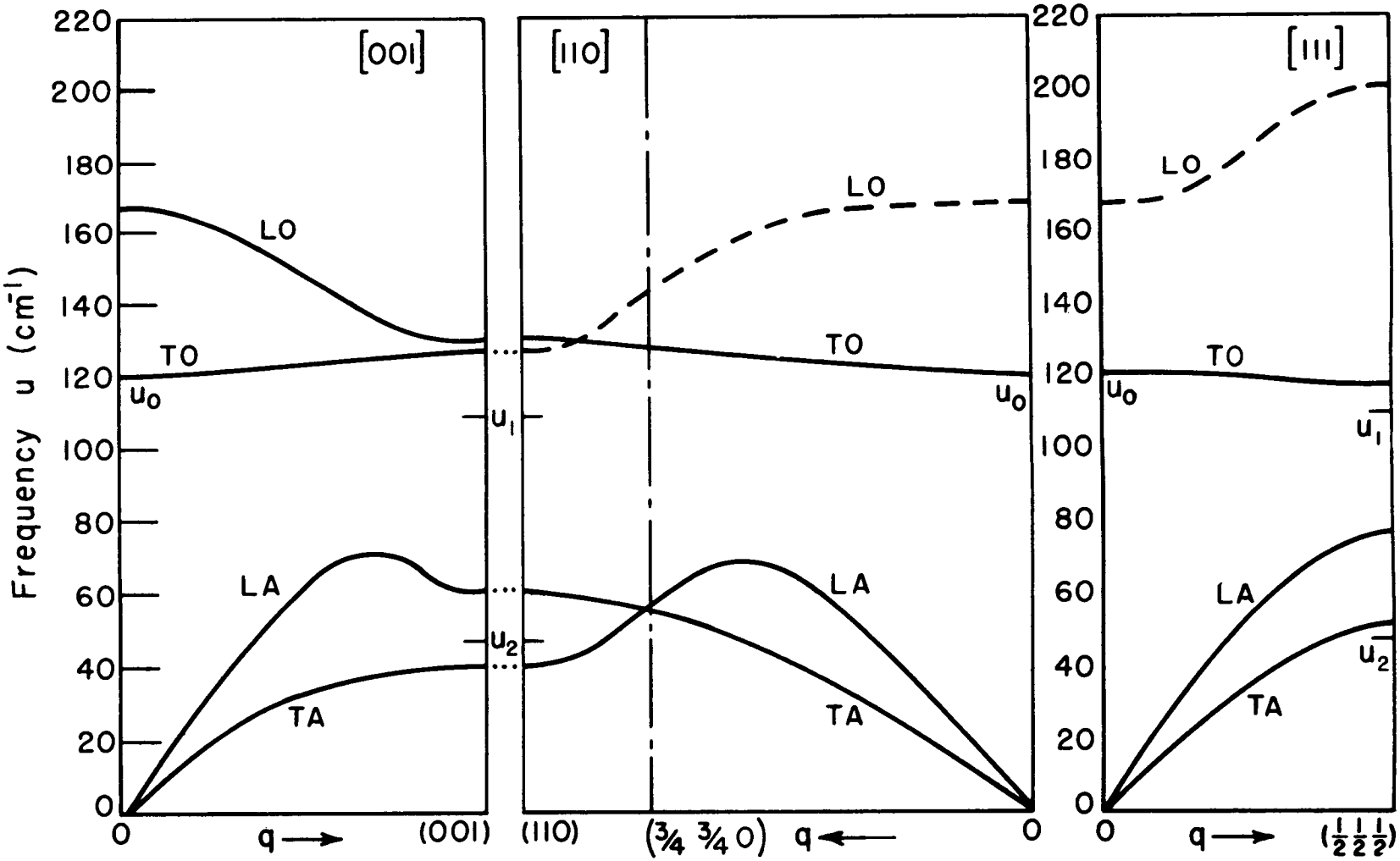

Fig. 2. Measured dispersion curves for NaI at 110°K for 3 symmetry directions (from Woods, Cochran, and Brockhouse).

combination which satisfies certain selection rules. The simplest such combination is that involving two lattice vibrations (phonons) u_a, u_b and the infrared photon ν. The selection rules[60] are, essentially, a conservation of energy and a conservation of "crystal momentum" or wave vector $\vec{q}$ (for the infrared photon $|\vec{q}| \cong 0$, as mentioned above). There are two possible combinations, a sum band in which two photons are created:

$$\nu = u_x + u_y, \quad \vec{q}_x = -\vec{q}_y;$$

and a difference band in which one phonon is destroyed while a second is created:

$$\nu = u_i - u_j, \quad \vec{q}_i = \vec{q}_j \ .$$

There is, for crystals whose unit cells contain centers of symmetry (such as the sodium chloride and diamond structures), an additional selection rule which restricts these transitions to those between different branches.[39] The temperature dependence of the bands is determined by quantities specifying the thermal average $\eta(u)$ of the quantum numbers of the state of frequency u,

$$\eta(u) = (e^{\frac{hu}{kT}} - 1)^{-1}. \tag{II-34}$$

Here T is the absolute temperature, h is Planck's constant, and k is the Boltzmann constant. The infrared absorption written in terms of the imaginary part of the dielectric constant ϵ'', has the form,

$$(II\text{-}35) \qquad \epsilon''(\nu) = \sum_{\substack{\nu = u_x + u_y \\ \vec{q}_x = -\vec{q}_y}} C^{+}_{xy} \frac{N(u_x)N(u_y)}{u_x u_y} [1+\eta(u_x) + \eta(u_y)] ,$$

for a sum band. If the absorption is written in terms of the extinction coefficient κ, or a frequency-dependent damping constant, the form of the expression remains the same. For a difference band the expression is

$$(II\text{-}36) \qquad \epsilon''(\nu) = \sum_{\substack{\nu = u_i - u_j \\ \vec{q}_i = \vec{q}_j}} C^{-}_{ij} \frac{N(u_i)N(u_j)}{u_i u_j} [\eta(u_j) - \eta(u_i)].$$

In these expressions the quantity N(u) is the density of phonon states of frequency u. Clearly, the absorption is expected to exhibit maxima of photon frequencies ν where both phonons u have large values of N(u). The quantities C^{+}_{xy} and C^{-}_{ij} contain appropriate constants and, more importantly, the matrix elements of the quantities by which the electromagnetic wave interacts with the crystal and the two phonons. It is only in this last point that the recent papers on this topic disagree. It should be noted that (II-35) and (II-36) should also serve to describe the infrared absorption in elemental dielectrics (diamond) and semiconductors (germanium and silicon) where the transverse optical mode of zero wave vector has no dipole moment and thus there is no single phonon absorption.

The first suggestion for this kind of two-phonon absorption process was given by Lax and Burstein;[61] their calculation used the higher order terms in the dipole moment to couple the radiation into the active phonon branches. Anharmonic terms in the potential function were utilized by Kleinman[62] and by Genzel and Bilz;[44, 63] we shall return briefly to the latter authors' work below. Szigeti (IV)[39] calculated the imaginary part of the dielectric constant, ϵ'', for a crystal with both third and fourth order potential terms and second and third order dipole moment terms. He found that both the second order dipole moment and the third order potential contribute to the subsidiary maxima we are here considering. He also found, in agreement with Born and Huang (as mentioned above), that all the higher order terms also contribute to the broadening of the central (eigenfrequency) absorption.

With the aid of Figure 2, let us now consider a few factors effecting the infrared absorption. First, the $\vec{q}$ conservation selection rule requires that the transitions take place parallel to the ordinate axis in the dispersion curves. Second, from an elementary

---

[61] M. Lax, E. Burstein, Phys. Rev. 97, 39 (1955).

[62] D. Kleinman, Phys. Rev. 118, 118 (1960).

[63] H. Bilz, L. Genzel, Z. Physik 169, 53 (1962).

standpoint, the density of states will be greatest near the edge of the Brillouin zone, particularly for those directions where the dispersion curve has zero slope at the zone boundary. We may justify this statement by the following argument: the density of modes in $\vec{q}$ space is assumed to be uniform, then the density of modes in $|\vec{q}|$ space would be proportional to $|\vec{q}|^2$. Finally, we take the density of states N(u) in $|\vec{q}|$ space proportional to the density of modes and to $\frac{d|\vec{q}|}{du}$ (the inverse of the slope of the dispersion curve). The question of the singularities and critical points in distributions such as the dispersion curves is one which has received considerable mathematically sophisticated attention recently.[64] However, we shall confine ourselves to the above elementary result, which indicates that, because of the nature of the variation of the density of states, the dominant phonon frequencies for the infrared absorption will be those at the edge of the zone.

At temperatures above the Debye temperature $\eta(u) + 1/2 \cong \frac{kT}{hu}$, so for a sum band

$$1 + \eta(u_x) + \eta(u_y) = \frac{kT}{h} \quad \frac{\nu}{u_x u_y} \quad ,$$

---

[64] See, e.g., L. Van Hove, Phys. Rev. 89, 1189 (1953); J. Phillips, Phys. Rev. 104, 1263 (1956), 113, 147 (1959).

and for a difference band

$$\eta(u_j) - \eta(u_i) = \frac{kT}{h} \frac{\nu}{u_i u_j} .$$

Above the Debye temperature, then, the infrared absorption due to the subsidiary maxima is proportional to the temperature. Note that, in general (c.f. Figure 2) the sum bands occur at frequencies above the eigenfrequency while the difference bands will fall below it. At low temperatures the situation is rather different:

$$\eta(u) \cong e^{-\frac{hu}{kT}} .$$

For the sum band the temperature dependence is weak:

$$1 + \eta(u_x) + \eta(u_y) = 1 + e^{-\frac{hu_x}{kT}} + e^{-\frac{hu_y}{kT}} \to 1,$$

$$T \to 0,$$

while for the difference band the temperature dependence is strong:

$$\eta(u_j) - \eta(u_i) = e^{-\frac{hu_j}{kT}} - e^{-\frac{hu_i}{kT}} \to 0$$

$$T \to 0 .$$

This effect has been vividly illustrated by Hadni[65] with measurements of the transmission of a thin plate of CsI at 300°K and at 4.2°K. At the high temperature there is complete absorption from frequencies

---

[65] A. Hadni, J. Claudel, E. Décamps, X. Gerbaux, P. Strimer, Compt. rend. 255, 1595 (1962).

somewhat larger than the eigenfrequency to tnose much smaller than it. At the low temperatures, however, the absorption for frequencies above the eigenfrequency shows some slight change, while for frequencies smaller than the eigenfrequency the absorption completely disappears.

In general the sum bands will be relatively narrow. Following Figure 2 for NaI, the frequencies of the bands would be

TA + LA: $101 < \nu < 128\ cm^{-1}$,

TA + TO: $168 < \nu < 184\ cm^{-1}$,

LA + TO: $182 < \nu < 194\ cm^{-1}$,

with other weaker bands at higher frequencies. Due to the crossing of the acoustic branches, however, the difference bands will be relatively broad. Again following Figure 2, the frequencies of the bands would be

LA - TA: $0 < \nu < 27\ cm^{-1}$

TO - LA: $40 < \nu < 77\ cm^{-1}$

TO - TA: $77 < \nu < 86\ cm^{-1}$

LO - TO: $3 < \nu < 83\ cm^{-1}$

with other possible combinations being weaker because of the temperature dependence. If the acoustic branches did not cross or at least approach one another closely, this description of the infrared absorption would not simply explain the amount of observed continuous

absorption in the far infrared. If the optical branches approach one another and do not lie too high, then their differences can contribute to the far infrared absorption. Figure 2 shows that the optical branches do closely approach one another in the [100] direction.[66] Of course, the optical branch difference bands will show a considerably greater temperature dependence than will those between the acoustic branches.

The above description of the infrared absorption away from the eigenfrequency has been well-supported by experiment, for the sum bands. Much of this work has been done on the elemental semiconductors, silicon and germanium. The eigenfrequency of these materials exhibit no first order dipole moment, and consequently have no strong infrared absorption to mask the weaker sum and difference bands. Little difference band data has been reported; this is not surprising since spectroscopy is much simpler in the region of the sum bands compared with that of the difference bands (which fall in the far infrared). A direct correspondence between the phonon structure, as determined from the neutron experiments, and the infrared absorption, for several sum bands and one difference band, has been reported by Brockhouse and Iyengar[67] for germanium. The

---

[66] See also the theoretical curves given by Tolpygo, loc. cit.

[67] B. Brockhouse, P. Iyengar, Phys. Rev. 111, 747 (1958).

subsidiary maxima for frequencies above the eigenfrequency in gallium phosphide have been related to a proposed set of phonons by Kleinman and Spitzer[68] on the basis of the temperature dependence of the absorptions. Johnson, et al., have studied the infrared absorption in germanium,[69] silicon,[70] indium antimonide,[71] and gallium arsenide[72] at several temperatures between 20°K and 300°K, and have assigned the observed maxima to sum bands on the basis of the observed temperature dependence. They included three phonon processes, which are also permitted by the above theories, albeit with a smaller probability than the two phonon processes. They have reported reasonable agreement in gallium arsenide between their phonon assignments and the results of a shell model phonon spectrum calculation by Cochran.[72] Genzel and Bilz[44] have tentatively assigned the subsidiary maxima observed on the low frequency side of the

---

[68] D. Kleinman, W. Spitzer, Phys. Rev. 118, 110 (1960).

[69] F. Johnson, et. al., note 3, W. Cochran, et al., footnote 72, below.

[70] F. Johnson, Proc. Phys. Soc. (London) 73, 265 (1959).

[71] S. Fray, F. Johnson, R. Jones, Proc. Phys. Soc. (London) 76, 939 (1960).

[72] W. Cochran, S. Fray, F. Johnson, J. Quarrington, W. Williams, J. Appl. Phys. 32, 2102 (1961).

eigenfrequency in sodium chloride and lithium flouride to difference bands, on the basis of the theoretical lattice vibration calculations of Karo.[73]

To summarize this two-phonon theory of the infrared absorption for frequencies below the eigenfrequency, then, we expect to be able to correlate the observed structure of the absorption with the phonon dispersion curve, and we expect the ratio of the measured values of ϵ'' for different temperatures to be given, from (II-36), by

$$\text{(II-37)} \qquad \frac{\epsilon''(\nu, T_1)}{\epsilon''(\nu, T_2)} = \sum_{\substack{\nu = u_i - u_j \\ \vec{q}_i = \vec{q}_j}} \frac{[\eta(u_j, T_1) - \eta(u_i, T_1)]}{[\eta(u_j, T_2) - \eta(u_i, T_2)]} \quad ,$$

where the summation has as many terms as there are pairs of lattice modes which satisfy the selection rules. If the phonon structure is known, and if only one pair of modes satisfies the selection rules, then the interpretation becomes especially easy.

Of the above-mentioned theories, only that of Genzel and Bilz[44,63] includes a complete description of the complex dielectric constant $\hat{\epsilon}$. They write, for the diatomic cubic crystal,

---

[73] A. Karo, J. Chem. Phys. 31, 1489 (1958).

$$\text{(II-38)} \qquad \hat{\epsilon}(\nu) = \epsilon_\infty + \frac{(\epsilon_o - \epsilon_\infty)}{2}\left[\frac{1}{1+\Omega - i\delta} + \frac{1}{1-\Omega - i\delta}\right],$$

$$\Omega = \frac{\nu}{\nu_o},$$

where δ is now the frequency dependent damping constant. Upon separation into real and imaginary parts, (II-36) yields, analogously with the classical expression (II-14a) and (II-15a)

$$\text{(II-39)} \qquad \epsilon'(\nu) = \epsilon_\infty + \frac{(\epsilon_o - \epsilon_\infty)}{2}\left[\frac{1+\Omega}{(1+\Omega)^2 + \delta^2} + \frac{1-\Omega}{(1-\Omega)^2 + \delta^2}\right],$$

$$\text{(II-40)} \qquad \epsilon''(\nu) = \frac{(\epsilon_o - \epsilon_\infty)}{2}\left[\frac{(-\delta)}{(1+\Omega)^2 + \delta^2} + \frac{(-\delta)}{(1-\Omega)^2 + \delta^2}\right].$$

For regions where δ^2 is small compared to $(1+\Omega)^2$ and $(1-\Omega)^2$ e.g., well away from the eigenfrequency, we have

$$\text{(II-39')} \qquad \epsilon'(\nu) = \epsilon_\infty + (\epsilon_o - \epsilon_\infty)(1 - \Omega^2)^{-1},$$

$$\text{(II-40')} \qquad \epsilon''(\nu) = (-\delta)(\epsilon_o - \epsilon_\infty)\frac{1+\Omega^2}{(1-\Omega^2)^2} \cong (-\delta)(\epsilon_o - \epsilon_\infty)$$

$$\Omega^2 \ll 1.$$

Comparison of these expressions with the analogous classical ones (II-14a') and (II-15') discloses (a) the equation for $\epsilon'(\nu)$, remains unchanged, it is still linear with the quantity $(1 - \Omega^2)^{-1}$, while (b) the frequency dependence of ϵ'' is primarily now that of δ. The frequency dependent damping constant can be found, following (II-37') and (II-38'),

from

$$\text{(II-41)} \qquad \delta = \frac{(-\epsilon'')}{\epsilon' - \epsilon_\infty} \quad \frac{1 - \Omega^2}{1 + \Omega^2} \ , \ \delta << \left| 1 - \Omega^2 \right| .$$

Genzel and Bilz[44] provide expressions whereby δ may be directly calculated, if the phonon dispersion curves and densities of states are known for temperature T such that

$$\text{(II-42)} \qquad 0 < T \leq \frac{\Theta_D}{4} \ ,$$

where Θ_D is the Debye temperature. The form of the expressions for δ is, essentially, that of (II-36) and (II-37), above.

CHAPTER III
EXPERIMENTAL TECHNIQUES

In this chapter we shall describe the instrumentation and techniques used in making the room temperature and low temperature measurements, the preparation of the crystal samples, and the details of the computation of the optical constants.

A. Far infrared instrumentation

The far infrared vacuum grating spectrometer used for the present measurements was constructed at The Ohio State University by the present author and Dr. M.E. Vance, under the supervision of Profs. E.E. Bell and R.A. Oetjen.[1] A detailed description of this spectrometer and its performance will be given elsewhere.[2] In this

---

[1] R.F. Rowntree, M.E. Vance, E.E. Bell, R.A. Oetjen, Symposium on Molecular Structure and Spectroscopy, Columbus, Ohio, 1962; M.E. Vance, R.F. Rowntree, E.E. Bell, R.A. Oetjen, Preprint C-103, International Symposium on Molecular Structure and Spectroscopy, Tokyo, 1962. The construction of this spectrometer was partially supported by a grant from the National Science Foundation and a contract between The Ohio State University Research Foundation and the U.S. Air Force Cambridge Research Laboratories.

[2] R.F. Rowntree, M.E. Vance, E.E. Bell, R.A. Oetjen, in preparation, to be submitted to Applied Optics.

instrument the radiation from a high-pressure mercury arc lamp is dispersed by an echelette grating, the various orders of which are selectively chopped by an Interferometric Modulator[3] and detected by a Golay Cell. The resulting electrical signal is amplified, filtered, synchronously rectified, and displayed on a strip chart recorder. This spectrometer provides a combination of high resolution, high spectral purity, and ease of operation superior to any other reported instrument in the 100μ-1000μ (100 cm^{-1} - 10 cm^{-1}) region.

The factor of high spectral purity is extremely important for the present work, and its attainment is one of the major difficulties in far infrared spectroscopy. If the spectrometer chart record contains a significant contribution from spurious higher frequency radiation, the results obtained will be strongly effected, because the optical constants at higher frequencies differ greatly from those in the far infrared.

The spectral region of the present work (100 cm^{-1} - 10 cm^{-1}) was covered using four echelette dispersion gratings, with groove spacings of 180, 90, 45, and 20 lines/inch, blazed at 100, 50, 25, and 11.5 cm^{-1}, and used in the spectral regions 100 - 65 cm^{-1}, 75 - 33 cm^{-1}, 37 - 19 cm^{-1}, and 21 - 10 cm^{-1}, respectively. Thus the data taken

---

[3] M.E. Vance, Ph.D. Dissertation, The Ohio State University, 1962.

with any one grating overlapped that taken with another. The frequency corresponding to a given setting of the spectrometer was obtained from the relation $\nu = \tau \csc \theta$, where θ was the angle of rotation of the grating from the central image or mirror position; the grating constant, τ, for each grating was obtained from measurements of the observed angles θ for known absorption lines of atmospheric H_2O vapor[4] (for all gratings) and N_2O[5] (for the 20 lines/inch grating). In order to eliminate the effects due to the atmospheric H_2O absorptions, all the present crystal measurements were made with the instrument evacuated to a pressure of less than 0.1 mm of Hg.

For the measurements requiring polarized radiation (on $CaWO_4$), wire grating polarizers were used. The "wires" were actually fine lines of gold deposited on a sheet of Mylar.[6] The wires had a width of 0.01 mm and their centers were separated by 0.025 mm. At frequencies lower than 50 cm^{-1} the polarizers transmitted better than 80 percent of the incident radiation whose electric vector was perpendicular to the wires. At 100 cm^{-1} the transmission had dropped to

---

[4] W.S. Benedict, private communication.

[5] E. Palik, K. Rao, J. Chem. Phys. 25, 1174 (1956).

[6] These polarizers were purchased from Buckbee Mears Company, St. Paul, Minnesota.

40 percent; most of this decrease in transmission is believed to be caused by absorption in the Mylar. The transmission of radiation with its electric vector parallel to the wires was less than 2 percent for frequencies smaller than 150 cm^{-1}, thus the wire grating provided better than 95 percent polarization. A detailed report of the performance of these polarizers will be given elsewhere.[7]

B. Room temperature measurements

In general, the room temperature measurements were made before the low temperature ones and the refractive index measurements before the power transmission coefficient measurements. The room temperature refractive index measurements were made with the tnin crystal sample mounted in the cryostat and were otherwise identical with the measurements at low temperatures, described in the next section, except that there was no coolant in the cryostat.

For the room temperature transmission measurements of a given sample, the slab of crystal was glued to one of two aluminum plates, in each of which was cut an aperture slightly smaller than the size of the crystal. The aluminum plates were attached to a motor-driven carriage placed at a focus (henceforth called "the sample position") of the radiation beam in the spectrometer. The

---

[7] R.F. Rowntree, H.J. Sloan, in preparation, to be submitted to Applied Optics.

carriage was provided with limit switches so that the apertures of the two aluminum plates could be alternately, and reproducably, placed in the sample position. A solid aluminum plate could also be placed in the sample position. Before the start of each set of measurements, the positions of the two aluminum plates were carefully adjusted, so that the resulting chart pen deflection was the same for either aperture in the sample position. The crystal slab was then glued over one of the apertures.

The transmission measurements were made by setting the spectrometer for a predetermined frequency, placing the open aperture in the sample position, and adjusting the spectrometer slits so that the spectral slit width of the instrument was sufficiently wide that the channeled spectrum would not be resolved (the condition $\Delta\nu_I > 1/2n\ell$, mentioned in Chapter II, Section A, above). The amplifier gain was then adjusted to give a full scale deflection, t_h, on the chart record. The aperture covered by the crystal sample was then moved into the sample position and the resulting pen deflection, t_s, recorded. Finally, the solid aluminum plate was moved into the sample position and the resulting zero (no radiation) pen deflection, t_o, recorded. This point-by-point procedure was then repeated for a number of selected frequencies in a given dispersion grating spectral region. It was found that the detector-amplifier-recorder system was

sufficiently stable that the zero did not have to be recorded at every frequency. When a given group of measurements had been completed, each portion (t_h, t_s, t_o, for each frequency) of the record was averaged by eye, and the room temperature (300°K) power transmission coefficient $\mathcal{T}_{300}$ computed from

$$\mathcal{T}_{300} = \frac{t_s - t_o}{t_h - t_o} \quad .$$

Typically, a set of three measurements at one frequency required about fifteen minutes.

C. Reflection measurements

When the present work was begun we had not yet learned of the concurrent mid-infrared reflection measurements of Barker. Consequently, we carried out some reflection measurements on $CaWO_4$ to attempt to roughly identify its lowest frequency absorptions, which were expected to have the largest effect on the far infrared optical constants. Because the spectrometer had been designed to accept a wide range of experiments, the changes in the instrumentation required for the reflection measurements were few. The sample carriage was shifted so that the radiation beam was incident at an angle of 12° (rather than the 0° used for the transmission measurements), and a front surface aluminum mirror was glued in back of the open aperture in the sample carriage. An additional mask was placed in

front of the monochromator entrance slit to block out radiation reflected from the aluminum plate rather than the sample. The scheme of the reflection measurements was then essentially identical with that of the transmission work described above, except that t_h was here the signal due to the radiation specularly reflected from the aluminized mirror and t_s that due to the specular reflection from the sample. The power reflection coefficient R was then computed from

$$R = \frac{t_s - t_o}{t_h - t_o} \quad .$$

In all cases the sample was sufficiently absorbing that no back surface reflection effects could be expected.

Because the performance of the Interferometric Modulator decreased rapidly for frequencies greater than 100 cm^{-1}, the reflection measurements were made using conventional far infrared techniques:[8] disc chopping and reflection filtering by blazed gratings and by the selective reflection from crystals ("reststrahlen"), which occurs at frequencies somewhat higher than the eigenfrequency. The reflection filter combinations used for various frequencies is shown in Table 1.

---

[8] R. Oetjen, W. Haynie, W. Ward, R. Hansler, H. Schauwecker, E. Bell, J. Opt. Soc. Am. 42, 559 (1952); see also Note 3, Chapter I, above.

TABLE 1
REFLECTION FILTERING SCHEDULE

Frequency Region (cm^{-1})	Reflection Filter Position #1	Reflection Filter Position #2
70 - 100	12.5 lines/mm grating	CsBr
100 - 135	12.5 lines/mm grating	KI
130 - 150	KBr	KBr
145 - 170	KCl	KCl
165 - 250	NaCl	NaCl
250 - 400	CaF_2	CaF_2

The region up to 200 cm^{-1} was covered using the 180 lines/inch dispersion grating in first order, and the mercury lamp source and the Golay Cell with a crystal quartz window used for the transmission measurements. For the region above 200 cm^{-1} the 180 lines/inch grating was used in second order, the source was a coated platinum strip,[9] and the detector was a Golay Cell with a diamond window.

D. Low temperature techniques

The low temperature measurements were made using a

[9]P.B. Burnside, Ph.D. Dissertation, The Ohio State University, 1958. The author is indebted to Dr. Burnside for the preparation of the platinum strip used in the present work.

commercial[10] stainless steel double-chamber cryostat designed especially for use in the sample position of the far infrared spectrometer. The cryostat is capable of being used with liquid helium, however the problems associated with maintaining a sample at helium temperatures in the rather large radiation beam of the spectrometer have not yet been solved. Consequently, the present work was restricted to the use of liquid nitrogen as a coolant.

The samples were cemented to brass blocks which were screwed to the bottom of the inner chamber of the cryostat. Both "Pliobond"[11] cement and "GE 7031"[12] adhesive were used as glues, with the former proving to be the more satisfactory for the present, liquid nitrogen temperature (77^{o}K) work.

The radiation beam was admitted to the sample through windows of 0.62 mm polyethylene sealed, with 0-rings, to the outside of the cryostat. In order to reduce the heating of the sample, and the possibility of melting the windows, the higher frequency ($\nu > 150$ cm^{-1}) radiation from the mercury lamp source was attenuated by means of an echelette reflection grating (12.5 lines/mm) and a piece of black

---

[10] Manufactured by The Superior Air Products Co., Newark, New Jersey.

[11] W.J. Ruscoe Co., Akron, Ohio.

[12] The General Electric Co., Schenectady, New York.

polyethylene placed over a mirror in the optical path between the source and the sample.

The temperatures actually reached by the samples were measured by means of a thermistor[13] glued to the side of the sample. The thermistor was calibrated, at dry ice and liquid nitrogen temperatures, on the assumption (following the manufacturer's specifications) that its resistance was given by the expression $R(T) = R_o \exp \frac{B}{T}$. Calibration consisted of measuring the resistance at the two temperatures and computing B. The final expression by which the temperature was found from the thermistor resistance was

$$T = 77 \left[1 - .087 \ln \left(\frac{8 \times 10^4}{R(T)} \right) \right]^{-1} {}^{o}K .$$

Because of the uncertainties due to the questionable thermal contact between the sample and the thermistor, the inexact resistance measurements, and the effect of the leads on the resistance and temperature, the temperature measurements could have been in error by as much as ten percent.

The measured temperature varied between $82^{o}K$ and $105^{o}K$, with a mean value of $92^{o}K$. In view of the uncertainties involved, we

---

[13] Manufactured by the Victory Engineering Co., Union, New Jersey.

have chosen to cite the value of 90°K for the low temperature measurements.

For the refractive index determinations the thin crystal plates were mounted in the cryostat for both the room temperature and low temperature measurements, which were usually run consecutively. About three different settings of the spectrometer were used in recording the channeled spectrum for a given thin sample in one dispersion grating spectral region; typically, about one day (10 - 12 hours) was required to complete the three scans. Each scan involved adjusting the slits so that the maxima and minima were clearly resolved, then setting the amplifier gain and time constant to achieve a reasonable signal-to-noise-ratio, and finally selecting a grating rotation (spectral scanning) rate compatible with the time constant.

Since the sample in the cryostat could not be readily, and reproducably, moved in and out of the sample position, the low temperature power transmission coefficient could not be measured by the method described above for the room temperature work. Consequently, the following alternative method was devised. The thick sample was mounted in the cryostat and the room temperature (300°K) transmitted signal recorded at the same slit settings and frequencies used for the room temperature power transmission coefficient measurements (the gain was usually set somewhat higher); call this chart deflection t_{300}.

When this set of deflections, usually about ten plus about three zero-signal measurements, t_o, had been completed, the liquid nitrogen was then transferred into the cryostat. When the sample reached a steady low temperature, as indicated by the thermistor resistance and the increased recorder deflection (usually after 45 minutes), the pen deflection, t_{90}, at each frequency was recorded at the same slit and gain settings used at room temperature.

The zero signal level, t_o', was also recorded at low temperature for each frequency by moving an opaque shutter into the radiation beam between the source and the sample. This was necessary because of the placement of the sample before the chopper (in this case the Interferometric Modulator) in the optical path, thus permitting the radiation emitted by the sample to be modulated and detected. It was found experimentally, and subsequently varified by calculation, that there was a detectable difference between the power emitted by a "greybody" at 90°K, with an emissivity between 0.2 and 0.4 (corresponding to the measured partial absorption), and the power emitted by a blackbody at 300°K. By placing the shutter before the sample, however, the signal difference between "shutter out" and "shutter in" ($t_{90} - t_{o'}$) was still proportional to the power transmitted at 90°K.

After all the 90°K data was recorded the remaining coolant was blown out of the cryostat with compressed air and, when the sample

had returned to room temperature (requiring about an hour), the signal transmitted at several (all, if time permitted) of the frequencies was again recorded. If the room temperature transmission signal ($t_{300} - t_o$) at the beginning and end of a set of measurements differed by more than 10 percent, the data were discarded and the same procedure repeated on another day. If the 300°K transmission signal had stayed constant within 10 percent, the "before" and "after" values were averaged, and the 90°K power transmission coefficient computed in terms of the 300°K one by

$$\mathcal{T}_{90} = \mathcal{T}_{300} \frac{(t_{90} - t_o)}{(t_{300\,av} - t_o)} \quad .$$

The obvious disadvantage of this method was that it was highly dependent upon the stability of the spectrometer components (source, detector, Interferometric Modulator) over periods of ten hours or more, when from experience one knew that such stability was unlikely. In practice, about one half of the low temperature transmission measurements had to be repeated at least twice to achieve the required 10 percent agreement between the "before" and "after" 300°K data.

E. Sample preparation

The two MgO samples were purchased commercially[14] in the form of rectangular blocks approximately 30 x 14 x 7 mm and 25 x 15 x 14 mm, respectively.

The $CaWO_4$ was also procured commercially;[14] it was delivered in the form of rather irregularly-shaped boules, approximately 30 mm long, having a more or less elliptical cross-section with major and minor axes approximately 12 mm and 10 mm, respectively. The orientation of the crystalline c-axis in the boules was determined by cutting thin slices from each boule and examining the slices under a polarized microscope.[15] In both cases it was found that the c-axis lay perpendicular to the long axis of the boule, parallel to the minor axis of the elliptical cross-section. From one boule plates were cut with their parallel faces perpendicular to the c-axis; these were used without a polarizer to measure the ordinary ray ($E \perp$ c-axis) optical constants. Plates with their faces parallel to the c-axis were cut from the second boule; these were used with a polarizer, to measure both pairs of optical constants.

---

[14] The samples were grown by Semi-Elements, Inc., Saxonburg, Pennsylvania.

[15] The author wishes to thank Mr. James E. Bradley for the orientation of the boules.

The samples were prepared[16] for measurement by cutting on a diamond saw and then lapping until a surface reasonably transparent to visible light was obtained. In general a thin plate was cut for the channeled spectrum measurements and the remaining thick plate used for transmission coefficient measurements at low frequencies. Subsequently, thinner samples were cut, as needed, for the higher frequency measurements.

The thickness of the samples was measured with a micrometer caliper. The caliper was marked for separations of 0.01 mm and it was possible to interpolate visibly and read the caliper to 0.002 - 0.003 mm. Usually about eight different measurements, at different positions on the plate, were made on each crystal sample. The thickness variation seldom exceeded $\pm$ 0.004 mm, which we take as the uncertainty in the thickness measurements.

F. Computational techniques

As Moss[17] has pointed out, care must be taken in the use of the expressions (II-7) for the determination of the refractive index in

---

[16] The cutting and polishing of the samples was performed by Mr. Henry C. Pagean of the Electron Device Lab., Department of Electrical Engineering; the author is indebted to Mr. Pagean for his excellent work.

[17] T. Moss, Optical Properties of Semi-Conductors (Butterworths Scientific Publications, London, 1959) p. 13.

spectral regions where it is changing. The core of this problem involves the choice of the order number b. While in principle b can be eliminated from (II-7) by simple subtraction, in practice this procedure leads to large uncertainties in the value of n because it involves small differences of rather large numbers, i.e., the frequencies. Our solution to this problem is given below; a similar method has been described by Geick,[18] however his approach requires more computational steps.

As was mentioned earlier, the channeled spectrum of a given sample of thickness ℓ, in a given dispersion grating's spectral region, consists of a number of transmission maxima and minima. The grating angles θ corresponding to these extrema were determined from the chart record and the corresponding wavelengths (in the body of this report we have tried scrupulously to use only frequency as the spectral variable, however this computation is simpler in terms of wavelength and was actually so used) calculated from the grating equation $\lambda = 1/\nu = \tau^{-1} \sin\theta$. The maxima were then labeled with successive integers β, with $\beta = 0$ for the maximum of shortest wavelength; and the minima were labeled with successive odd half integers $\beta + 1/2$, with $\beta = 1/2$ for the minimum directly above the $\beta = 0$ maximum. Thus (II-7) becomes, with b_o the order number for λ_o,

---

[18] R. Geick, Z. Physik 161, 116 (1960).

$$b_o\lambda_o = 2n\ell \qquad \text{max.}$$

(III-1)

$$(b_o - 1/2)\lambda_{\frac{1}{2}} = 2n\ell \qquad \text{min.}$$

$$(b_o - 1)\lambda_1 = 2n\ell \qquad \text{max.}$$

$$(b_o - 3/2)\lambda_{\frac{3}{2}} = 2n\ell \qquad \text{min.}$$

$$\vdots$$

$$(b_o - \beta)\lambda_\beta = 2n\ell \qquad \text{max.}$$

$$[b_o - (\beta + 1/2)]\lambda_{\beta+\frac{1}{2}} = 2n\ell \qquad \text{min.}$$

$$\vdots$$

On the assumption that the refractive index does not change appreciably between successive maxima or minima, we may eliminate the right hand sides of (III-1), yielding

$$(b_o-\beta)\lambda_\beta = [b_o - (\beta + 1)]\lambda_{\beta+1} \qquad \text{max.}$$

(III-2)

$$[b_o-(\beta-1/2)]\lambda_{\beta-\frac{1}{2}} = [b_o-(\beta + 1/2)]\lambda_{\beta+\frac{1}{2}} \qquad \text{min.}$$

$$\lambda_{\beta-\frac{1}{2}} < \lambda_\beta < \lambda_{\beta+\frac{1}{2}} < \lambda_{\beta+1} \ .$$

Solving for b_o yields

(III-3)
$$b_o = \frac{(\beta'+1)\lambda_{\beta'+1} - \beta'\lambda_{\beta'}}{\lambda_{\beta'+1} - \lambda_{\beta'}} \qquad \begin{matrix}\beta' = \beta \text{ max} \\ \beta' = \beta - 1/2 \text{ min}\end{matrix}$$

Thus the program consisted of computing the products $\beta' \lambda_{\beta'}$, finding b_o for each pair of successive similar extrema, and finally of averaging all the values so obtained and determining the b_o to be used (since in (II-6) we have required that b be an integer). In spectral regions where $b < 20$ (the 20 lines/inch and 45 lines/inch grating regions, $\nu < 37$ cm^{-1}), this procedure provided an unambiguous determination of b_o:

$$\overline{b_o} = \text{integer} \pm 0.2.$$

In the higher frequency regions, b_o was selected to match the above-determined lower frequency values.

With b_o selected, the optical thickness, $n\ell$, and the refractive index, n, were computed from (III-1) and measured thickness ℓ. The resulting values for n were plotted and a smooth curve drawn through them.

In Chapter II, two expressions for the power transmission coefficient $\mathcal{T}$ were given:

$$\text{(II-8)} \qquad \mathcal{T} = \frac{(1-R)^2 D}{1-R^2 D^2}, \quad D = \exp(-4\pi\kappa\nu\ell),$$

$$\text{(II-9)} \qquad \mathcal{T} = (1-R)^2 D, \quad R^2 D^2 \ll 1 .$$

We will now determine the values of $\mathcal{T}$ for which (II-9) may be used. As may be seen from the results (Chapter IV, below) a typical value, in the present work, is n = 3.0, R = .25. If the condition in (II-9) is chosen to read

$$R^2D^2 \leq 0.01,$$

then

$$D \leq 0.4$$

and so

$$\mathcal{T} < 0.225;$$

for D = 1

$$\mathcal{T} = .60.$$

Thus we see that (II-9) may only be used for a sample transmitting less than 22 percent. To have made all the transmission measurements at $\mathcal{T} < 0.22$ while retaining the desired accuracy (see below) would have required the use of a large number of samples with small differences in thickness, and a consequent increased risk of breakage during cutting and grinding. In addition, because of the large increase in transmission of cooling to 90°K, the values of $\mathcal{T}_{90}$, obtained by the method described in an earlier section, were seldom less than 0.3. Consequently, (II-8) had to be used in much of the present work.

A convenient form of the solution of (II-8) for D, remembering that, from (II-10), it is D^{-1} that is used to compute κ, is

$$(III\text{-}5) \qquad D^{-1} = \frac{\left[\frac{2R^2\mathcal{J}}{(1-R)^2}\right]}{-1+\sqrt{1+\left\{\left[\frac{2R^2\mathcal{J}}{(1-R)^2}\right]^2 \frac{1}{R^2}\right\}}} \quad .$$

With (III-5), and judicious use of a six place numerical table,[19] D^{-1} could be computed by five desk calculator operations. The extinction coefficient was then computed from

$$(II\text{-}10) \qquad \kappa = (4\pi \ell \nu)^{-1} \ln D^{-1} \quad .$$

It was found that the use of values of $\mathcal{J}$ larger than about 0.45 yielded unsatisfactory results. The reason for this is shown by the following argument: take the logarithmic derivatives of (II-8) and (II-10)

$$\frac{d\mathcal{J}}{\mathcal{J}} = \frac{dD}{D}\left(1 - \frac{2R^2D^2}{1-R^2D^2}\right) \quad ,$$

$$\frac{dD}{D} = \frac{d\kappa}{\kappa} \ln D,$$

then

$$(II\text{-}11) \qquad \frac{d\kappa}{\kappa} = \ln^{-1} D \left(\frac{1-R^2D^2}{1-3R^2D^2}\right) \frac{d}{\mathcal{J}} \quad .$$

---

[19] L. Zimmerman, Vollständige Tafeln der Quadrate aller Zahlen bis 100009 (Edwards Brothers, Inc., Ann Arbor, 1946).

If $\Delta\mathcal{T}$ is the uncertainty in the full-scale deflection, then

$$10^2 \left| \frac{\Delta\kappa}{\kappa} \right| ,$$

the percent uncertainty in the extinction coefficient, may be found from (II-11) in terms of the percent uncertainty in the transmission,

$$10^2 \left| \frac{\Delta\mathcal{T}}{\mathcal{T}} \right| .$$

Figure 3 is a plot of $\frac{\Delta\kappa}{\kappa}$ and $\frac{\Delta\mathcal{T}}{\mathcal{T}}$ versus $\mathcal{T}$, for $\Delta\mathcal{T} = 0.02$, a typical value for the present work.

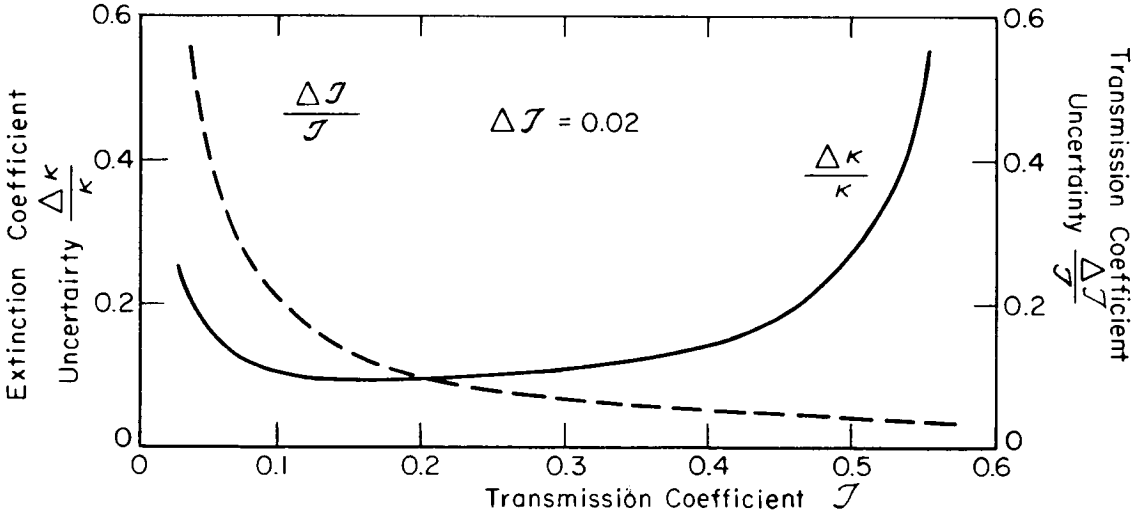

Fig. 3. A comparison of the uncertainties in the transmission coefficient and the extinction coefficient.

Figure 3 shows that, for a two percent uncertainty in the full-scale deflection, calculations from transmission values greater than about 45 percent or less than about 4 percent will yield uncertainties in the extinction coefficient greater than 20 percent. Calculations

from transmission values between 5 percent and 40 percent, however, will yield extinction coefficients with uncertainties between 10 and 15 percent.

CHAPTER IV
RESULTS OF THE MEASUREMENTS

A. Calcium tungstate

The refractive indices of $CaWO_4$ were computed from measurements on four samples. Two plates, 0.968 mm and 0.776 mm thick, were cut with their parallel faces parallel to the crystalline c-axis; two others, 0.871 mm and 0.329 mm thick, were cut perpendicular to the c-axis. The spectral regions and temperatures at which the various samples were used is shown in Table II. The perpendicular-cut samples were measured with unpolarized radiation and yielded only the ordinary ray ($E \perp$ c-axis) optical constants. The parallel cut samples were measured with polarized radiation and displayed either the ordinary or extraordinary ray ($E \parallel$ c-axis) constants, depending on the orientation of the polarizer relative to the crystal.

A tracing of typical chart records of a channeled spectrum is shown in Figure 4. The upper curve was obtained with the cryostat removed from the spectrometer, the middle curve is the channeled spectrum at 300°K, and the lowest curve the channeled spectrum at 90°K. The order numbers, b, of the maxima are indicated on the figure. The three curves are displaced vertically from one another;

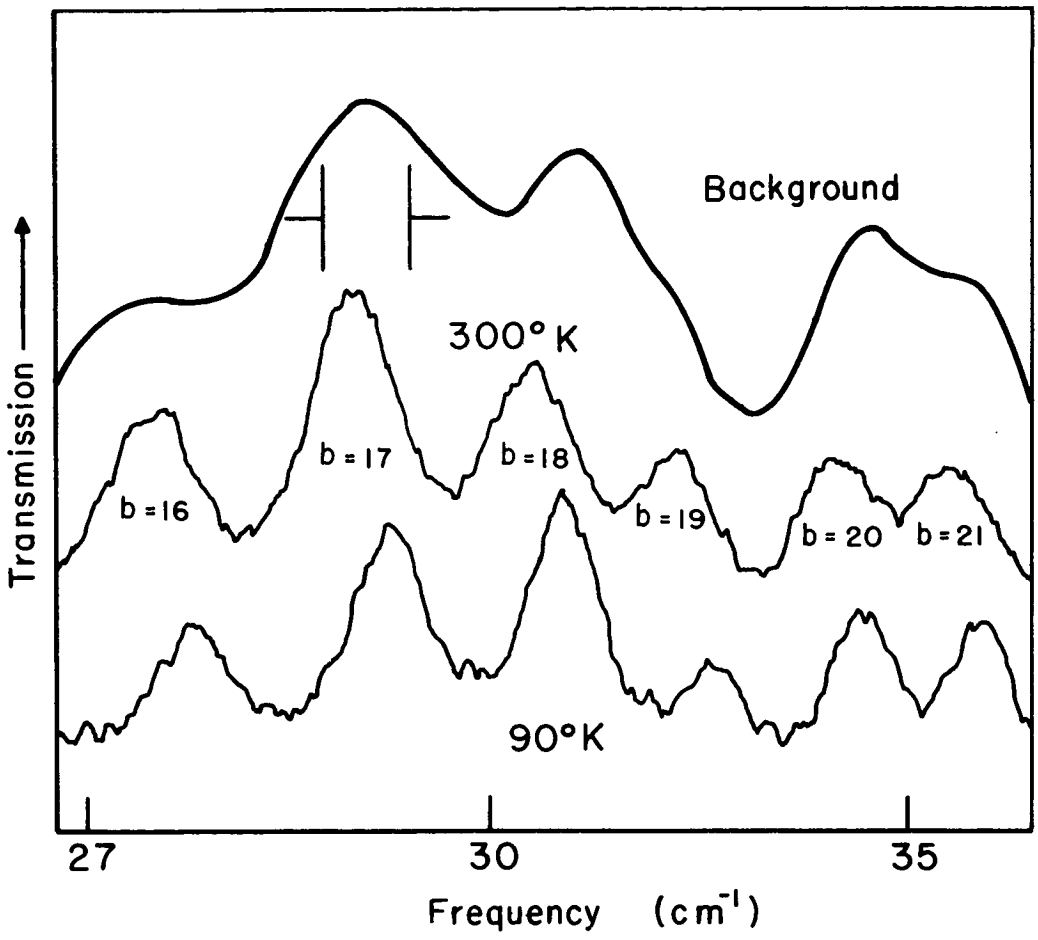

Fig. 4. A tracing of a typical chart record of channeled spectra at 300°K and 90°K. Sample: 0.07 mm $CaWO_4$; radiation polarized parallel to the c-axis; 45 lines/inch dispersion grating. The ordinate scales of the three curves are different.

TABLE 2

$CaWO_4$ SAMPLES USED FOR CHANNELED SPECTRA MEASUREMENTS

Sample	How Measured	Temperature	Spectral Region
	Ordinary ray ($E \perp c$-axis)		
0.968 mm	with polarizer	300°K	14 - 51 cm^{-1}
		90°K	21 - 37 cm^{-1}
0.871 mm	without polarizer	300°K	14 - 59 cm^{-1}
		90°K	22 - 84 cm^{-1}
0.776 mm	with polarizer	300°K	37 - 55 cm^{-1}
		90°K	35 - 67 cm^{-1}
0.329 mm	without polarizer	300°K	56 - 94 cm^{-1}
	Extraordinary Ray ($E \parallel c$-axis)		
0.968 mm	with polarizer	300°K	14 - 51 cm^{-1}
		90°K	21 - 36 cm^{-1}
0.776 mm	with polarizer	300°K	33 - 74 cm^{-1}
		90°K	35 - 82 cm^{-1}

if they were drawn with the same ordinate scale the 90°K curve would lie slightly above the 300°K curve and the background would be considerably higher. Figure 4 clearly shows the shift of the maxima and minima to higher frequencies on cooling; this corresponds (from (II-7)) to a decrease in the refractive index.

Since the linear thermal expansion coefficient of $CaWO_4$ is not given in the literature, it seemed reasonable to assume that it was similar to the other hard, natural crystals such as quartz, sapphire.

and MgO,[1] which had expansion coefficients smaller than 2×10^{-5} (degree C)$^{-1}$. It is also known that the expansion coefficient decreases considerably when the temperature is lowered to that of liquid nitrogen. Consequently, it appeared reasonable to assume that the change in thickness of the $CaWO_4$ samples, on cooling to 90°K, was less than the uncertainty in the measurement of the room temperature thickness, approximately $\pm$ 0.004 mm, or $\pm$ 0.5 percent for the three thicker samples and $\pm$ 1.2 percent for the 0.329 mm sample. Thus we concluded that the effects of the thermal expansion could be ignored and the room temperature measured thickness used in the computation of the optical constants at both 300°K and 90°K.

The results of the $CaWO_4$ refractive index measurements at 300°K and 90°K are plotted versus frequency in Figure 5 for the ordinary ray and in Figure 6 for the extraordinary ray. Each open circle is an experimentally measured point. The solid line was drawn as a "best fit" to the experimental points in the region of small scatter, and the squares are the values used in further calculations. The vertical bars are a measure of the uncertainty in the position of the squares. The dashed lines are the result of fitting the data of the squares to (II-14') and then extrapolating. This is discussed in Chapter VI, below.

---

[1] See Chapter V, below.

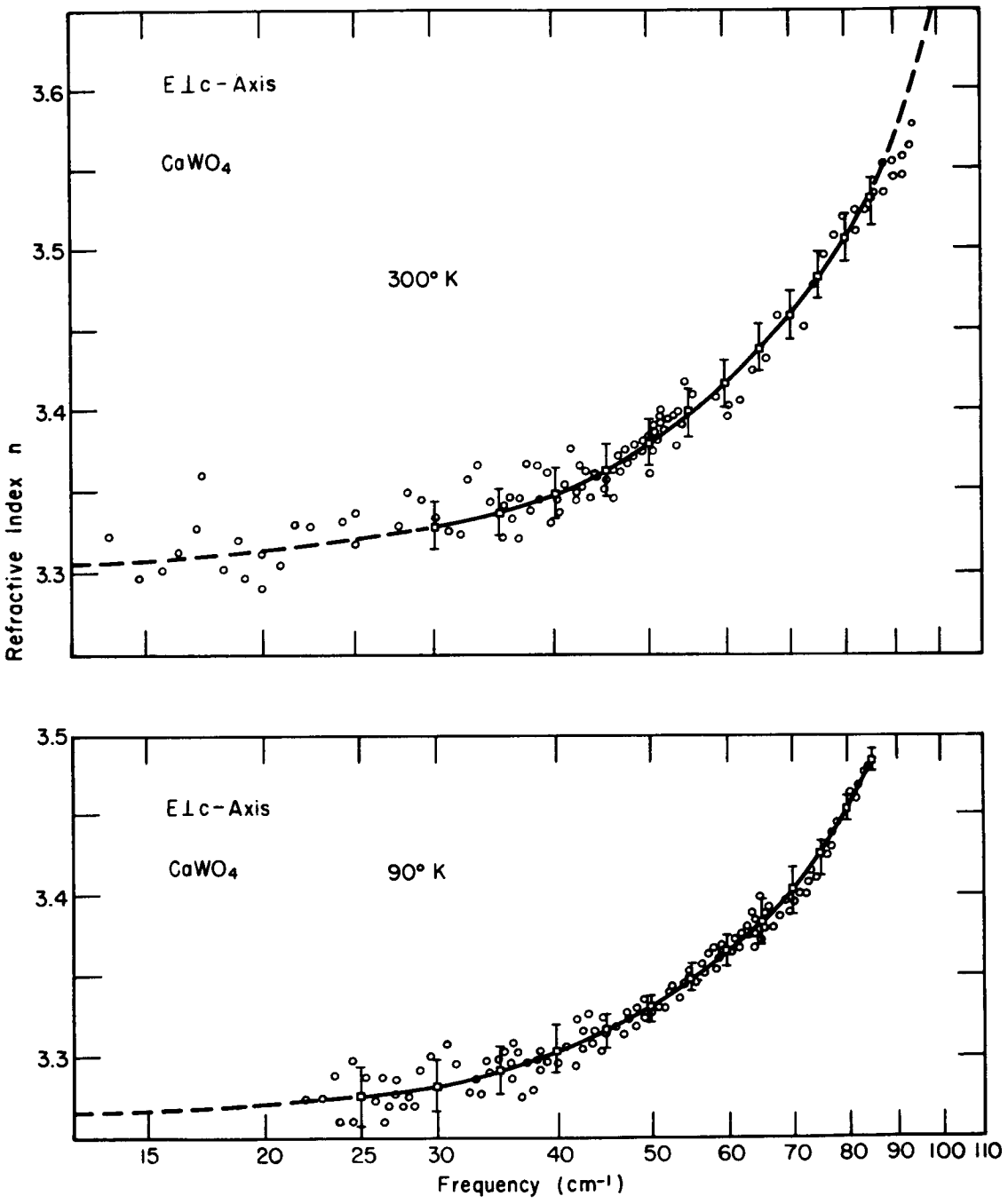

Fig. 5. Measured refractive index of $CaWO_4$, ordinary ray, at 300°K and 90°K.

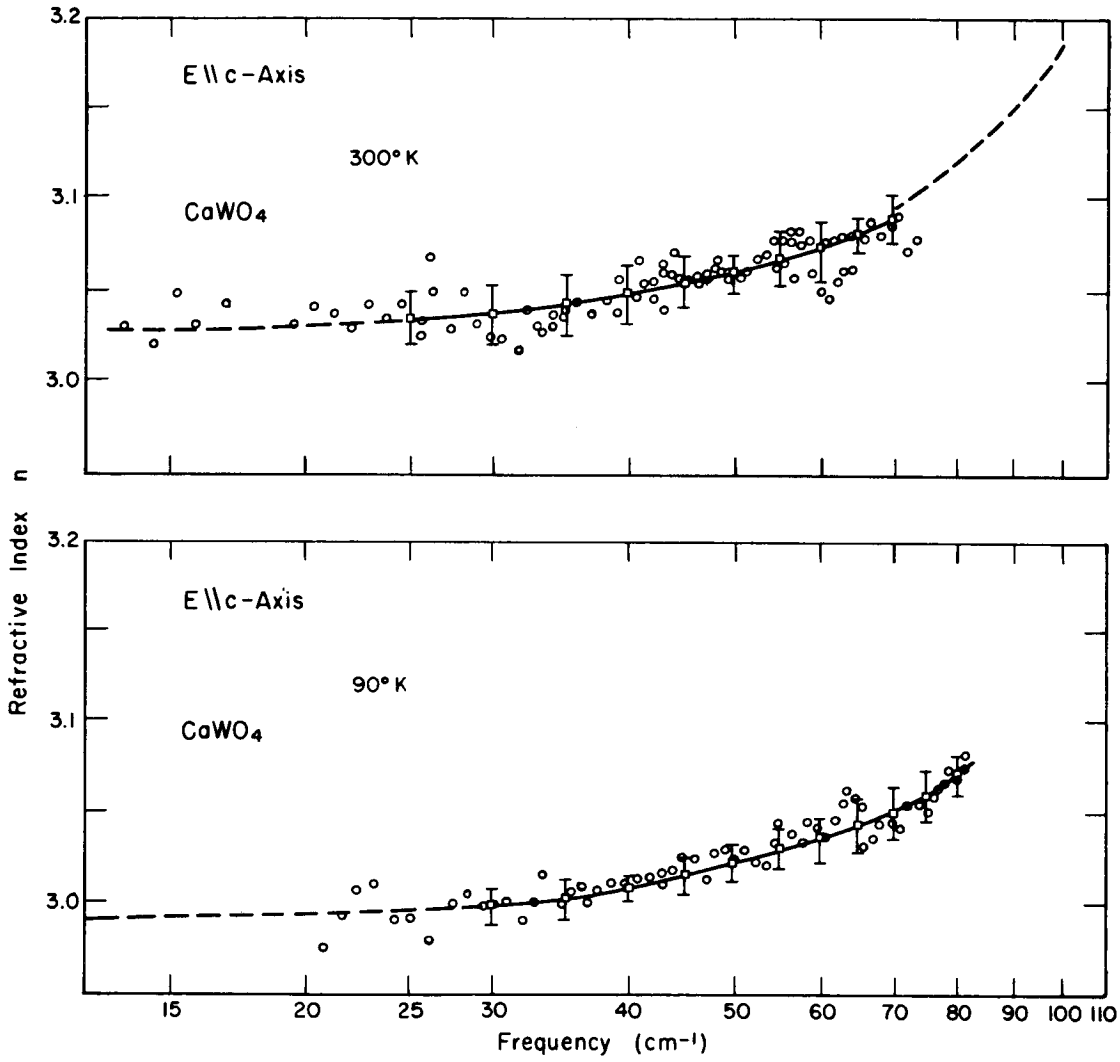

Fig. 6. Measured refractive index of $CaWO_4$, extraordinary ray, at 300°K and 90°K.

There was no significant variation in any spectral region between the experimental points obtained from different samples. This included the ordinary ray data taken with samples of different orientations cut from two different boules. The agreement obtained would serve to indicate that the accuracy of the orientation, and the sample consistency between boules, were adequate for the accuracy of the present measurements. A visual inspection of the samples disclosed some indications of inhomogeneity, and all of the samples cracked after two of three cycles of cooling to 90°K, which might also have indicated the existence of strains or other inhomogeneities. However, no optical effects were detected which could be traced to these factors.

The extinction coefficients for $CaWO_4$ were computed from measurements on four samples. Three plates, 3.25 mm, 1.94 mm, and 0.959 mm thick, were cut with their parallel faces parallel to the crystalline c-axis. One plate, 4.12 mm thick, was cut with its faces perpendicular to the c-axis. In general, the measurements of a given sample covered at least two dispersion grating spectral regions. The present transmittance (100$\mathcal{J}$) of the 4.12 mm sample at 300°K and 90°K is shown in Figure 7. The vertical bars are an estimate of the uncertainty in the measurements at each frequency. The lines marked "reflection loss only" represent the transmittance, computed from (II-8) that would be expected if there were no absorption (D=1) and the

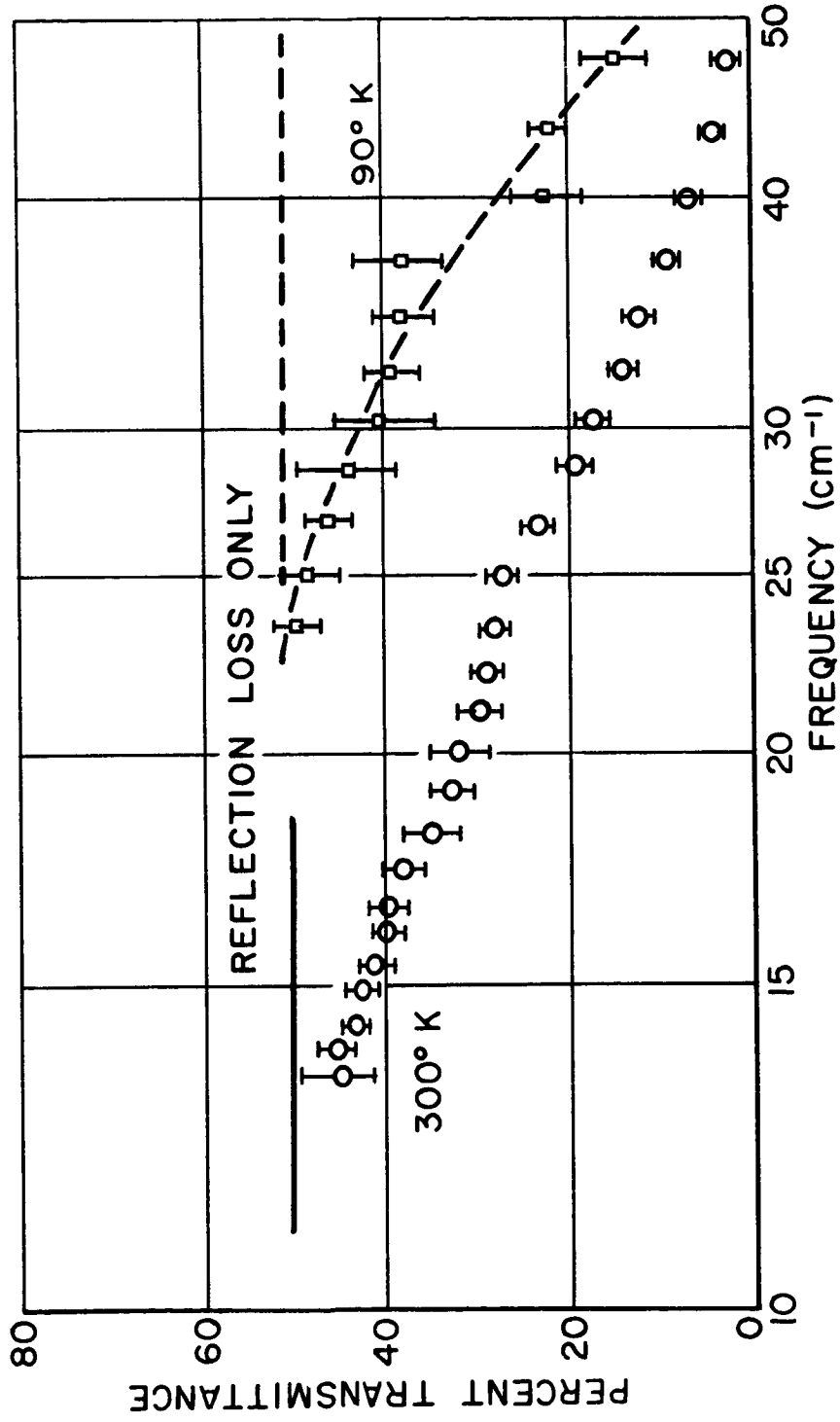

Fig. 7. Measured transmittance of 4.12 mm $CaWO_4$, ordinary ray, at 300°K and 90°K.

only losses were those due to reflections from the crystal faces, with the channeled spectra effects averaged out.

Because the 90°K transmittance was computed using the 300°K values (as described in Chapter III, above), 90°K points could not be found for frequencies where the 300°K transmittance was too small to be accurately measured; on the other hand, frequencies for which 90°K transmittance approaches the "reflection loss only" level could not be used for a computation of the extinction coefficient (this was also mentioned in Chapter III, above). For these reasons, we obtained only about one half as many experimental values of the 90°K extinction coefficient as compared with the 300°K extinction coefficient.

The results of the measurements of the 300°K and the 90°K extinction coefficients are shown in Figure 8 for the ordinary ray and Figure 9 for the extraordinary ray. The solid lines were drawn to provide a visually-determined "best fit" to the experimental points. Values were taken from these lines for use in the further calculations discussed in Chapter VI, below.

The results of the $CaWO_4$ reflection measurements are shown in Figure 10. The data for $E \perp$ c-axis were taken with the 4.12 mm perpendicular-cut sample and did not require use of the polarizer. The $E \parallel$ c-axis data were taken with a polarizer from the 3.25 mm parallel-cut sample. Because the wire grating's polarization efficiency had

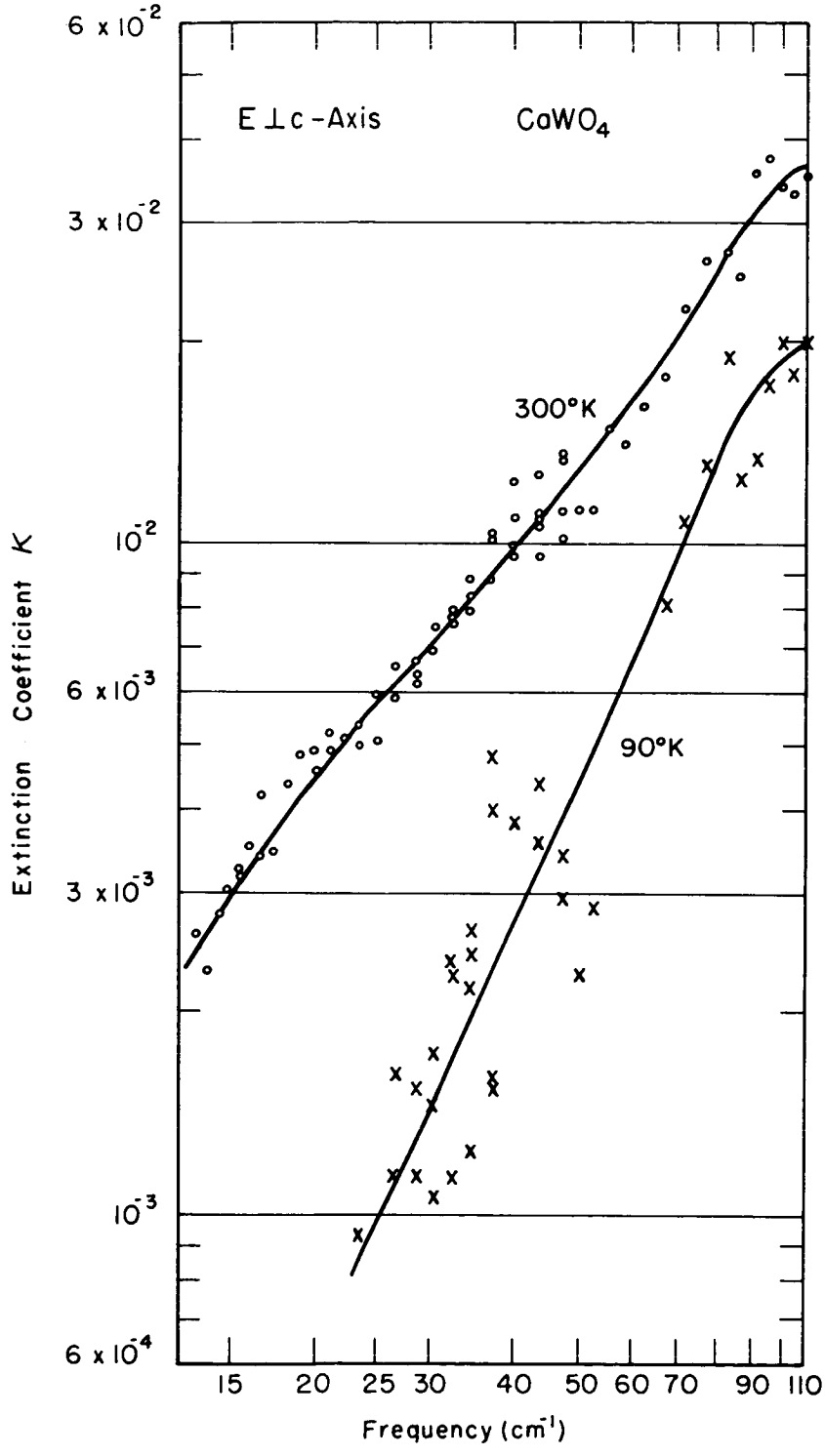

Fig. 8. Measured extinction coefficient κ of $CaWO_4$, ordinary ray, at 300°K and 90°K.

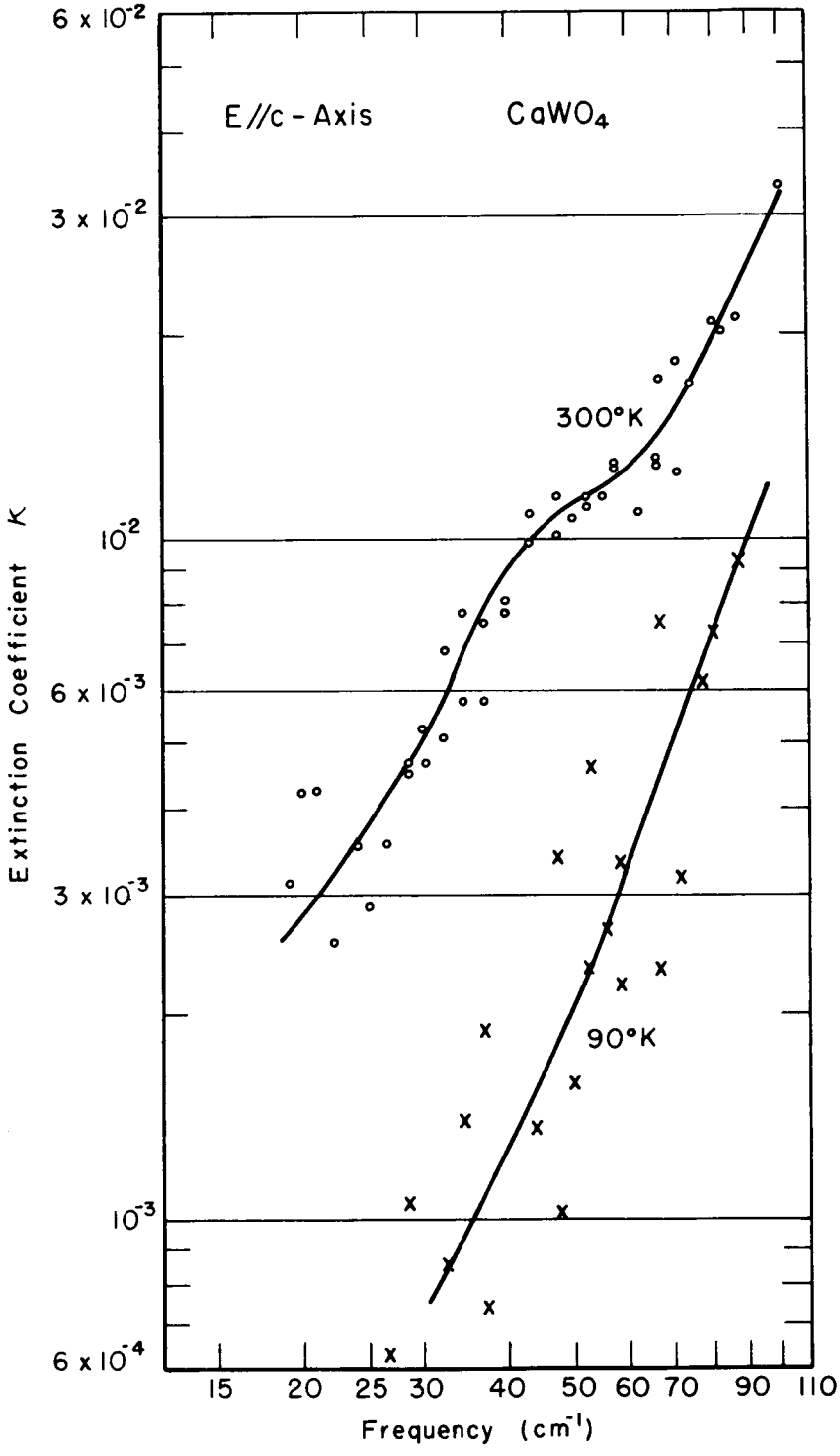

Fig. 9. Measured extinction coefficient κ of $CaWO_4$, extraordinary ray, at 300°K and 90°K.

fallen to about 60 percent at 400 cm^{-1} (from > 95 percent for frequencies below 150 cm^{-1}), no data were taken at higher frequencies. The solid lines in Figure 10 show the reflectance as calculated from the measured refractive indices by (II-4). As before, the measured points are shown by circles and their uncertainties by the vertical bars.

B. Magnesium oxide

The refractive index measurements for MgO were made on two samples; one, 0.693 mm thick, was used in the entire spectral region, and a second, 0.436 mm thick, was used between 82 cm^{-1} and 100 cm^{-1}. The samples showed no visible indications of inhomogeneities, and withstood repeated coolings to 90°K without cracking.

The linear expansion of MgO has been measured by Durand;[2] he reported that the change in length on cooling from 300°K to 85°K was 0.143 percent. Since the uncertainty in the room temperature measurement of the thickness was approximately 0.6 percent for the 0.693 mm sample and 0.9 percent for the 0.436 mm sample, the room temperature thickness was used for both the 300°K and the 90°K computations.

The results of the MgO refractive index measurements are shown in Figure 11. Again, the circles are the experimentally measured points, the solid line the visually-determined "best fit" to the data,

---

[2] M. Durand, Physics 7, 297 (1936).

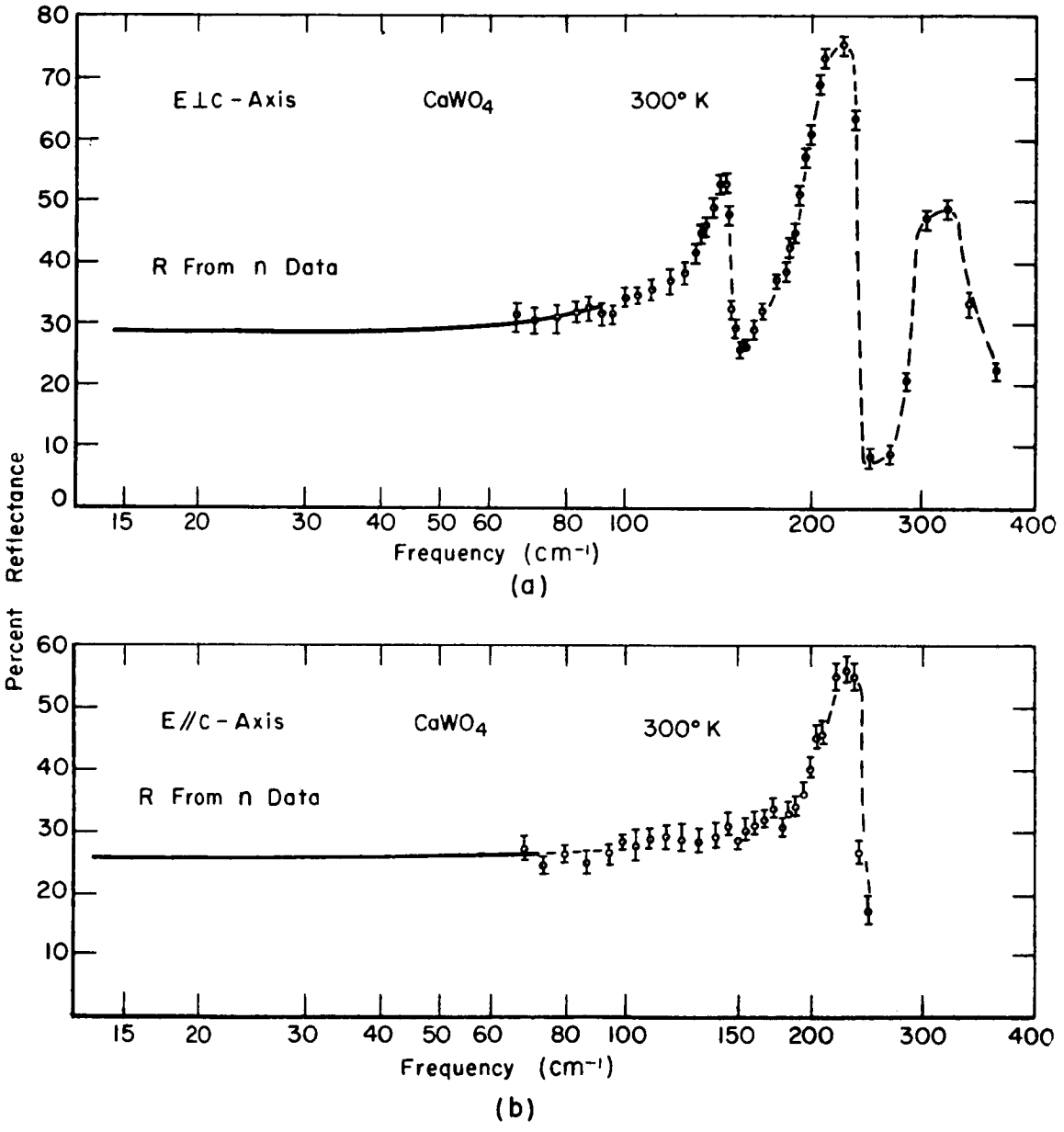

Fig. 10. Measured reflectance of $CaWO_4$ at 300°K.
(a) Ordinary ray, sample cut perpendicular to c-axis (no polarizer);
(b) Extraordinary ray, sample cut parallel to c-axis (with polarizer).

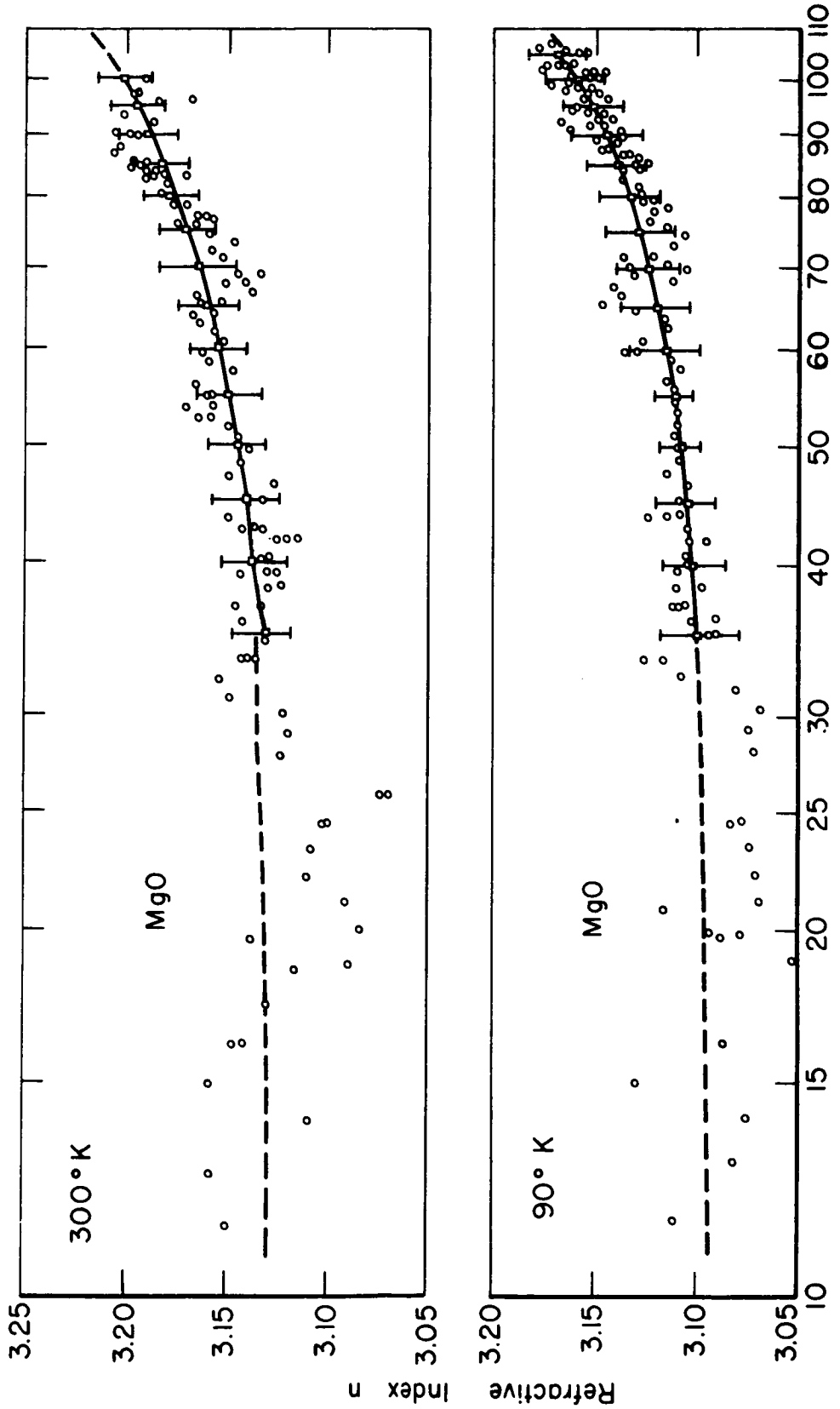

Fig. 11. Measured refractive index n of MgO at 300°K and 90°K.

the dashed line the extrapolation on the basis of (II-14a'); the squares are the values used in further calculations, with their uncertainty given by the vertical bars.

The extinction coefficients of MgO were computed from measurements made on samples 14.85, 6.62, 4.79, and 2.83 mm thick. The results of these measurements are shown in Figure 12. As before, the solid lines were fitted visually to the data, and the values used in further work taken from the lines.

C. Errors and uncertainties

The refractive indices were computed from measurements of the frequencies of the maxima and minima of a channeled spectrum and from the measured thickness of the sample. Inaccuracies in the measurement of the frequencies of the extrema could be caused by an incorrect frequency calibration of the spectrometer, or by errors in the determination of the grating angles of the extrema on the chart record. The latter cause would probably tend to produce a random, rather than a systematic, error, and the results (Figures 5, 6, 11) exhibit such a scatter. A calibration error, on the other hand, would be expected to produce a more systematic error within a given dispersion grating spectral region, but such an error should vary from grating to grating, since they were calibrated independently. If the error lies in the grating drive, however, it is expected to appear

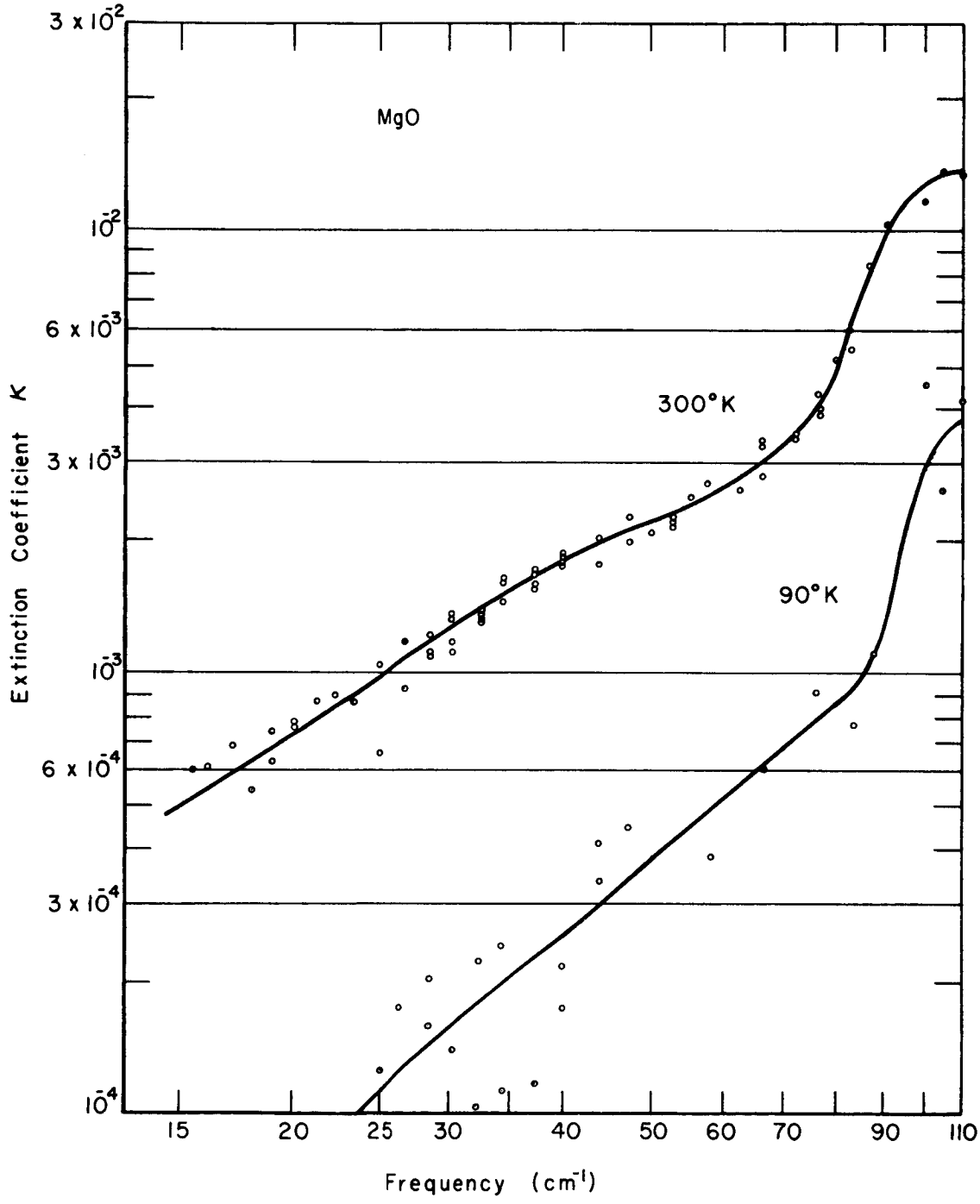

Fig. 12. Measured extinction coefficient κ of MgO at 300°K and 90°K.

more or less similarly in each grating region; just such an effect has been observed. Inspection of Figures 5, 6, 11 shows a slightly larger scatter of the experimental points in the regions near 36 - 38 cm^{-1} and 65 - 70 cm^{-1}, which correspond to the overlap of the regions of the 45 and 90 lines/inch and 90 and 180 lines/inch gratings, respectively. In both of these regions the values obtained from the coarser grating tended to lie about 0.4 percent above those obtained with the finer grating. A similar disagreement was previously observed in these overlap regions in spectra recorded on another instrument using these same gratings.[3] The source of this error has not been identified; and, fortunately, its effect on the present work appears to be small.

The increased scatter of the measured refractive index values at frequencies below 30 cm^{-1} was a disappointment. It was expected that the most accurate values would be obtained in this region where the order numbers were small and the extrema well separated. Of course, the calibration in this region was expected to be somewhat less accurate, because the H_2O and N_2O absorption lines were considerably broader than at higher frequencies; indeed, this was the first time that quantitative measurements had been made with the 20 lines/inch grating.

---

[3] This was called to the author's attention by Dr. P.B. Burnside.

We believe, however, that the major blame for this failure can be laid elsewhere. The upper curve, the spectrometer background recorded with no sample, of Figure 4 shows a quasi-periodic structure with a spacing of 3 - 5 cm^{-1}. This structure is observed throughout the spectral region from 10 to 200 cm^{-1}, at other laboratories[4] as well as ours. The amplitude of the variation increases from 1 to 2 percent at 200 cm^{-1} to as much as 50 percent at 15 cm^{-1}. While the source of these fluctuations has not been positively identified, we now believe that it lies in the internal construction of the Golay detector. We expect to discuss this effect in detail elsewhere.[5] For the present, however, we note that the channeled spectrum, from which we compute the refractive index, is superimposed upon this fluctuating background and that consequently the extrema of the recorded channeled spectrum will be shifted if they fall between the extrema of the background. The effects of this can be large only where the background changes are large, i.e., in the low frequency region. We believe that this is the primary cause of the increased scatter of points below 30 cm^{-1}.

Because of the above effect, we have used only the experimental points between approximately 30 and 80 cm^{-1}, as described above, in

---

[4] L. Genzel, private communication; R.B. Sanderson, private communication.

[5] E.E. Bell, R.F. Rowntree, in preparation.

making further calculations. In this region we believe the combined errors, due to calibration and uncertainty in the extrema positions, to be no greater than the extreme scatter of the experimental points: approximately $\pm$ 0.5 percent.

Errors in the thickness measurements would not effect the scatter of points, but would only serve to displace them in unison along the ordinate scale. We stated earlier that the uncertainty in the thickness measurements was approximately $\pm$ 0.5 percent for most of the samples from which channeled spectra were taken. Consequently, we expect that the error in the measured refractive indices, the solid lines in Figures 5, 6, 11, does not exceed $\pm$ 1.0 percent.

The uncertainty in the extinction coefficient measurements is dominated by the uncertainty in the measured power transmission coefficient. The combined uncertainties of thickness measurement and frequency determination contributed certainly little more than 1 percent, while it was shown in Chapter III, Section F, above, that a 2 percent uncertainty in the measured transmission would produce a 10 to 15 percent uncertainty in the extinction coefficient. Since the transmission coefficient measurements had uncertainties between 1 and 3 percent, the computed extinction coefficients could have errors of between 5 and 20 percent. The scatter of the room temperature points, on Figures 8, 9, 12, is seen to be no more than 20 percent. The points

representing measurements on different samples showed no systematic variation, and there was good agreement between measurements taken on the same sample with different gratings. If we assume that the smooth curves we have drawn are a good average of the data, then the error in the values taken from it are probably best represented by the scatter of points.

The 90°K extinction coefficient values in Figures 8, 9, 12, show a considerably greater scatter than do the 300°K results. This is to be expected from the method of measurement, described in Chapter III, Section D, above. Since it is difficult to estimate the uncertainty introduced by the instability of the spectrometer, the scatter of points in Figures 8, 9, 12, is probably the best measure of the error in the 90°K extinction coefficient results. Inspection of the figures shows that this error may be as large as $\pm$ 50 percent.

The radiation was assumed to be incident normally on the sample for all the above results. Actually, since the sample was at an image point, the beam was a converging one with an angular half-width of about 12°. Because the refractive index was relatively large, however, Snell's Law showed that the radiation path in the sample could still be considered normal to the faces, to the accuracy of the present work.

CHAPTER V
RELATED DATA AND OTHER WORK

A. Calcium tungstate

As was mentioned in the introduction, very few measurements of the physical properties of $CaWO_4$ have been reported in the literature. The crystal structure of $CaWO_4$ is tetragonal.[1] A diagram[2] of the structure of a unit cell of $CaWO_4$ is shown in Figure 13; the relative sizes of the atoms are distorted for clarity.

Coblentz[3] measured the infrared reflectivity of an unoriented sample of $CaWO_4$ and found a peak of high reflectivity between 800 and 900 cm^{-1}. Recently, Barker[4] has made measurements of the reflectance of $CaWO_4$ at room temperature from the near infrared to 100 cm^{-1} for radiation polarized both parallel and perpendicular to

---

[1] R. Wyckoff, Crystal Structures (Interscience Publishers, Inc., New York, 1948).

[2] P. Ewald, C. Herman, Strukturbericht 1913-1928 (Aka. Verlag, Leipzig, 1931), p. 348.

[3] W. Coblentz, Supplementary Investigations of Infrared Spectra, Publication No. 97, The Carnegie Institution of Washington, 1908, p. 16.

[4] A.S. Barker, Jr., private communication.

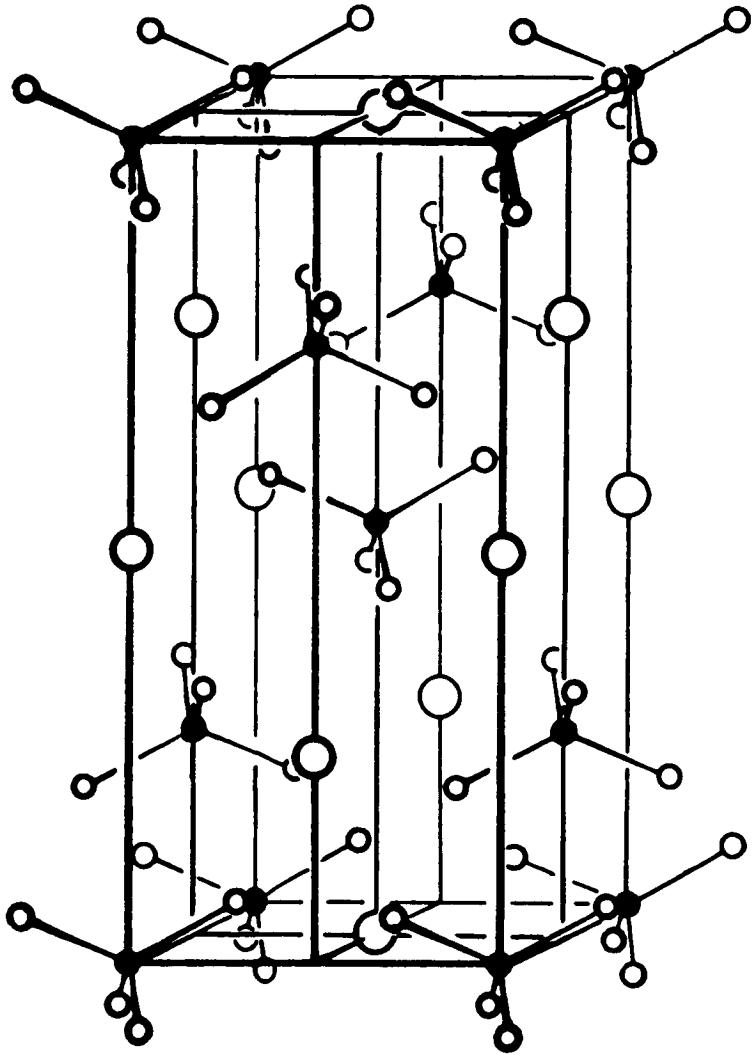

Fig. 13. The structure of the unit cell of $CaWO_4$ (from Ewald and Herman). Large open circles: Ca; small open circles: O; solid circles: W. cell dimensions: $a_o = 5.24$ Å, $c_o = 11.38$ Å.

the optic axis. He has then fitted the reflectance data, via (II-3), to the classical dispersion relations (II-14), (II-15), and obtained a set of dispersion parameters as shown in Table 3. The static dielectric constants are, of course, not free parameters but are obtained from (II-16).

TABLE 3

THE DISPERSION PARAMETERS FROM BARKER+ FOR $CaWO_4$ (300°K)

	E c-axis (ordinary ray)				E c-axis (extraordinary ray)			
Parameter	j=1	j=2	j=3	j=4	j=1	j=2	j=3	j=4
$\nu_j(cm^{-1})$	143	198	307.5	793	192	240	435	778
A_j	2.0	4.6	0.88	0.83	0.6	3.8	0.22	0.98
γ_j	0.1	0.1	0.042	0.01	0.16	0.08	0.03	0.01
ϵ_∞	3.35				3.35			
ϵ_o	11.66				8.95			

+Note 4

If we recall that the eigenfrequency lies approximately at the low frequency edge of the reflectance maximum, then Coblentz's observations are consistent with Barker's highest frequency modes. Standard handbooks[5] list values for the refractive indices of $CaWO_4$

[5] E.g., Landolt-Bornstein, Physikalisch-chemische Tabellen (J. Springer, Berlin, 1952) 6th ed.

in the visible spectral region. The dielectric constants ($\epsilon' = n^2$) corresponding to these values progress smoothly from $\epsilon' = 3.74$ at 0.475μ to $\epsilon' = 3.65$ at 0.667μ for the ordinary ray, and from $\epsilon' = 3.81$ at 0.475μ to $\epsilon' = 3.71$ at 0.667μ for the extraordinary ray. While the values for ϵ' in the visible are usually larger than ϵ_∞ by a few percent, the 10 percent difference between the measured values and those arrived at by Barker seem somewhat unusual.

B. Magnesium oxide

The infrared spectrum of MgO has been the subject of a number of investigations, as was mentioned previously in the introduction. The results of these several studies have been contradictory.

From transmission measurements on MgO powder[6] the eigenfrequency was reported to be at 14.2μ ($700\ cm^{-1}$). In subsequent work on fumed samples (where magnesium ribbon was burned in air and the combustion product collected on a transparent substrate), eigenfrequencies of 23μ ($435\ cm^{-1}$),[7] 17.3μ ($580\ cm^{-1}$),[8] and 17.5μ ($570\ cm^{-1}$),[11] as well as subsidiary maxima at $\sim 25\mu$ ($400\ cm^{-1}$),[8,11] were reported. Measurements, on thin, cleaved samples of the bulk material, were

---

[6] S. Tolksdorf, Z. physik, Chem. 132, 616 (1928).

[7] J. Strong, Phys. Rev. 37, 1565 (1931).

[8] J. Fock, Z. Physik 90, 44 (1934).

in general agreement on the gross structure[10,11] of the subsidiary maxima at frequencies higher than the eigenfrequency, but not on the question of possible fine structure.[9] Reports of the reflectance[9,10,11] from the bulk material failed to agree on both the spectral structure observed and the magnitude of the maximum reflectance.

Stephens and Malitson[12] made accurate measurements of the refractive index, and the temperature coefficient of refractive index, of single-crystal MgO in the visible and infrared regions and fitted the results to a Sellmeier-type equation. Saksena and Viswanathan[13] examined the earlier work on MgO and rewrote Stephens and Malitson's expression for the refractive index in the form of (II-14). From this they deduced that the eigenfrequency should lie at 25.26μ (396 cm^{-1}), which was at the long wavelength side of the reflectance maximum, in agreement with the results for other similar crystals.

---

[9]R. Barnes, R. Brattain, F. Seitz, Phy. Rev. 48, 582 (1935).

[10]E. Burstein, J. Oberley, E. Plyler, Proc. Indian Acad. Sci. A28, 388 (1948).

[11]J. Willmott, Proc. Phys. Soc. (London) A63, 389 (1950).

[12]R. Stephens, I. Malitson, J. Research Natl. Bur. Standards 49, 249 (1952).

[13]B. Saksena, S. Viswanathan, Proc. Phys. Soc. (London) B69, 129 (1956).

The most recent measurements on MgO have been those of Smart,[14] using a grating-CsI prism spectrometer. His measurements were made on vacuum-evaporated samples; the required temperatures were obtained by using a beam of electrons to heat the MgO. He made reflection and transmission measurements, at room temperature and at liquid nitrogen temperature, in the region between 200 and 800 cm^{-1}. In addition Inglis, in the same laboratory, measured the far infrared channeled spectrum of a thin sample of MgO at liquid nitrogen temperature to frequencies below 50 cm^{-1}. Smart then programmed a high-speed computor to perform Kramers-Kronig relation-type computations[15] and obtained values for the optical constants of MgO (and a number of other crystals) throughout the infrared. Smart also obtained a room temperature eigenfrequency of 396 cm^{-1}, and a peak reflectance of 100 percent of that of his aluminized reference mirror; the liquid nitrogen temperature reflectance was slightly higher. Smart also performed a numerical integration of his measured infrared absorption and compared the result, via the Kramers-Kronig relation (II-21), to the difference between the short wavelength (from Stephens

---

[14] C. Smart, Ph.D. Thesis, University of London, 1962, unpublished. See also W. Price, G. Wilkinson, et al., Molecular Spectroscopy Report, U.S. Army Contract DA-91-591-EUC 1958-1959 (ASTIA AD 231 584, TAB 60-2-3, p. 61).

[15] See Chapter II, Section C.1, above.

and Malitson) and static (from his computations) refractive indices and obtained reasonable agreement for the room temperature data but not for those at liquid nitrogen temperatures. Similar room temperature agreement was also found for NaCl, KCl, and ZnS.

The various dispersion parameters at 300°K and 90°K for MgO are tabulated in Table 4 and will be referred to in Chapter VI, below.

TABLE 4

SPECTRAL DATA FOR MgO

Parameter	Value	Source[+]
ν_o (300°K)	396 cm^{-1}	Smart
(90°K)	410 cm^{-1}	Smart
γ (300°K)	0.074	Smart
(90°K)	0.066	Smart
ϵ_∞ (300°K)	2.956	Stephens and Malitson
ϵ_∞ (90°K)	2.95	see text
ϵ_o (300°K)	9.8 ± 0.15	Højendahl
	9.8	Smart
	9.65 ± 0.19	Von Hippel
ϵ_o (90°K)	9.42	Smart

[+]See notes 12, 14, 16, 17, 19.

The ϵ_o value reported by Højendahl[16] was determined from measurements of the capacitance of a mixture of MgO powder and a liquid of

[16]K. Højendahl, Kgl. Danske Videnskab, Selskab 16, No. 2 (1938).

known dielectric constant. The value of ϵ_o reported by Von Hippel[17] was stated to be correct to ± 2 percent; the method of measurement was not described. It should be noted that Fuchs, working in Von Hippel's laboratory in 1961, used the ϵ_o value of Højendahl in his report.[18] The 90°K value of ϵ_∞ was computed as follows: from Stephens and Malitson's Sellmeier-type equation ϵ_∞ was found to be the dielectric constant at 1.3μ. Stephens and Malitson quote values for dn/dT only for the visible: the values progress linearly from 1.9×10^{-5} (degree C)$^{-1}$ at 0.405μ to 1.4×10^{-5} (degree C)$^{-1}$ at 0.70μ. If this is extrapolated to 1.3μ dn/dT is rather less than 1.0×10^{-5} (degree C)$^{-1}$. It is also known[19] that the magnitude of dn/dT decreases with temperature, consequently it appears that a choice of

$$\Delta\epsilon_\infty = 2n \frac{dn}{dT} \Delta T = 0.007,$$

$$\epsilon_\infty(90^\circ K) = \epsilon_\infty(300^\circ K) - \Delta\epsilon_\infty = 2.949 \simeq 2.95$$

is a reasonable value for ϵ_∞ (90°K) for the present work.

---

[17] A.R. Von Hippel (ed.) Dielectric Materials and Applications (John Wiley and Sons, Inc., 1954), p. 301.

[18] R. Fuchs, Temperature Dependence of the Dielectric Constant of Ionic Crystals, Technical Report 167, Lab. Insulation Research, MIT, Cambridge, 1961.

[19] R. Krishnan, Progress in Crystal Physics (S. Viswanathan, Chetput, Madras, 1958), Vol. 1, p. 147.

Some additional physical quantities of MgO needed for the calculations in Chapter VI are tabulated in Table 5; all values are for 300°K, except as noted. The compressibility was calculated from the elastic constants by[20]

$$K = \frac{3}{c_{11} + 2c_{12}} \quad .$$

The value of $\frac{\partial \epsilon_\infty}{\partial P}$ was calculated from the measured value of $\rho \frac{\partial n}{\partial \rho}$,[21] where ρ is the density, by

$$\frac{\partial \epsilon_\infty}{\partial P} = -2nK\rho \frac{\partial n}{\partial \rho}, \quad K = \frac{1}{V} \frac{\partial V}{\partial P} \quad .$$

The volume expansion coefficient Γ is related to the linear expansion coefficient γ by $\Gamma = 3\gamma$. The polarizability of MgO is found from the Lorentz-Lorenz equation,[5]

$$\frac{4\pi}{3} \alpha_\infty = \frac{\epsilon_\infty - 1}{\epsilon_\infty + 2} \quad .$$

The free ion polarizability data of Fajans and Joos[22] was deduced, assuming additivity, from refraction measurements of solutions.

---

[20] M. Durand, Phys. Rev. 50, 453 (1936), henceforth Durand I.

[21] E. Burstein, P. Smith, Phys. Rev. 74, 229 (1948).

[22] K. Fajans, G. Joos, Z. Physik 23, 1 (1924).

The data of Pauling[23] was deduced, semi-theoretically, from Stark effect data.

TABLE 5

RELATED DATA FOR MgO

Quantity	Value	Source[+]
Nearest Neighbor Distance r_o	2.10×10^{-8} cm	Wycoff
Reduced Mass M	16.02×10^{-24} gm	HCP
Polarizability:		
$\alpha^+(Mg^{++})$	1.2×10^{-25} cm^3 0.94×10^{-25} cm^3	Fajans, Joos Pauling
$\alpha^-(O^{--})$	27.5×10^{-25} cm^3 38.5×10^{-25} cm^3	Fajans, Joos Pauling
α_∞(MgO)	18.5×10^{-25} cm^3	Computed from ϵ_∞
$\frac{\partial \epsilon_o}{\partial T}$	18.3×10^{-4} (degree C)$^{-1}$	Krishnan
$\frac{\partial \epsilon_o}{\partial P}$	-3.1×10^{-11} dynes/cm^2	Mayburg
$\frac{\partial \epsilon_\infty}{\partial T}$	$\sim 1.0 \times 10^{-5}$ (degree C)$^{-1}$	see text
$\frac{\partial \epsilon_\infty}{\partial P}$	9.0×10^{-13} dynes/cm^2	Computed from Burnstein, Smith
Linear Expansion Coefficient γ (300°K)	10.98×10^{-6}(degree C)$^{-1}$ 10.5×10^{-6}(degree C)$^{-1}$	Sharma Durand II
(118°K)	3.4×10^{-6}(degree C)$^{-1}$	Durand II

[23] L. Pauling, Proc. Roy. Soc. (London) A114, 191 (1927).

TABLE 5 - continued

Quantity	Value	Source[+]
Elastic Constants:		
c_{11} (300°K)	29.86×10^{11} dynes/cm^2	Durand I
(90°K)	28.75×10^{11} dynes/cm^2	Durand I
c_{12} (300°K)	8.77×10^{11} dynes/cm^2	Durand I
(90°K)	8.54×10^{11} dynes/cm^2	Durand I
c_{44} (300°K)	15.48×10^{11} dynes/cm^2	Durand I
(90°K)	15.67×10^{11} dynes/cm^2	Durand I
Compressibility		
K (300°K)	6.54×10^{-13} cm^2 /dyne	Computed from
(90°K)	6.38×10^{-13} cm^2 /dyne	c_{11}, c_{12}
Debye Temperature		
Θ_D (0°K)	946°K	Barron, et al.
(0°K)	946°K	Durand I
(90°K)	~725°K	Barron, et al.
(300°K)	~740°K	Barron, et al.

+ See footnotes 1, 14, 20-29.

---

[24] Handbook of Chemistry and Physics (Chemical Rubber Publishing Co., Cleveland, 1962), 44th ed., inside front cover.

[25] Krishnan, op. cit., p. 192.

[26] S. Mayburg, Phys. Rev. 79, 375 (1950).

[27] S. Sharma, Proc. Indian Acad. Sci. A32, 268 (1950).

[28] M. Durand, Physics 7, 297 (1936), henceforth Durand II.

[29] T. Barron, W. Berg, J. Morrison, Proc. Roy. Soc. (London) A250, 70 (1959).

CHAPTER VI
DISCUSSION OF THE RESULTS

A. Calcium tungstate

One of the most prominent features of the far infrared spectrum for $CaWO_4$, or other non-isotropic crystals, is the degree to which its anisotropy is displayed. In the visible region the birefringence (difference in refractive indices) of $CaWO_4$ is of the order of 1 percent, while Figures 5 and 6 show it to be of the order of 10 percent in the far infrared. In addition, in the visible region, $CaWO_4$ exhibits "positive birefringence" (n (ordinary) < n (extraordinary)), while in the far infrared it has "negative birefringence" (n (ordinary) > n (extraordinary)). Similarly, the dichroism (or difference in absorption between the ordinary and extraordinary rays), while not known for the visible and near infrared, is quite pronounced in the far infrared. The difference in the extinction coefficients for the two polarizations (Figures 8 and 9) is considerable. As was illustrated in Figure 7, the high frequency transmission "edge" shifts significantly to higher frequencies on cooling to $90^{\circ}K$.

Following Chapter II, Section B, above, we prefer to evaluate the measured optical constants n and κ in terms of the real and imaginary parts of the dielectric constant,

(II-11) $$\hat{\epsilon} = \epsilon' - i\epsilon'',$$

$$\epsilon' = n^2 - \kappa^2,$$

$$\epsilon'' = 2n\kappa \ .$$

In (II-14') we showed that classical dispersion theory predicts a linear relationship between ϵ' and the square of frequency, for frequencies considerably smaller than the lowest resonant frequency. In Figures 14 and 15 the squares of the "best fit" refractive index values from Figures 5 and 6 are plotted versus the square of frequency. The largest values of the extinction coefficient in this spectral region are sufficiently small ($\kappa < 3 \times 10^{-2}$) that κ^2 is insignificant compared with n^2. The vertical bars in Figures 14 and 15 are the uncertainties in ϵ' due to the uncertainty in n indicated similarly in Figures 5 and 6. Inspection of Figures 14 and 15 shows that the linear relationship between ϵ' and ν^2 seems to be well-supported. The values of the static dielectric constants ϵ_o for the ordinary and extraordinary rays at 300°K and 90°K were determined by drawing straight lines through the points in Figures 14 and 15 and extending these lines to $\nu^2 = 0$. These lines are shown for the 90°K

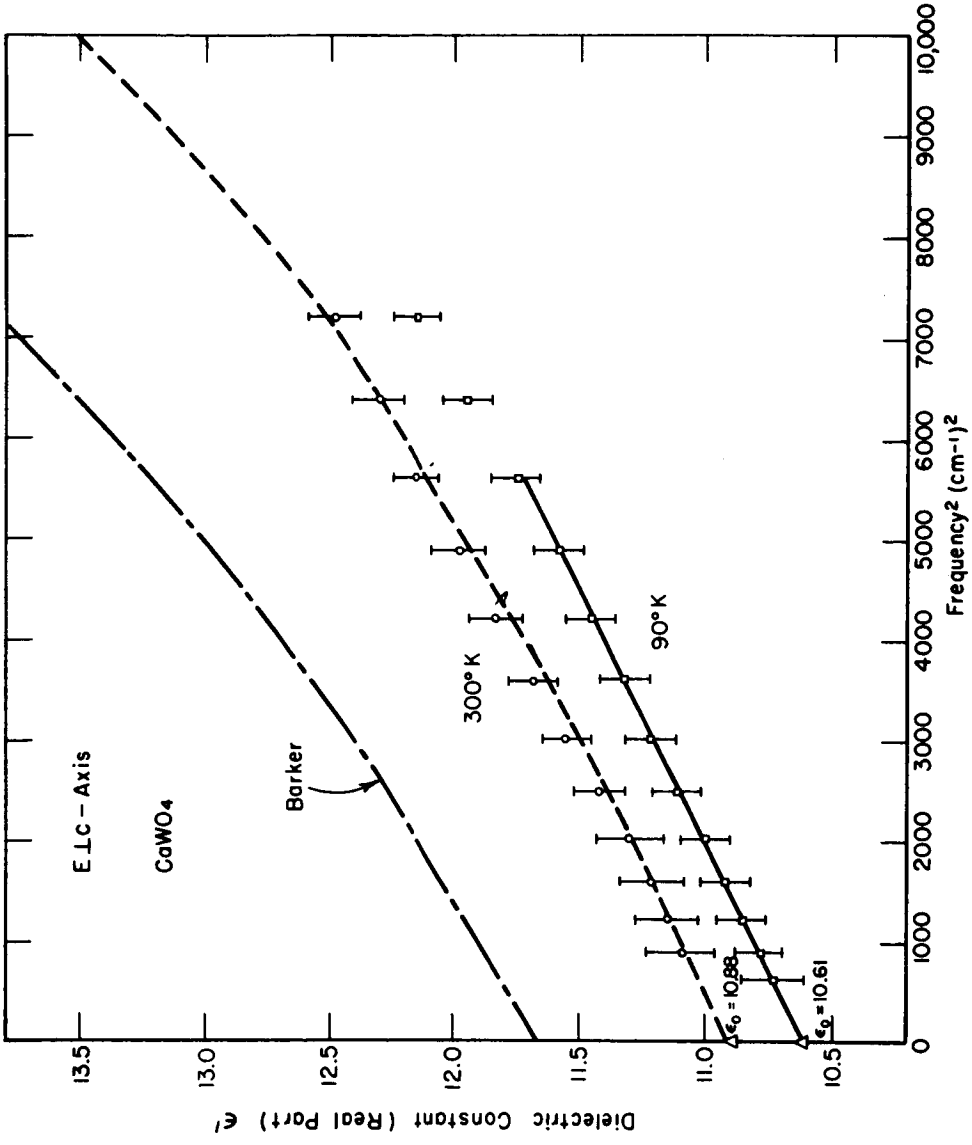

Fig. 14. The dielectric constant (real part) ϵ' of $CaWO_4$, ordinary ray, at 300°K and 90°K, from the present measurements and from the 300°K dispersion parameters of Barker.

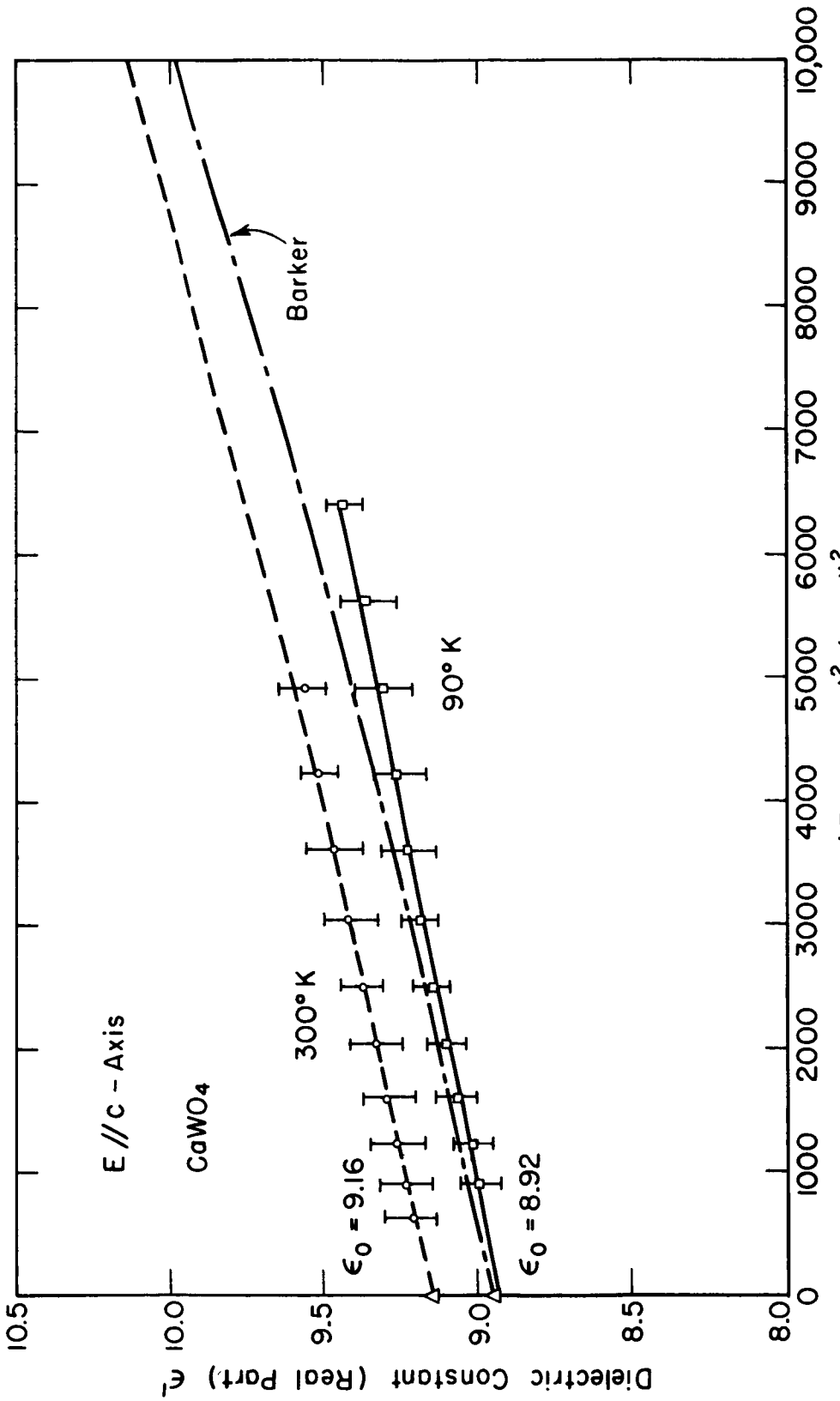

Fig. 15. The dielectric constant (real part) ϵ' of $CaWO_4$, extraordinary ray, at 300°K and 90°K, from the present measurements and from the 300°K dispersion parameters of Barker.

results only in Figures 14 and 15; all the values of ϵ_o so obtained are indicated on the figures. The uncertainty in n, for the values plotted, is $\pm$ 1 percent, thus the uncertainty in ϵ' is $\pm$ 2 percent. However, ϵ_o is found from the straight line which is a very close fit to all the ϵ' points, not just the two necessary to determine it. Consequently, the author believes the uncertainty in ϵ_o is less than that of each ϵ' value; an uncertainty of $\pm$ 1 percent appears to be a conservative value.

The values of ϵ' predicted by the dispersion parameters deduced by Barker (Table 3) are also shown in Figures 14 and 15. The extraordinary ray prediction is rather good as it stands, while the ordinary ray prediction is somewhat too large, in both intercept and slope. Keeping unchanged the frequencies determined by Barker, and the other parameters of the two highest frequency resonances, the strengths A_1 and A_2, of the two lowest frequency resonances, and the values of ϵ_∞, for each polarization, were adjusted to better match the present experimental data. The fits so obtained are shown by the dashed lines drawn through the 300°K points in Figures 14 and 15. These lines were also used to determine the dashed line extensions of the refractive index results in Figures 5 and 6.

The imaginary part of the dielectric constant, ϵ'', at several frequencies was computed from the values of n and κ, as indicated by

the "best fit" lines in Figures 5, 6, 8, and 9, and the values plotted versus frequency in Figures 16 and 17. The values of ϵ'' predicted by the dispersion parameters of Barker are also shown in Figures 16 and 17. The solid curves through the 300°K experimental points were obtained by adjusting the damping constants, γ_1 and γ_2, of the two lowest frequency resonances for each polarization (using the new values of A_j obtained from fitting the ϵ' data). These curves do fit the experimental points rather well, except at the high frequencies, indicating that classical theory does provide an adequate description of the far infrared optical constants of $CaWO_4$. This is somewhat surprising in view of the failure of classical theory to adequately describe ϵ'' for simple crystals,[1,2,3] such as MgO.

The values of the $CaWO_4$ dispersion parameters, after adjustment to fit the present measurements, are shown in Table 6. The only large change is that of the lowest frequency resonance for the ordinary ray. In a subsequent note, Barker has indicated that he has now lowered the strength of this resonance to 1.6 (he finds the other changes indicated in Table 6 acceptable). It is worth noting

---

[1] L. Genzel, H. Happ, R. Weber, Z. Physik 154, 13 (1959).

[2] H. Happ, H. Hofmann, E. Lux, G. Seger, Z. Physik 166, 510 (1962).

[3] L. Genzel, G. Seger, Z. Physik 169, 66 (1962).

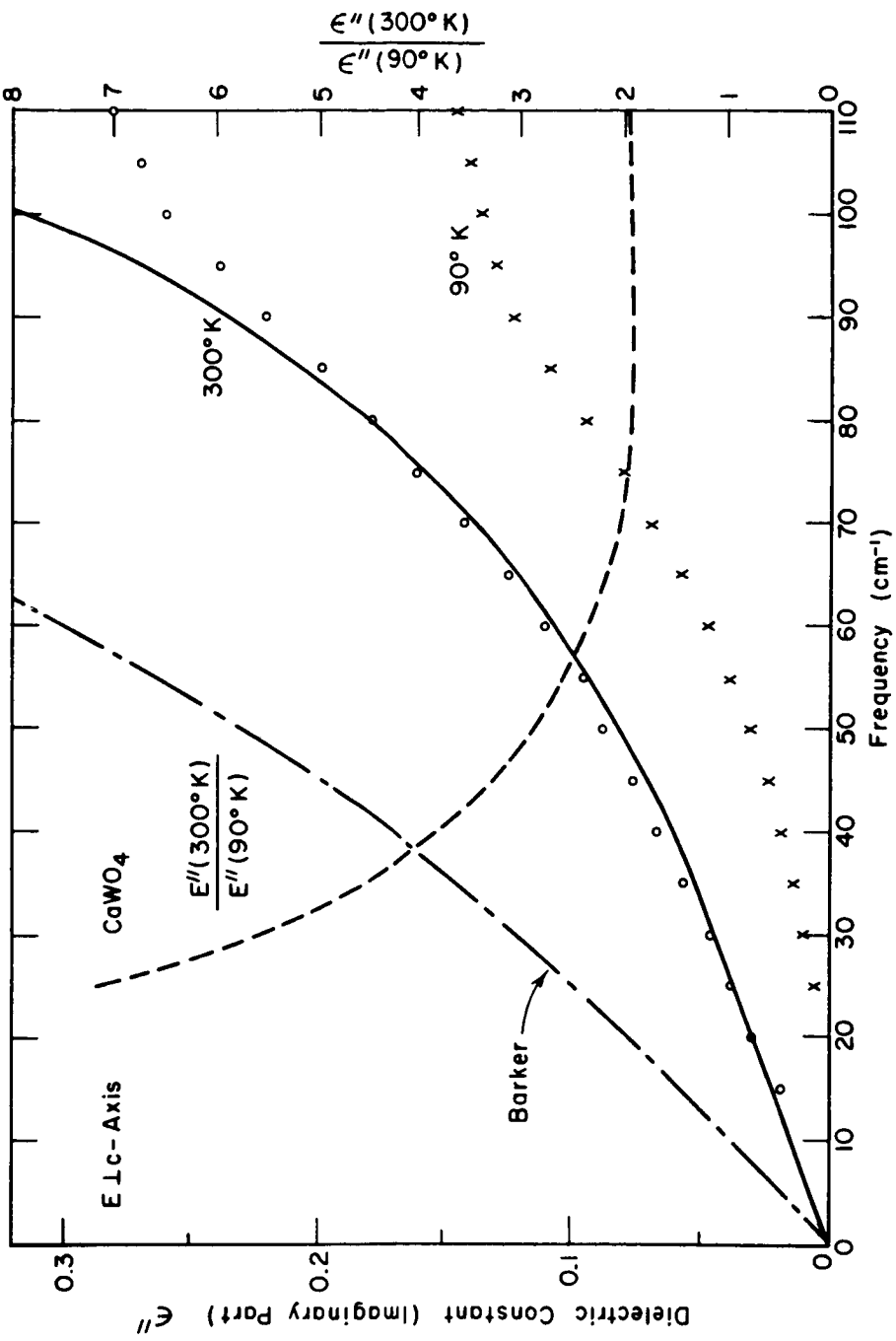

Fig. 16. The dielectric constant (imaginary part) ϵ'' of $CaWO_4$, ordinary ray, at 300°K and 90°K, from the present measurements and from the 300°K dispersion parameters of Barker. The ratio of the measured values at the two temperatures is also plotted.

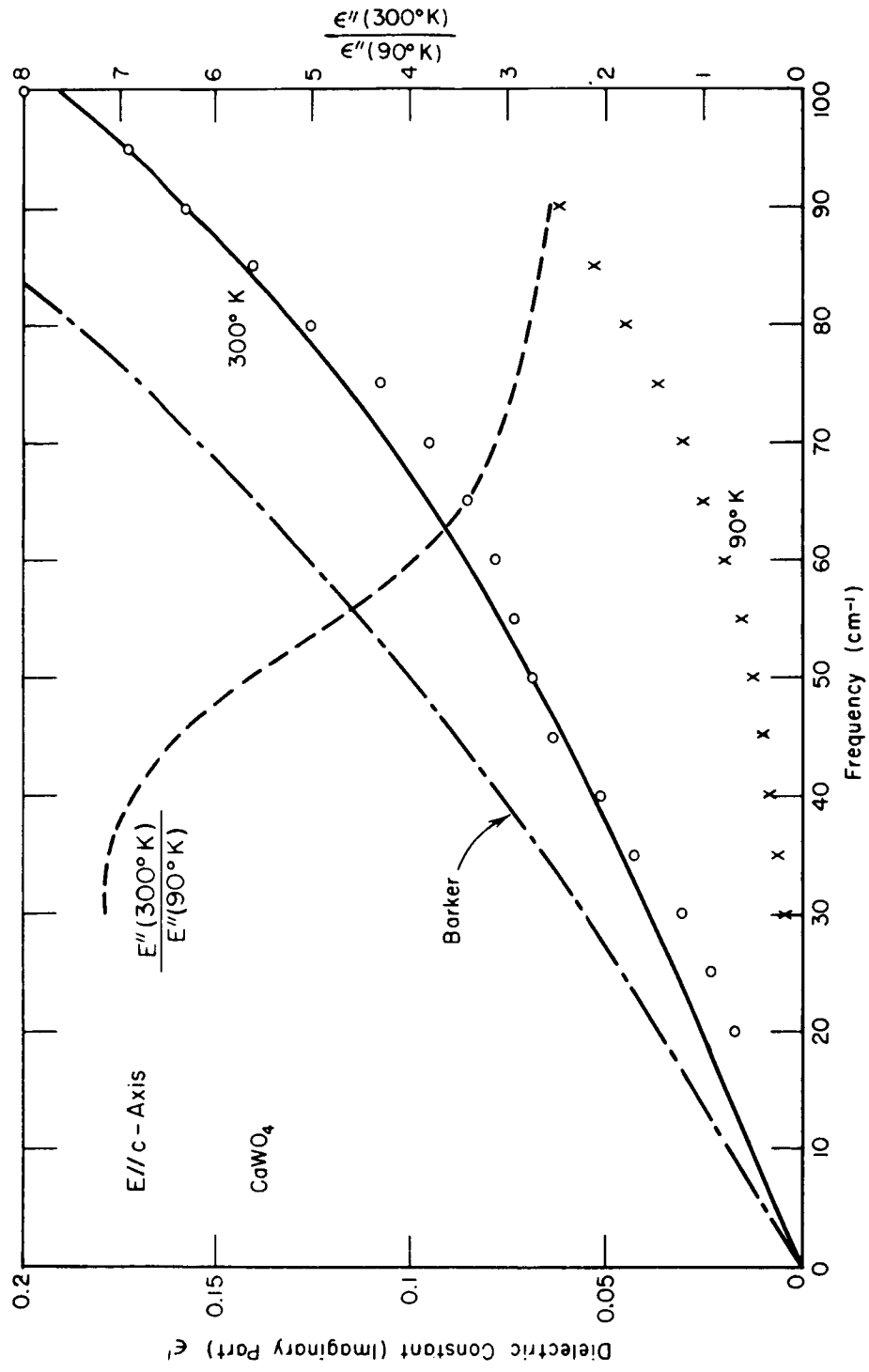

Fig. 17. The dielectric constant (imaginary part) ϵ'' of $CaWO_4$, extraordinary ray, at 300°K and 90°K, from the present measurements and from the 300°K dispersion parameters of Barker. The ratio of the measured values at the two temperatures at also plotted.

that the values of ϵ_∞ required to fit the far infrared data are much closer to the values of ϵ' found from visible refractive index data than are the ϵ_∞ values used by Barker, as was mentioned in Chapter V, above.

TABLE 6

ADJUSTED DISPERSION PARAMETERS FOR $CaWO_4$ ($300^\circ K$)

	E ⊥ c-axis (ordinary ray)				E ∥ c-axis (extraordinary ray)			
Parameter	j=1	j=2	j=3	j=4	j=1	j=2	j=3	j=4
ν_j (cm^{-1})	143	198	307.5	793	192	240	435	778
A_j	1.0	4.6	0.88	0.83	0.5	3.8	0.22	0.98
γ_j	0.05	0.04	0.042	0.01	0.10	0.06	0.03	0.01
ϵ_∞	3.60				3.65			
ϵ_o (computed)	10.91				9.15			
ϵ_o (measured)	10.88 ± 0.11				9.16 ± 0.09			

In principle, it would be possible to make some assumptions about the frequency shifts of the resonances on cooling, and to deduce a set of dispersion parameters to fit the $90^\circ K$ measurements. However, since there is no other $90^\circ K$ data to provide a comparison, and indeed, the data on the frequency shifts of complex crystals is extremely scarce, there appears to be little justification for such an effort for the present work.

Barker[4] has compared the present work's reflectance measurements (Figure 10) with his own work, and has indicated that there is reasonable agreement up to approximately 220 cm^{-1}. Above this frequency the maxima in Figure 10 lie significantly below those obtained by Barker. This is hardly surprising because the present work suffered from two experimental difficulties. First, the effectiveness of the polarizers was decreasing rapidly above 200 cm^{-1}. Second, the data above 200 cm^{-1} were taken using the dispersion grating in second order, while relying on the reststrahlen filters to strongly reduce the first order relative to the second; the fact that enough first order radiation remained to lower the reflectance peaks is hardly surprising.

In Figures 16 and 17 the ratio of ϵ'' at 300°K to ϵ'' at 90°K is also plotted. Since there is no data available on the phonon spectra of complex crystals, let alone for $CaWO_4$, it would seem unduly presumptuous to start to interpret this ratio by means of (II-37). In addition, it should be noted that, due to the considerable uncertainty in the 90°K values of κ, and consequently ϵ'', the value of the ratio $\epsilon''(300°K)/\epsilon''(90°K)$ may be considerably in error.

---

[4]A.S. Barker, Jr., private communication.

The gross features of the present results for $CaWO_4$ are similar to those obtained by Roberts and Coon[5] on crystal quartz and sapphire (corundum, Al_2O_3) at 300°K in the region between 30 and 250 cm^{-1}. They found that quartz had positive biregringence in the far infrared as well as the visible, and that ϵ_o (extraordinary ray) was approximately 5 percent larger than ϵ_o (ordinary ray). They reported a somewhat higher frequency transmission "edge" for the ordinary ray than for the extraordinary ray. Roberts and Coon found that sapphire had positive birefringence in the far infrared while it had negative birefringence in the visible. The difference between ϵ_o (ordinary ray) and ϵ_o (extraordinary ray) was about 20 percent. The difference in transmission between the two polarizations was similar to that found for $CaWO_4$ in the present work. Roberts and Coon reported that, in agreement with the present work, classical dispersion theory provided a good fit with the measured refractive index values. They obtained reasonably good agreement between classical theory and their transmission measurements for sapphire, but not for quartz.

---

[5] S. Roberts, D. Coon, J. Opt. Soc. Am. 52, 1023 (1962).

B. Magnesium oxide

MgO has a transmission "edge" at a higher frequency in the far infrared than any other previously reported polyatomic crystal, with the exception of crystal quartz.[5] However, because of its higher reflection losses resulting from the larger refractive index($n \cong 3.2$ versus $n \cong 2.1$ for quartz), MgO will probably not replace crystal quartz as a window material for detectors and other far infrared devices. MgO also exhibits a significant decrease in absorption on being cooled to $90^{\circ}K$.

As was the case with $CaWO_4$, above, the optical constants of MgO will be discussed in terms of the real and imaginary parts of the dielectric constant. The squares of the selected values of the refractive index, from the "best fit" line in Figure 11, are plotted versus the square of frequency in Figure 18. Again, the value of κ^2 is insignificant compared with n^2 in the present frequency range. The vertical bars show the uncertainty in ϵ' corresponding to the uncertainty in n indicated in Figure 11. It is clear that the linear relationship predicted by (II-14') is well-satisfied. The lines through the points were actually drawn using (II-14a') and the values of ν_o and ϵ_∞ given in Table 4; the value of ϵ_o was adjusted to fit the experimental points. The dashed lines in the refractive index curve, Figure 11, were plotted from this data. It should be noted, from the quality of

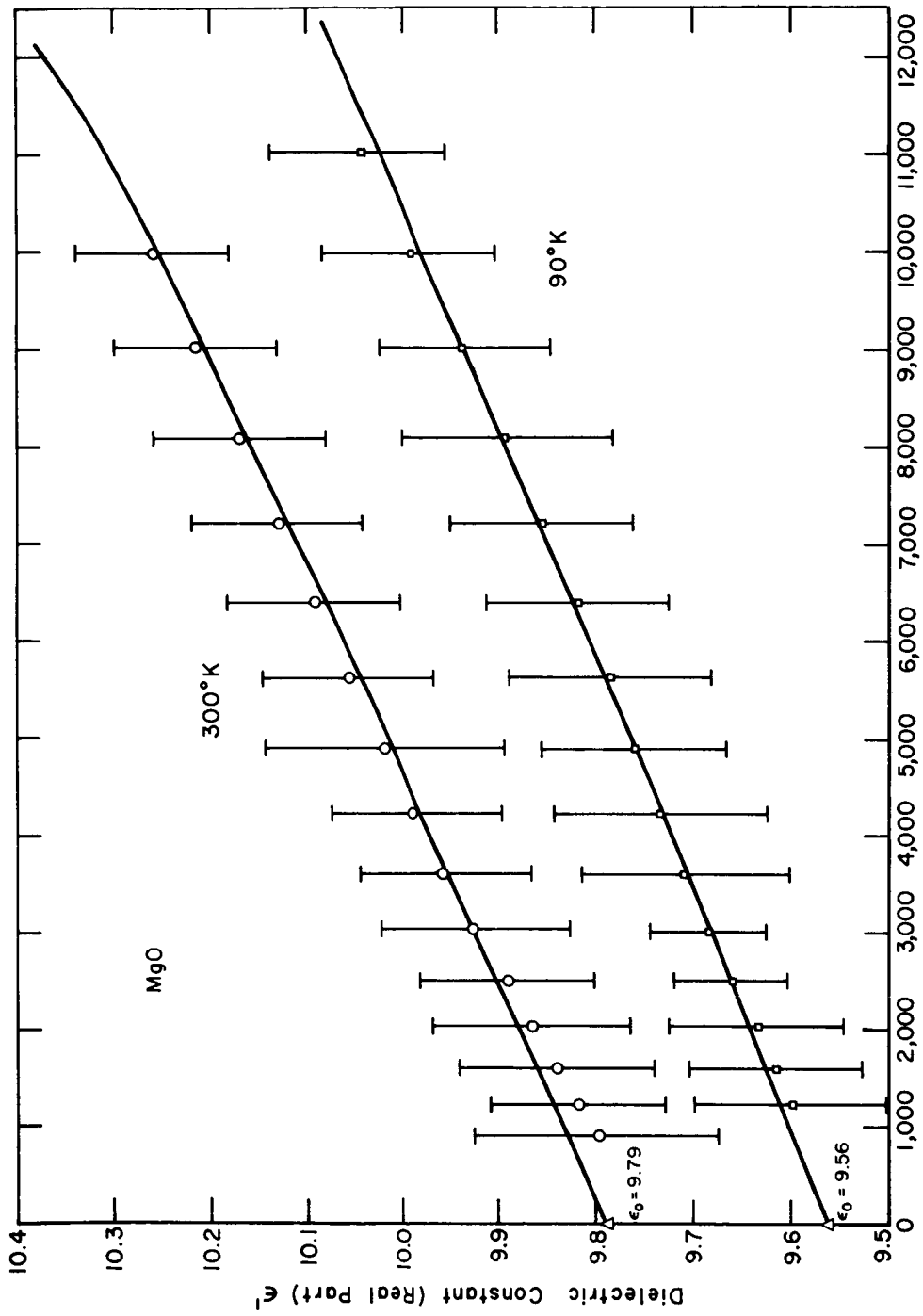

Fig. 18. The dielectric constant (real part) ϵ' of MgO at 300°K and 90°K.

the fit obtained by this procedure, that the present experimental data substantiate the MgO eigenfrequency assignment of $\sim$400 cm^{-1} of Saksena and Viswanathan, and Smart. Clearly, if the eigenfrequency was at $\sim$570 cm^{-1}, as assigned by the earlier workers, then the slope of the line, drawn on the basis of (II-14') or (II-14a'), would be approximately one half of that in Figure 18, and the fit to the experimental data would be very poor. This substantial agreement between predictions of the classical dispersion theory and the measured far infrared values of ϵ' for cubic diatomic crystals has been previously reported for CsBr.[2]

The value of the static dielectric constant, ϵ_o, obtained by fitting the ϵ' data to (II-14a') is certainly more accurate than the $\pm$ 2 percent limits of the uncertainty in the individual ϵ' points; again, a $\pm$1 percent value seems to be a conservative choice. The 300°K result, $\epsilon_o = 9.79 \pm 0.1$ is in good agreement with the work of Højendahl and Smart, however the value quoted by Von Hippel is somewhat further removed. The 90°K result, $\epsilon_o = 9.56 \pm 0.1$, is reasonably close to the value obtained by Smart; the uncertainty in the latter's result is not known. The present results for the 90°K refractive index (Figure 11) are in good agreement with those reported by Smart and Inglis.

The 300°K temperature coefficient of the dielectric constant, given in Table 5, predicts a value of $\epsilon_o = 9.41$ at 90°K; however, it is known that the magnitude of the temperature coefficient increases with temperature. On the simplest assumption, that $\frac{d\epsilon_o}{dT} \propto T$, we find ϵ_o (90°K) = 9.54, compared with the measured value of 9.56; the agreement may be accidental.

1. The infrared absorption

The 300°K and 90°K values of ϵ'', the imaginary part of the dielectric constant, computed from the measured values of n and κ, are shown in Figure 19. Clearly, ϵ'' does not vary linearly with frequency as predicted by classical dispersion theory (II-15'). This failure of classical theory has been previously reported for a number of alkali halides.[1,2,3] The values of ϵ'', for $\nu < 70$ cm^{-1}, which classical theory would predict from the damping constant, γ, found by Smart in the region of the eigenfrequency, are a factor of five larger than the measured values at 300°K and an order of magnitude larger than the measured values at 90°K.

The general shape of the ϵ'' curves is similar to those reported for various other cubic diatomic crystals: NaCl,[1] KBr,[1] CsBr,[2] CaF_2,[2] Lif.[3] The rapid change in ϵ'', occurring between 80 and 105 cm^{-1} in MgO, is also observed, at different frequencies, in the other crystals. There have been no reports of sharp peaks, in the

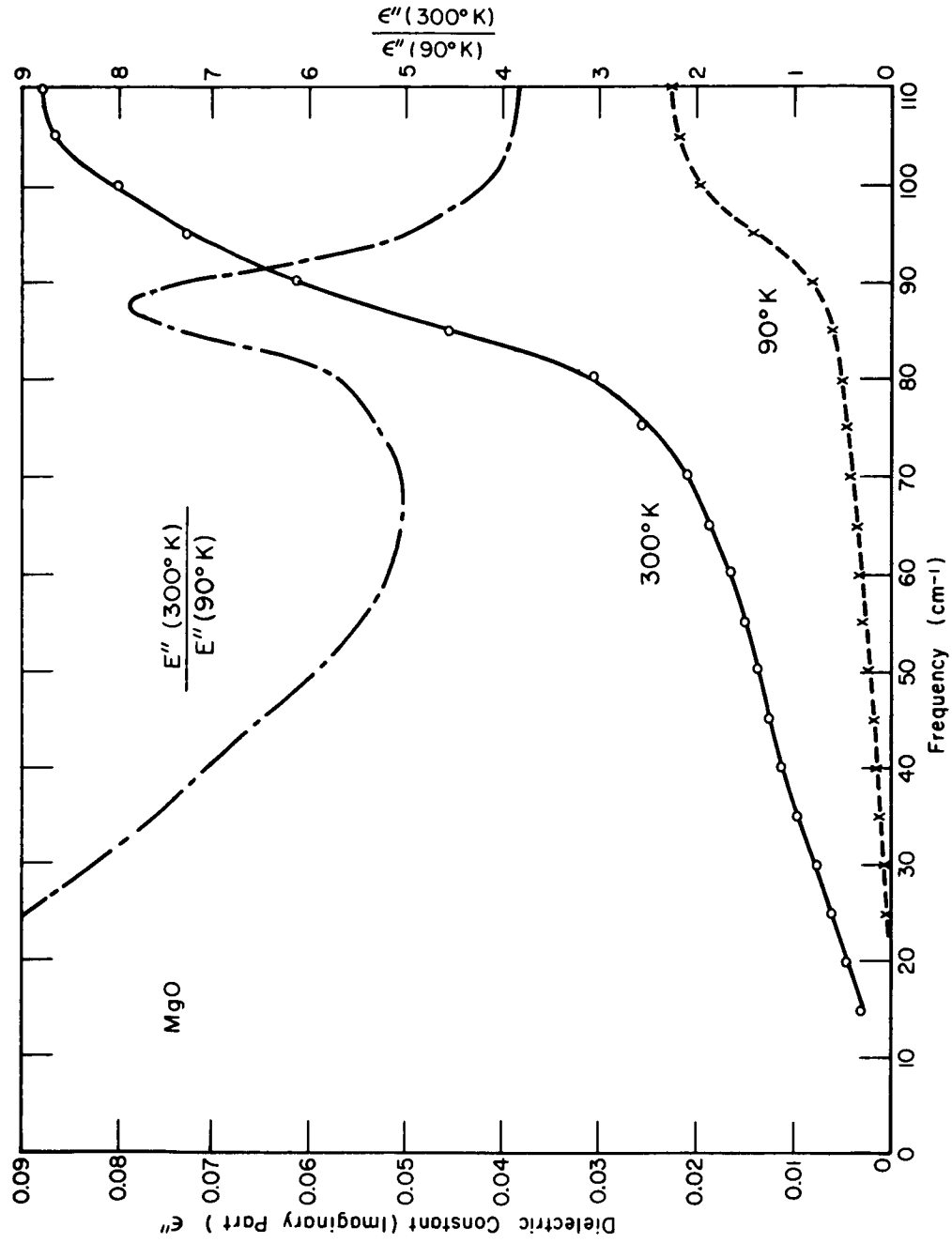

Fig. 19. The dielectric constant (imaginary part) ϵ'' of MgO at 300°K and 90°K. The ratio of the two values is also plotted.

region below the eigenfrequency, but only the changes in slope, similar to the curves in Figure 19.

The present results, when written in terms of the absorption coefficient, are similar, in their gross aspects, to those reported by Price, Wilkinson, et al.[6] Some of the disagreement arises from an apparent inconsistency in two graphs of their 300°K results; the present work agrees with one graph, but not the other. Their liquid nitrogen temperature results do not show the increase in absorption, beginning at 90 cm^{-1}, corresponding to the increase in ϵ'' in Figure 19. Indeed, according to their results, the amount of absorption, which the present work found at 100-110 cm^{-1}, would not occur until approximately 200 cm^{-1}. It should be noted, however, that in their comparison of the integrated absorption with the change in refractive index, following the Kramers-Kronig relation (II-21), the integrated 90°K absorption was too small by a factor of 1.6. This might indicate that their 90°K absorption data were in error.

The ratio $\epsilon''(300^{\circ}K)/\epsilon''(90^{\circ}K)$ is also plotted in Figure 19. This curve should be interpreted with caution, because of the large uncertainty in the 90°K extinction coefficient values. In particular,

---

[6] W. Price, G. Wilkinson, et al., Molecular Spectroscopy Report, U.S. Army Contract DA-91-591-EUC, 1959-1960 (ASTIA AD 262 665, TAB 61-4-4, p. 190).

the peak at 87 cm^{-1} may be spurious, due either to errors in the low temperature ϵ'' values or to a shift in the phonon frequencies between 300°K and 90°K, although the latter cause would not be expected to produce such a prominent effect in a difference band.

The interpretation of the far infrared absorption of MgO in terms of the two phonon processes requires a knowledge of the phonon spectra. Unfortunately, no such data are available to the present author; however there is reason to believe that neutron scattering measurements are being performed on MgO and that the results should be available in the not too distant future.[7] In order to assist the interpretation of the present work in the light of the theory of Genzel and Bilz, when the phonon data is available, the values of the frequency-dependent damping constant, δ, have been computed, from (II-39), for the present measurements and are listed in Table 7. Since the Debye temperature of MgO is large (Table 5), the 90°K data will certainly satisfy the condition (II-40).

It would be rash to even assume that the MgO phonon spectrum follows closely that of NaI (Figure 2), because recent results, both theoretical and experimental, on closely related crystals indicate that, in some cases, the longitudinal acoustic branch at the Brillouin zone

---

[7] M. Bhat, private communication.

boundary has a higher frequency than the transverse optical branch. In addition, it is expected that the absorption at frequencies below the eigenfrequency will contain contributions from more than one difference band. This latter fact will especially complicate the interpretation of the temperature dependence of the ratio $\epsilon''(300^{\circ}K)/\epsilon''(90^{\circ}K)$, following (II-37).

TABLE 7

THE MEASURED DAMPING CONSTANT δ OF GENZEL AND BILZ FOR MgO

$\nu(cm^{-1})$	$-\delta$ (300°K)	$-\delta$ (90°K)	$\nu(cm^{-1})$	$-\delta$ (300°K)	$-\delta$ (90°K)
15	0.46×10^{-3}	-	65	2.51×10^{-3}	0.53×10^{-3}
20	0.66	-	70	2.78	0.58
25	0.89	0.10×10^{-3}	75	3.34	0.65
30	1.13	0.14	80	3.90	0.72
35	1.37	0.19	85	5.72	0.83
40	1.59	0.23	90	7.66	1.09
45	1.77	0.28	95	8.93	1.82
50	1.92	0.34	100	9.65	2.51
55	2.09	0.39	105	10.25	2.70
60	2.25	0.45	110	10.14	2.78

We can, however, attempt a few rough interpretations, without any knowledge of the phonons. We assume that the absorption is due to only one difference band and not the superposition of several. The use of (II-37) is simplified, for the case of only one difference band at a given photon frequency ν, if it is rewritten, using (II-34), in the form

$$\text{(II-37')} \qquad \frac{\epsilon''(\nu, T_1)}{\epsilon''(\nu, T_2)} = \frac{\sinh \frac{\nu}{2\tau_1} \left[\cosh\left(\frac{U}{2\tau_2}\right) - \cosh\left(\frac{\nu}{2\tau_2}\right)\right]}{\sinh \frac{\nu}{2\tau_2} \left[\cosh\left(\frac{U}{2\tau_1}\right) - \cosh\left(\frac{\nu}{2\tau_1}\right)\right]} ,$$

where

$$u_i = U + \frac{\nu}{2}, \quad u_j = U - \frac{\nu}{2}, \quad (\nu = u_i - u_j)$$

and

$$\tau_1 = \frac{kT_1}{h}, \quad \tau_2 = \frac{kT_2}{h} .$$

Since the present work is only concerned with the case where $T_1 = 300^{\circ}K$ and $T_2 = 90^{\circ}K$, plots of $\frac{\epsilon''(\nu,\ 300^{\circ}K)}{\epsilon''(\nu,\ 90^{\circ}K)}$ versus U, with ν as a parameter, were prepared. For $20 < \nu < 100\ cm^{-1}$ these plots could be well-represented by one curve. Then, from $\epsilon''(300^{\circ}K)/\epsilon''(90^{\circ}K)$ from Figure 19, at a specific frequency ν, U can be found from the plot of (II-37'), and thus u_i and u_j can be determined.

In Figure 2 it was shown that the zone boundary frequencies, u_1 and u_2, from the one dimensional model, provided some guide, albeit a not too accurate one, to the separation between the optical and acoustic branches in NaI. For MgO these one dimensional model frequencies are $u_1 = 308\ cm^{-1}$ and $u_2 = 250\ cm^{-1}$. A difference band involving phonons of these frequencies would produce an absorption in the region of 58 cm^{-1} and, from (II-37'), $\epsilon''(300^oK)/\epsilon''(90^oK) \cong 11.8$. In view of the question of the meaning of u_1 and u_2 for the three dimensional crystal, and the uncertainties in ϵ'' (90^oK), the 87 cm^{-1} peak in the $\epsilon''(300^oK)/\epsilon''(90^oK)$ curve in Figure 19 might conceivably be associated with such a combination.

If the ratio $\epsilon''(300^oK)/\epsilon''(90^oK)$ is accurate, then the rapid increase in ϵ'' beyond 90 cm^{-1} is due to transitions between phonons with frequencies of $\sim 175\ cm^{-1}$ and $\sim 75\ cm^{-1}$. Similarly, the 25 to 50 cm^{-1} absorption is associated with phonon branches at 230 - 245 cm^{-1} for the upper level and 165 - 230 cm^{-1} for the lower level. It would appear difficult to match these phonon frequencies to some set of dispersion curves similar to those in Figure 2. Clearly, the phonon spectra must be known for further interpretation.

2. The dielectric constant

In the discussion of classical dispersion theory in Chapter II, above, it was pointed out that the temperature dependence in the dispersion parameters is contained in the damping constant γ_g, while the

oscillator strengths A_g are expected to be independent of temperature. The static dielectric constant, ϵ_o, is thus expected to be essentially independent of temperature, because it is determined (II-16) by the oscillator strengths and the high frequency dielectric constant (which shows only a slight temperature dependence). The results of the measurements show, however, that ϵ_o exhibits a measurable temperature dependence. We must note, however, that the experimentally measured eigenfrequency also shifts with temperature. Inspection of the definition of the oscillator strength, A_g, in (II-13), shows that it is inversely proportional to the square of the resonant frequency ν_g. Consequently, we may expect the temperature shift of the static dielectric constant to be associated with the temperature shift of the eigenfrequency. From (II-16'), for the cubic diatomic crystal,

$$\epsilon_o - \epsilon_\infty = A,$$

thus we might expect

$$\frac{(\epsilon_o - \epsilon_\infty)_{300}}{(\epsilon_o - \epsilon_\infty)_{90}} = \frac{\nu_o^2\,(90^\circ K)}{\nu_o^2\,(300^\circ K)} \quad .$$

For MgO, the value of the right hand side of this expression is 1.07 while the value of the left hand side is 1.03. The values are not unreasonable, in view of the accuracy of the measurements.

In Chapter II, Section C.2, above, a number of formulas were given which relate the static and high frequency dielectric constants, the eigenfrequency, and other physical quantities, for cubic diatomic crystals. It was mentioned that some of these relations had been evaluated for MgO using, however, the previously reported 580 cm^{-1} eigenfrequency. Since we now believe that this value has been demonstrated to be incorrect, and that the true eigenfrequency ($\sim$400 cm^{-1}) is rather different, it appears worthwhile to re-evaluate these various formulas using the eigenfrequency data from Smart and the dielectric constant data from the present work, at both 300°K and 90°K.

The required physical quantities, from Tables 4 and 5, were substituted in the various formulas from Chapter II, and the results listed in Table 8. The parameter s is the ratio, e^*/e, of the computed effective charge to the actual electronic charge. The quantity K^*/K is the ratio of the computed compressibility to the value listed in Table 5. A compilation of results, similar to those of Table 8, has been given by Perry, et al.,[8] for a number of alkali and other halide crystals. We will discuss the data in Table 8 in view of the comments of the authors deriving the formulas and in terms of the results of Perry, et al.

---

[8] G. Jones, D. Martin, P. Mawer, C. Perry, Proc. Roy. Soc. (London) A261, 10 (1961).

TABLE 8

COMPUTED EFFECTIVE CHARGE PARAMETERS AND COMPRESSIBILITIES FOR MgO

Equation	Result	Author
(II-25)	$s = 0.60$ (300°K)	Szigeti I
	$s = 0.61$ (90°K)	
(II-26)	$\frac{K^*}{K} = 0.91$ (300°K)	Szigeti II
	$\frac{K^*}{K} = 0.88$ (90°K)	
(II-27)	$\frac{K^*}{K} = 0.70$ (300°K)	Lundqvist
	$\frac{K^*}{K} = 0.69$ (90°K)	
(II-28)	$s = 0.83$ (300°K)	Lundqvist
	$s = 0.82$ (90°K)	
(II-29)	$s = 0.52$ (300°K)	Havinga, F&J[+]
	$s = 0.30$ (300°K)	Havinga, P[+]
(II-30)	$s = 0.48$ (300°K)	Havinga
(II-31)	see text	Havinga
(II-33)	$\frac{K^*}{K} = 1.05$ (300°K)	Cochran

[+]F & J: polarizability data from Fajans and Joos;

P: polarizability data from Pauling.

The values of s from Szigeti I (II-25) for the alkali halides range between 0.7 and 0.9; the 0.6 value for MgO is somewhat lower. It should be noted that this is obtained using the double valency (Z=2); if we forgo the concept of valency, then "the effective ionic charge" of MgO is 1.2, about 50 percent larger than those of the alkali halides. The change in s, between 300°K and 90°K, is small.

The value of K^*/K from (II-26) falls in the middle of the range of values found for the alkali halides. This contradicts Szigeti's statement, supported by a result using the incorrect eigenfrequency, that MgO would show a much greater variation from $K^*/K = 1$. He predicted this on the basis of the elastic anisotropy, indicated by the failure of the Cauchy relation $c_{44} = c_{12}$, for MgO but not (approximately) for the alkali halides. The use of 90°K data produces a small change away from $K^*/K = 1$. This result does not support the argument that the deviations from unity in (II-26) are due to the use of 300°K data in a relation derived for 0°K.

The Lundqvist formula for the compressibility (II-27) produces values K^*/K considerably smaller than those obtained from Szigeti II (II-26). Perry, et al., tested (II-27) only for KI at room temperature and at 4°K. In both cases they obtained results from (II-27) larger than they did from (II-26). It should be noted that while KI comes much

closer than MgO to satisfying the Cauchy relation, for KI $c_{12} > c_{44}$ while for MgO $c_{12} < c_{44}$.

The Lundqvist expression for s, (II-28), yields values considerably larger than those from Szigeti I. Perry, et al., also tested (II-28) at low temperatures only for KI, and obtained reasonable agreement. At room temperature, however, their values from (II-28) were also consistently larger than those from Szigeti I. It would appear that the Lundqvist model may overemphasize the effects of the mechanical anisotropy on the dielectric behavior of the crystal.

The formula of Havinga (II-29), using the free ion polarizabilities, produces results which are too small. Part of the difficulty doubtless lies with the polarizability of the oxygen ion. In the case of the halide ions, the polarizabilities from Fajans and Joos, and from Pauling, differ by only a few percent, while for O^{-2} they differ by 30 percent. Perry, et al., obtained rather good agreement between (II-29) and Szigeti I, (II-25).

The agreement with Szigeti I, using the second of Havinga's formulas, (II-30), is somewhat poorer than that which he obtained for NaCl and KCl. For MgO, Havinga's third formula, (II-31), actually yields an imaginary value for s. Havinga's derivation of these last two formulas assumed that the primary effects of changes in temperature and pressure would be on the repulsive force between

the ions. The failure of these expressions, particularly the latter, would indicate that this is not the case for MgO. This view is supported by the fact that $\frac{d\epsilon_\infty}{dP}$ is negative for MgO and positive for the alkali halides.

A full test of the expression of Cochran (II-33) requires data from a number of compounds containing the same ions, so that d_+ and d_- can be deduced from (II-32). Since such as assortment of data is not available, we make the assumption (following Woods, Cochran, and Brockhouse[9]) that the electronic deformation effects occur primarily in the negative ion. Then $d_+ = 0$, and from (II-32) $d_- = 1-s$. Using the value of s from (II-25), (II-33) can then be evaluated. The value of K^*/K so obtained is slightly larger than unity, consistent with Cochran's results for the alkali halides.

We may attempt to draw a few conclusions from this collection of results for MgO. First, the effective charge of MgO is smaller than those found for the alkali halides, if the double valency (Z=2) is retained. Second, the value of the effective charge at 90°K is little different from that at 300°K. Third, the ratio K^*/K is little different from that found for the alkali halides, apparently indicating that the

---

[9] A. Woods, W. Cochran, B. Brockhouse, Phys. Rev. 119, 980 (1960).

mechanical anisotropy evident in the elastic constants has little effect on the dielectric properties.

CHAPTER VII
CONCLUSIONS

A. Summary of the present work

The present work has demonstrated the utility of The Ohio State University far infrared spectrometer for the measurement of the infrared properties of dielectric crystals in the spectral region between 10 and 100 cm^{-1}. From more than 1500 separate measurements, over 900 values of the optical constants n and κ, at 300°K and 90°K, have been computed for MgO and $CaWO_4$ in this frequency range. From these values curves have been plotted showing the optical constants, and the real and imaginary parts of the dielectric constant, as a function of frequency at two temperatures. The static dielectric constants have been found from these curves.

The real parts of the dielectric constants for both materials have been shown to follow the predictions of classical dispersion theory. Good agreement has been found between measured 300°K values of the far infrared optical constants of $CaWO_4$ and the values predicted from classical dispersion parameters deduced from reflection measurements in the mid infrared at another laboratory.

This work shows the failure of classical dispersion theory to predict the structure of the far infrared absorption for cubic diatomic crystals, such as MgO. The interpretation of the infrared absorption of MgO in the light of the theory of two phonon processes awaits the measurement of the phonon dispersion curves. Some previous misinterpretations of relations between the dielectric constants and the eigenfrequency of MgO have been corrected.

B. Suggestions for further work

A few improvements in the spectrometer and its associated components would aid future work of this kind. A lamellar grating of better surface quality[1] would probably permit the operation of the Interferometric Modulator at higher frequencies, up to 200 cm^{-1}, eliminating the need for reststrahlen filters and simplifying the foreoptics. Use of the spectrometer above 200 cm^{-1} is probably pointless, because of the availability of CsI prism instruments for work above 200 cm^{-1}. Elimination, or at least a reduction, of the large background variations, through use of an improved detector, should permit more accurate recording of channeled spectra in the lowest frequency region. The introduction of some type of direct frequency calibration system[2] would improve the accuracy of the interpretation of channeled spectra.

---

[1] Such a grating is now being fabricated.

[2] Work on such a calibration system is now in progress.

Some improvement in the cryogenic facilities would also be useful. The ability to move the sample in the cryostat, or move the cryostat as a whole, would permit direct point-by-point transmission measurements and bring the accuracy of the low temperature measurements up to the level of those at room temperature. While such techniques have been used at liquid nitrogen temperatures,[3,4] their extension to the helium temperatures offers serious difficulties. The extension of the low temperature techniques of the present work to lower temperatures and, through the use of small heaters, to intermediate temperatures would be extremely useful.

Of the materials for investigations similar to the present work, the most promising, of course, are those for which the phonon dispersion curves, or sum band analyses, are available:[5] NaI, KBr,[6] Ge, Si, GaAs, InSb. Additional materials will doubtless be added to this list in the near future. While other crystals[7] with the scheelite

---

[3] R.L. Brown, Ph.D. Dissertation, The Ohio State University, 1959.

[4] A. Mitsuishi, J. Phys. Spc. Japan 16, 533 (1961). H. Yoshinaga, S. Fujita, S. Minami, A. Mitsuishi, R. Oetjen, Y Yamada, J. Opt. Soc. Am. 48, 315 (1958).

[5] See Chapter II, Section D, above.

[6] A. Woods, B. Brockhouse, W. Cochran, M. Sakamoto, R. Sinclair, Bull. Am. Phys. Soc. 5, 462 (1960).

[7] E.g., $CaMoO_4$.

structure are available commercially, there appears at present to be little reason to pursue the measurement of the far infrared properties of complex crystals, rather than the simpler materials mentioned above. Some simpler uniaxial crystals, e.g., MgF_2, MnF_2, are readily available also. Several non-single crystal materials,[8] available in relatively large pieces, could be usefully investigated, particularly at low temperatures, to aid future instrumentation.

The theory of dielectrics presently has a great need for data on the low temperature values of the static dielectric constants, and their temperature coefficients, of alkali halides and other simple crystals. Work in this vein is in progress at at least one laboratory,[9] using radio-frequency and microwave techniques. It may well be that, however, because of the engineering problems of such work at low temperatures, more accurate determinations of these values can be obtained from the channeled spectrum method of the present work.

Clearly, the subjects for profitable investigation, using the techniques demonstrated by the present work, greatly exceed the instrumentation to pursue them.

---

[8] The most likely candidates would be fused quartz and Irtran I (pressed MgF_2).

[9] D.H. Martin, unpublished comments at International Symposium on Far Infrared Spectroscopy, Cincinnati, 1962.

BIBLIOGRAPHY

Books

Born, M., Huang, K., Dynamical Theory of Crystal Lattices (The Clavendon Press, Oxford, 1954).

Born, M., Wolf, E., Principles of Optics, (Pergamon Press, New York, 1959).

Brillouin, L., Wave Propagation in Periodic Structures (Dover Publications, Inc., New York, 1953).

Ditchburn, R., Light (Interscience Publishers, Inc., New York, 1953).

Ewald, P., Herman, C., Strukturbericht 1913-1928 (Aka. Verlag, Leipzig, 1931).

Handbook of Chemistry and Physics (Chemical Rubber Publishing Company, Cleveland, 1962), 44th ed.

Kittel, C., Introduction to Solid State Physics (John Wiley and Sons, Inc., New York, 1956).

Krishnan, R., Progress in Crystal Physics (S. Viswanathan, Chetput, Madras, 1958), Vol. 1.

Lark-Horovitz, K., Johnson, V., (eds.), Methods of Experimental Physics (Academic Press, New York, 1959), Vol. 6, Part B.

Landolt-Bornstein, Physikalisch-chemische Tabellen (J. Springer, Berlin, 1952), 6th ed.

Moss, T., Optical Properties of Semi-Conductors (Butterworths Scientific Publications, London, 1959).

Seitz, F., Modern Theory of Solids (McGraw-Hill Book Company, Inc., New York, 1940).

Singer, J., (ed), Advances in Quantum Electronics (Columbia University Press, New York, 1961).

Strong, J., Concepts of Classical Optics (W. H. Freeman and Co., San Francisco, 1958).

Smith, R., Wave Mechanics of Crystalline Solids (John Wiley and Sons, Inc., New York, 1961).

Von Hippel, A., (ed.), Dielectric Materials and Applications (John Wiley and Sons, Inc., New York, 1954).

Wyckoff, R., Crystal Structures (Interscience Publishers, Inc., New York, 1948).

Ziman, J., Electrons and Phonons (Clarendon Press, Oxford, 1960).

Zimmerman, L., Vollständige Tafeln der Quadrate aller Zahlen bis 100009 (Edwards Brothers, Inc., Ann Arbor, 1946).

Periodicals

Barnes, R., Brattain, R., Seitz, F., Phys. Rev. 48, 582 (1935).

Barnes, R., Czerny, M., Z. Physik 72, 447 (1931).

Barron, T., Berg, W., Morrison, J., Proc. Roy. Soc. (London) A250, 70 (1959).

Bentley, F., Jones, W., Spectrochim. Acta 16, 135 (1960).

Bilz, H., Genzel, L., Happ, H., Z. Physik 160, 535 (1960).

Bilz, H., Genzel, L., Z. Physik 169, 53 (1962).

Boyle, W., Rodgers, W., J. Opt. Soc. Am. 49, 66 (1959).

Brockhouse, B., Steward, A., Revs. Mod. Phys. 30, 236 (1958).

Brockhouse, B., Iyengar, P., Phys. Rev. 111, 747 (1958).

Burstein, E., Oberley, J., Plyler, E., Proc. Indian Acad. Sci. A28, 388 (1948).

Burstein, E., Smith, P., Phys. Rev. 74, 229 (1948).

Cochran, W., Phil. Mag. 4, 1082 (1959).

Cochran, W., Proc. Roy. Soc. (London) A253, 260 (1959).

Cochran, W., Fray, S., Johnson, F., Quarrington, J., Williams, N., J. Appl. Phys. 32, 2102 (1961).

Dick, B., Overhouser, A., Phys. Rev. 112, 90 (1958).

Dean, T., Jones, G., Martin, D., Mawer, P., Perry, C., Optica Acta 7, 185 (1960).

Durand, M., Phys. Rev. 50, 453 (1936).

Durand, M., Physics 7, 297 (1936).

Fajans, K., Joos, G., Z. Physik 23, 1 (1924).

Fray, S., Johnson, F., Jones, R., Proc. Phys. Soc. (London) 76, 939 (1960).

Fock, J., Z. Physik 90, 44 (1934).

Geick, R., Z. Physik 161, 116 (1960).

Geick, R., Z. Physik 166, 122 (1961).

Genzel, L., Weber, R., Z. angew. Physik 10, 127 (1958).

Genzel, L., Weber, R., Z. angew. Physik 10, 195 (1958).

Genzel, L., Happ, H., Weber, R., Z. Physik 154, 13 (1959).

Genzel, L., Seger, G., Z. Physik 169, 66 (1962).

Golay, M., Rev. Sci. Inst. 18, 357 (1947).

Hadni, A., Claudel, J., Décamps, E., Gerbaux, X., Strimer, P., Compt. rend. 255, 1595 (1962).

Hanlon, J., Lawson, A., Phys. Rev. 113, 472 (1959).

Happ, H., Hofman, H., Lux, E., Seger, G., Z. Physik 166, 510 (1962).

Hass, M., Phys. Rev. 119, 633 (1960).

Havinga, E., Phys. Rev. 119, 1193 (1960).

Højendahl, K., Kgl. Danske Videnskab. Selskab. 16, No. 2 (1938).

Iona, M., Phys. Rev. 60, 822 (1941).

Johnson, F., Proc. Phys. Soc. (London) 73, 265 (1959).

Jones, G., Martin, D., Mawer, P., Perry, C., Proc. Roy. Soc. (London) A261, 10 (1961).

Karo, A., J. Chem. Phys. 31, 1489 (1958).

Kellerman, E., Phil. Trans. Roy. Soc. (London) 238, 513 (1940).

Kleinman, D., Spitzer, W., Phys. Rev. 118, 110 (1960).

Kleinman, D., Phys. Rev. 118, 118 (1960).

Kramers, H., Atti Congr. dei Fisici, Como, 545 (1927).

Kronig, R., J. Opt. Soc. Am. 12, 547 (1926).

Krumhansl, J., J. Appl. Phys. 33, 307 (1962).

Lax, M., Burstein, E., Phys. Rev. 97, 39 (1955).

Levin, E., Offenbacher, E., Phys. Rev. 118, 1142 (1960).

Low, F., J. Opt. Soc. Am. 51, 1300 (1961).

Lundqvist, S., Arkiv Fysik 9, 435 (1955).

Lundqvist, S., Arkiv Fysik 12, 263 (1957).

Lyddane, R., Sachs, R., Teller, E., Phys. Rev. 59, 673 (1941).

Macdonald, J., Brachman, M., Revs. Mod. Phys. 28, 393 (1956).

Mayburg, S., Phys. Rev. 79, 375 (1950).

Mitsuishi, A., J. Phys. Soc. Japan 16, 533 (1961).

Momin, A., Proc. Indian Acad. Sci. A37, 254 (1953).

Odelevski, V., Izv. An USSR, Ser Fiz. 14, 232 (1950).

Oetjen, R., Haynie, W., Ward, W., Hansler, R., Schauwecker, H., Bell, E., J. Opt. Soc. Am. 42, 559 (1952).

Palik, E., J. Opt. Soc. Am. 50, 1329 (1960).

Palik, E., Rao, K., J. Chem. Phys. 25, 1174 (1956).

Pauling, L., Proc. Roy. Soc. (London) A 114, 191 (1927).

Phillips, J., Phys. Rev. 104, 1263 (1956).

Phillips, J., Phys. Rev. 113, 147 (1959).

Plyler, E., Yates, D., Gebbie, H., J. Opt. Soc. Am. 52, 860 (1962).

Putley, E., J. Phys. Chem. Solids 22, 241 (1961).

Roberts, S., Coon, D., J. Opt. Soc. Am. 52, 1023 (1962).

Robinson, T., Proc. Phys. Soc. (London) B 65, 910 (1952).

Robinson, T., Proc. Phys. Soc. (London) B 66, 969 (1953).

Saksena, B., Viswanathan, S., Proc. Phys. Soc. London B 69, 129 (1956).

Sharma, S., Proc. Indian Acad. Sci. A 32, 268 (1950).

Smith, H., Phil. Trans. Roy. Soc. London 241, 105 (1948).

Spitzer, W., Kleinman, D., Phys. Rev. 121, 1324 (1961).

Stephens, R., Malitson, I., J. Research Natl. Bur. Standards 49, 249 (1952).

Strong, J., Phys. Rev. 37, 1565 (1931).

Strong, J., Phys. Rev. 38, 1818 (1931).

Strong, J., Brice, B., J. Opt. Soc. Am. 25, 207 (1935).

Strong, J., Vanesse, G., J. Opt. Soc. Am. 49, 844 (1959).

Szigeti, B., Trans. Faraday Soc. 45, 155 (1949).

Szigeti, B., Proc. Roy. Soc. (London) A 204, 51 (1950).

Szigeti, B., Proc. Roy. Soc. (London) A 252, 217 (1959).

Szigeti, B., Proc. Roy. Soc.(London)A 258, 377 (1960).

Szigeti, B., Proc. Roy. Soc.(London)A 261, 274 (1961).

Tolpygo, K., Izv. AN USSR, Ser. Fiz., 21, No. 1 (1957), (Trans. Bulletin 21, 44 (1957)).

Tolpygo, K., Izv. AN USSR, Ser. Fiz. 24, No. 2 (1960), (Trans. Bulletin 24, 167 (1960)).

Tolpygo, K., Uspekhi Fiz. Nauk 74, 269 (1961), Soviet Phys.-Uspekhi 4, 485 (1961).

Tolksdorf, S., Z. physik. Chem. 132, 161 (1928).

Van Hove, L., Phys. Rev. 89, 1189 (1953).

Willmott, J., Proc. Phys. Soc.(London) A 63, 389 (1950).

Woods, A., Cochran, W., Brockhouse, B., Phys. Rev. 119, 980 (1960).

Woods, A., Brockhouse, B., Cochran, W., Sakamoto, M., Sinclair, R., Bull. Am. Phys. Soc. 5, 462 (1960).

Yamashita, J., Progr. Theoret. Phys. (Kyoto) 8, 280 (1952).

Yamashita, J., Progr. Theoret. Phys. (Kyoto) 12, 454 (1954).

Yamashita, J., Kurosawa, T., J. Phys. Soc. Japan 10, 610 (1955).

Yoshinaga, H., Oetjen, R., Phys. Rev. 101, 526 (1956).

Yoshinaga, H., Fujita, S., Minami, S., Mitsuishi, A., Oetjen, R., Yamada, Y., J. Opt. Soc. Am. 48, 315 (1958).

Reports and Dissertations

Brown, R., Ph. D. Dissertation, The Ohio State University, 1959.

Burnside, P., Ph. D. Dissertation, The Ohio State University, 1958.

Fuchs, R., Temperature Dependence of the Dielectric Constant of Ionic Crystals, Technical Report 167, Lab. Insulation Research, MIT, 1961.

Hansler, R., Ph. D. Dissertation, The Ohio State University, 1952, unpublished.

McCubbin, T. K., Far Infrared Spectroscopy from 100 to 700 Microns, Ph. D. Dissertation, The Johns Hopkins University, 1951.

Price, W., Wilkinson, G., et al., Molecular Spectroscopy Report, U. S. Army Contract DA-91-591-EUC 1959-1960 (ASTIA AD 262665, TAB 61-4-4, p. 190).

Smart, C., Ph. D. Thesis, University of London, 1962, unpublished.

Rowntree, R., Chang, W., Symposium on Lasers and Applications, Columbus, November 1962.

Vance, M., Ph. D. Dissertation, The Ohio State University, 1962.